Aus der Klinik für Kardiologie

der Medizinischen Fakultät Charité – Universitätsmedizin Berlin

DISSERTATION

Myocardial deformation imaging in patients with inflammatory cardiomyopathy

zur Erlangung des akademischen Grades

Doctor medicinae (Dr. med.)

vorgelegt der Medizinischen Fakultät

Charité – Universitätsmedizin Berlin

von

Aleksandar Staykov Aleksandrov

aus Burgas, Bulgarien

Datum der Promotion: 08.12.2017

Table of contents

Abstrakt

Einleitung: Die inflammatorische Kariomyopathie (iCM) ist eine wesentliche Ursache für eine dilatative Kardiomyopathie (DCM) und diese wiederum einer der häufigsten Gründe für eine Herztransplantation. Keine der routinemäßigen nicht-invasiven Untersuchungsmethoden ist zuverlässig genug, die Diagnose iCM zu stellen. Die zweidimensionale (2D) und dreidimensionale (3D) Speckle Tracking Echocardiographie (STE) ermöglichen eine präzise Beurteilung bereits geringer Veränderungen der myokardialen Kontraktilität. Ziel unserer Studie war es, die Zuverlässigkeit und die diagnostische Genauigkeit der 2D und 3D STE bei Patienten mit bioptisch nachgewiesener iCM zu bewerten.

Methodik: 255 Patienten mit Verdacht auf iCM, bei denen Endomyokardbiopsien durchgeführt worden waren, wurden in die Studie eingeschlossen. Bei allen Patienten wurden Echokardiographien durchgeführt und Bilder für Messung von 2D longitudinalen Strains und Strain Rate gespeichert. Bei 57 Patienten wurden 3D Echokardiographiedatensätze aufgenommen und analysiert. Entsprechend der histopathologischen Befunde und der immunohistochemischen Analyse wurden die Patienten in drei Gruppen eingeteilt: keine Myokardinflammation, DCM und iCM.

Ergebnisse: Bei 57 Patienten wurde keine Myokardinflammation nachgewiesen, bei 60 Patienten wurde eine DCM und bei 138 eine iCM nachgewiesen. 2D globaler longitudinaler Strain (GLS) war bei Patienten mit iCM im Vergleich zu Patienten ohne Myokardinflammation signifikant abgeschwächt (-14.50±5.40% vs. -18.39±4.05%, $p<0.001$), selbiges wurde auch für die globale systolische longitudinale Strain Rate (-0.92± 0.32 s^{-1}, vs. -1.11±0.26 s^{-1}, $p<0.001$) und die globale frühdiastolische longitudinale Strain Rate nachgewiesen (1.16±0.45 s^{-1} vs. 1.53±0.41 s^{-1}, $p<0.001$). 3D GLS war signifikant vermindert bei Patienten mit iCM verglichen mit Patienten ohne Myokardinflammation (-12.73±4.58% vs. -17.88±4.34%, $p=0.003$). Der globale area Strain (GAS), der globale zirkumferenzielle Strain (GCS) und der globale radiale Strain (GRS) waren auch bei Patienten mit iCM signifikant reduziert im Vergleich zu Patienten ohne Myokardinflammation (-22.09±7.46% vs. -30.01±6.12%, $p=0.003$; -13.22±4.53 % vs. -17.39±3.84%, $p=0.013$ bzw. 32.89±14.14% vs. 49.18±14.01%, $p=0.002$).

Die STE Parameter schienen für den Nachweis einer iCM hochprädiktiv zu sein. Der 3D GRS zeigte die höchsten prädiktiven Vorhersagewerte (Fläche unter der Receiver-Operating-Characteristic Kurve von 0.793), gefolgt von 3D GLS, GAS und GCS (Fläche unter der Receiver-Operating-Characteristic Kurve von 0.790; 0.773 bzw. 0.773).

Wir fanden starke und signifikante Korrelationen zwischen den 2D und 3D STE Indizes und der linksventrikulären (LV) Ejektionsfraktion, LV-Dimensionen und Volumen, maximale LV-Ausflusstraktgeschwindigkeit und Gewebe Doppler Parametern.

Schlussfolgerung: Unsere Ergebnisse zeigen, dass 2D und 3D STE Indizes das Potential haben, die frühe Vorhersage einer Myokardinflammation zu erleichtern und könnten als zusätzliche nicht-invasive diagnostische Untersuchungen dienen.

Abstract

Introduction: Inflammatory cardiomyopathy (iCM) is a major cause of dilated cardiomyopathy (DCM) and leading cause for heart transplantation. None of the routine noninvasive methods is reliable enough in establishing the diagnosis of iCM. Two-dimensional (2D) and three-dimensional (3D) speckle tracking echocardiography (STE) enable an accurate assessment of minor segmental alterations on myocardial contractility. The aim of our study was to assess the reliability and diagnostic accuracy of 2D and 3D STE in patients with endomyocardial biopsy-proven iCM.

Methods: Two hundred fifty-five patients with suspected iCM on whom endomyocardial biopsies had been performed were included in study. All of them underwent echocardiographic investigations and images of 2D longitudinal strain and strain rate measurements were recorded. In 57 patients 3D echocardiographic datasets were obtained and analyzed. According to the results of the histopathological and immunohistochemical analysis, the patients were classified into three groups: no myocardial inflammation, DCM and iCM.

Results: In 57 patients, no myocardial inflammation was detected, 60 patients were with DCM and 138 patients had iCM. 2D global longitudinal strain (GLS) was significantly attenuated in patients with iCM compared to the patients without myocardial inflammation (-14.50±5.40% vs. -18.39±4.05%, $p<0.001$), the same was observed for global systolic longitudinal strain rate (-0.92± 0.32 s^{-1}, vs. -1.11±0.26 s^{-1}, $p<0.001$) and global early diastolic longitudinal strain rate (1.16±0.45 s^{-1} vs. 1.53±0.41 s^{-1}, $p<0.001$). 3D GLS was significantly reduced in iCM patients compared to those without myocardial inflammation (-12.73±4.58% vs. -17.88±4.34%, $p=0.003$), global area strain (GAS), global circumferential strain (GCS) and global radial strain (GRS) were also significantly attenuated in patients with iCM compared to patients without myocardial inflammation (-22.09± 7.46 % vs. -30.01±6.12 %, $p=0.003$; -13.22±4.53 % vs. -17.39±3.84%, $p=0.013$; and 32.89±14.14% vs. 49.18±14.01%, $p=0.002$, respectively).

STE parameters appeared highly predictive for detection of iCM. The 3D GRS showed the highest predictive values (area under the receiver operating curve of 0.793), followed by 3D GLS, GAS and GCS (area under the receiver operating curve of 0.790; 0.773 and 0.773, respectively).

We found strong and significant correlations between 2D and 3D STE indexes and left ventricular (LV) ejection fraction, LV dimensions and volumes, maximal LV outflow tract velocity and tissue Doppler parameters.

Conclusion: Our results showed that 2D and 3D STE indexes have the potential to facilitate early prediction of myocardial inflammation and could serve as useful noninvasive diagnostic tools.

1. Introduction

1.1. Inflammatory cardiomyopathy

1.1.1. Preamble

Based on the definition of the World Health Organization (WHO), myocarditis is an inflammatory disease of the heart muscle caused by viral, bacterial or fungal infection, systemic diseases, autoimmune dysregulation, drugs or toxins and diagnosed by established histological, immunological, and immunohistochemical criteria.[1] Inflammatory cardiomyopathy (iCM) is myocarditis in association with cardiac dysfunction.[1] The diagnosis of iCM can only be achieved by analysis of endomyocardial biopsy (EMB), since none of the non-invasive methods is reliable enough. Histological or immunohistological evidence of an inflammatory cell infiltrate with or without myocyte damage, with or without viral persistence in the myocardium, is the gold standard for the diagnosis of myocarditis and iCM.[2] The actual incidence of iCM is unknown, as EMB, the diagnostic gold standard, is used infrequently.[3] From a clinical point of view, it has heterogeneous clinical presentations ranging from subclinical paucisyptomatic forms to life-threatening arrhythmias, cardiogenic shock, and sudden death.[4] In patients presenting with mild symptoms and minimal ventricular dysfunction, myocarditis often resolves spontaneously without specific treatment.[3] Myocarditis can result in dilated cardiomyopathy (DCM) with progression to heart failure (HF) in up to 30% of cases, where prognosis is poor, with a survival rate less than 40% after 10 years.[5] Myocarditis is the major cause of sudden unexpected death in patients <40 years of age and may account for up to 20% of mortality from cardiovascular causes.[6] The treatment of many forms of myocarditis is symptomatic, but immunohistochemical and molecular biological analysis of EMB as well as autoantibody serum testing is important to identify those patients in whom specific therapy is appropriate.[3] Prognosis in myocarditis patients varies according to the underlying aetiology, clinical presentation and disease stage.[3]

1.1.2. Definition and classification

According to the Dallas criteria implemented in 1986, myocarditis is defined as an "inflammatory infiltrate of the myocardium with necrosis and/or degeneration of adjacent myocytes, not typical of ischemic damage associated with coronary artery disease (CAD)".[7]

The 1995 report of the WHO/ International Society and Federation of Cardiology Task Force on the Definition and Classification of Cardiomyopathies gave the following definitions:

- **Myocarditis:** Inflammatory disease of the myocardium diagnosed by established histological, immunological and immunohistochemical criteria.
- **Inflammatory Cardiomyopathy**: Myocarditis in association with systolic and/ or diastolic cardiac dysfunction.
- **Dilated Cardiomyopathy**: DCM is characterized by dilation and impaired contraction of the left or both ventricles that is not explained by abnormal loading conditions or CAD.[1]

Myocarditis can be classified by cause, histology, immunohistology, clinicopathological and clinical criteria.[2]

The histological diagnosis of myocarditis includes different forms, classified according to the type of inflammatory cell infiltrate: lymphocytic, eosinophilic, polymorphic, giant cell myocarditis, and cardiac sarcoidosis. The following criteria for subsets of myocarditis were recommended by the Working Group on Myocardial and Pericardial Diseases from the European Society of Cardiology (ESC):

- **Viral myocarditis:** Histological evidence for myocarditis associated with positive viral polymerase chain reaction (PCR).
- **Autoimmune myocarditis:** Histological evidence for myocarditis with negative viral PCR, with or without serum cardiac autoantibodies.
- **Viral and immune myocarditis:** Histological evidence for myocarditis with positive viral PCR and positive cardiac autoantibodies.

A follow-up EMB may reveal persistent viral myocarditis, histological and virological resolution, or persistent virus-negative myocarditis, with or without serum cardiac autoantibodies, e.g. post-infectious autoimmune disease.[3]

1.1.3. Epidemiology

Due to the variable clinical manifestation, the unsatisfactory sensitivity and specificity of the non-invasive diagnostic tools and the infrequent usage of EMB, the exact incidence of myocarditis remains unclear.[8,9]

In a homogeneous population of young military service men, Karjalainen and colleagues reported an incidence of myocarditis of 0.17 per 1.000 man-years[10], but the real numbers are expected to be substantially higher due to the often subclinical presentation of acute myocarditis and misinterpretation of unspecific symptoms.[11] Biopsy-proven myocarditis is found in 9–16% of adult patients with unexplained non-ischaemic DCM.[3] According to autopsy series 1–10% of the general population suffer from undiagnosed myocarditis.[6, 12] In cases of unexplained deaths in young adults aged 35 or younger, the prevalence of myocarditis was highly variable, ranging from 20 to 42%.[5,9]

The disease may affect individuals of all ages; although it is most frequent in the young.[3] Myocarditis has a slightly greater prevalence in men than in women. Recent trials and registries of myocarditis report a female to male ratio between 1:1.5 and 1:1.7.[13]

1.1.4. Etiology

Although the etiology of myocarditis often remains undetermined, a large variety of infectious agents (viruses, bacteria, spirochetes, rickettsia, fungi, protozoa, helminthes, etc.) and non-infectious causes (systemic diseases, autoimmune diseases, drugs, and toxins) have been associated with the development of the disease.[3, 14] The spectrum of the infectious agents varies with the geographical region, the age of the patient, application of different therapeutic procedures and the presence of concomitant diseases.[5] Viral infection is the most common cause in Western Europe and North America, with adenovirus and enterovirus (including coxsackievirus) historically being the most frequently identified viruses. Recently, the most commonly detected viral genomes in EMB samples were parvovirus B19 (PVB19) and human herpesvirus-6 (HHV6).[15] Other viruses associated with myocarditis less frequently include cytomegalovirus (CMV) and Epstein-Barr virus (EBV), hepatitis C virus. Coinfection with two more viruses has been found in more than 25% of

myocarditis patients.[16] Human immunodeficiency virus (HIV) has been associated with myocarditis and DCM.[15]

Lymphocytic and giant cell myocarditis are presumed idiopathic or autoimmune if no viruses are identified in EMB and other known causes are excluded. Autoimmune myocarditis may occur with exclusive cardiac involvement or in the context of autoimmune disorders with extracardiac manifestations, most frequently in sarcoidosis, hypereosinophilic syndrome, scleroderma, and systemic lupus erythematosus.[3]

1.1.5. Clinical presentation

The clinical presentation of iCM is highly variable. It ranges from subclinical disease, chest pain and arrhythmias to fulminant HF or sudden cardiac death. The large spectrum of clinical forms depends on several factors, such as genetic determinants of the infective agent, the genetics, age, gender and immunocompetence of the host.[5] A viral prodrome, including fever, rash, myalgias, arthralgias, fatigue, and respiratory or gastrointestinal symptoms frequently, but not always, precede the onset of myocarditis by several days to a few weeks. Patients may present with chest pain, dyspnea, fatigue, palpitations, decreased exercise tolerance, or syncope. In all cases of suspected myocarditis, it is mandatory to rule out CAD and other cardiovascular disease, e.g. arterial hypertension (AH), or extracardiac non-inflammatory diseases that could explain the clinical presentation.[3]

Chest pain in acute myocarditis may mimic typical angina and be associated with electrocardiographic changes, including ST-segment elevation.[15] In patients with clinical signs of myocarditis and biopsy-proven PVB19 myocarditis in the absence of significant CAD, coronary vasospasm is one of the main causes of atypical chest pain.[16] Cardiac rhythm disturbances are not uncommon and may include new-onset atrial or ventricular arrhythmias. Disturbances in the conduction system may cause high-grade atrioventricular (AV) block leading to dizziness or syncope. Patients with fulminant myocarditis typically present with severe HF symptoms that may rapidly lead to cardiogenic shock, whereas patients with giant cell myocarditis commonly present with HF symptoms that relentlessly progress to probable early death despite optimal treatment.[15]

1.1.6. Diagnosis

Patients with suspected myocarditis should undergo a complete cardiological work-up, including standard cardiological examination, electrocardiogram (ECG), blood analyses with standard cardiac enzymes, and serum tests for anti-heart auto-antibodies, imaging techniques-echocardiogram and especially cardiac magnetic resonance (CMR) imaging, and EMBs for histological, molecular and immunohistochemical analysis.[9] Patients who meet the diagnostic criteria for clinically suspected myocarditis proposed by the Working Group on Myocardial and Pericardial Diseases from the ESC should undergo CMR and EMB, or should be referred to tertiary centers where these diagnostic procedures could be performed.[3]

1.1.6.1. Electrocardiogram

The ECG of a patient with myocarditis can demonstrate a variety of abnormalities, none of which are pathognomonic. The sensitivity of the ECG is low in myocarditis (47%).[9, 17] Generally, patients can exhibit dysrhythmias, conduction system abnormalities, or ST-segment or T-wave changes consistent with ischemia.[12] The most common ECG abnormality in myocarditis is sinus tachycardia with nonspecific ST/T-wave changes.[12, 17] Supraventricular and ventricular dysrhythmias can also be observed. Possible disturbances in the conduction system in myocarditis may include any of the following: sinus arrest, I to III degree AV block, or intraventricular (left or right bundle branch) block.[18] The other primary ECG manifestation of myocarditis is the so-called pseudoinfarction pattern, which can manifest as ST-segment elevation, ST-segment depression, T-wave inversion, poor R-wave progression or Q waves.[17, 19] Some ECG changes are more suggestive of myocarditis than others. For example, ST-T segment elevation in myocarditis is typically concave (rather than convex in myocardial ischemia) and diffuse without reciprocal changes.[3]

1.1.6.2. Laboratory biomarkers

Inflammatory markers

Nonspecific serum markers of inflammation, including erythrocyte sedimentation rate, C-reactive protein (CRP), and leukocyte count, are often elevated, but they do not confirm the diagnosis of acute myocarditis.

Cardiac biomarkers

Cardiac biomarkers of myocardial injury are elevated in minority of patients with myocarditis but, if elevated, may be helpful in confirming the diagnosis.[15] The level of MB fraction of creatine kinase (CK) has a high specificity, but a limited sensitivity for the diagnosis of myocarditis.[20] Cardiac troponins are more sensitive of myocyte injury in patients with clinically suspected myocarditis than CK levels, but they are non-specific and, when normal, do not exclude myocarditis.[3] Cardiac hormones such as brain natriuretic peptides, circulating cytokines, markers related to extracellular matrix degradation, and new biomarkers such as pentraxin, galectin, and growth differentiation factor 15 are sensitive, but non-specific in patients with myocarditis.[3]

Viral antibodies

Serologic studies for detecting infections with cardiotropic viruses are frequently performed in the clinical routine. However, concordance between results of serology and the results of EMB is only present in about 10% of cases. Positive viral serology does not imply myocardial infection, but rather indicates the interaction of the peripheral immune system with an infectious agent.[21] Viral serology is of limited utility in the diagnosis of viral myocarditis, because most viral infections believed to be involved in the pathogenesis of myocarditis are highly prevalent in the general population.[22]

However, positive PCR results obtained with EMB should always be accompanied by a parallel investigation on blood samples collected at the time of the EMB. A sample of peripheral blood from patients with suspected myocarditis allows molecular testing for the same viral genomes as those sought in the myocardial tissue.[23]

1.1.6.3. Echocardiography

In the workup of myocarditis, echocardiography still represents the first-choice imaging modality, since it offers the acquisition of comprehensive anatomic and functional data very quickly at the patient's bedside.[24] However, conventional echocardiography has traditionally played a limited role in the diagnosis of suspected myocarditis due to the lack of specific distinguishing features, low sensitivity and/or apparently normal examination results encountered in less severe forms of myocarditis.[20, 25]

Echocardiography helps to rule out other causes of HF, such as valvular, congenital, or amyloid heart disease, to evaluate and monitor changes in cardiac chamber size, wall thickness, systolic and diastolic functions, the presence of intracavitary thrombi and pericardial effusion. The echocardiographic findings of myocarditis may vary widely, showing marked LV dilation, global ventricular dysfunction with or without pericardial effusion, regional wall motion abnormalities (WMAs), and diastolic dysfunction with preserved ejection fraction (EF). Histologically proven myocarditis may resemble dilated, hypertrophic, and restrictive cardiomyopathy (CM) and can mimic ischaemic heart disease.[3] Diastolic filling patterns are abnormal in most patients, with a restrictive pattern frequently present. Pericardial effusion, typically small, is not uncommon.[15] Echocardiographic features suggestive of myocarditis are often nonspecific, but can be helpful in identifying a fulminant course.[26] Felker et al. developed echocardiographic criteria to help distinguish between fulminant and acute myocarditis. Patients with fulminant myocarditis had normal LV diastolic dimensions, hypocontractile left ventricle and increased septal thickness at presentation, secondary to the greater inflammatory response resulting in interstitial edema and loss of ventricular contractility, while patients with acute myocarditis had increased LV dimensions, normal wall thickness and decreased LV function.[17, 27]

In recent years, new methods, such as tissue Doppler (TD), speckle-tracking echocardiography (STE) and contrast-enhanced echocardiography, have broadened the diagnostic possibilities of echocardiography.[24, 28-37]

However, 2D STE parameters were evaluated in patients with acute myocarditis, but not with iCM, and the diagnosis was established with CMR. We consider that these new echocardiographic techniques should be prospectively studied against EMB in order to confirm their clinical role in patients with iCM and to test the sensitivity and specificity of these methods.

1.1.6.4. Nuclear imaging

Kühl et al. found that antimyosin scintigraphy had a high specificity, but a lower sensitivity for the detection of myocarditis.[38] Due to their limited specificity, radiation burden and the practical difficulties of myocardial scintigraphy, the use of scintigraphic techniques has declined over the past years and they are not routinely recommended for the diagnosis of myocarditis, with the possible exception of sarcoidosis.[3, 24]

1.1.6.5. Cardiovascular magnetic resonance imaging

A recent white paper from the International Consensus Group on Cardiovascular Magnetic Resonance in Myocarditis states that a CMR study should be performed in symptomatic patients with clinical suspicion of myocarditis.[39] Three imaging criteria for confirming the diagnosis of myocarditis (the "Lake Louise Criteria") by CMR have been proposed:

In the setting of clinically suspected myocarditis, CMR findings are consistent with myocardial inflammation, if at least two of the following criteria are present:

1. Regional or global myocardial signal intensity increase in T2-weighted images.
2. Increased global myocardial early gadolinium enhancement ratio between myocardium and skeletal muscle in gadolinium-enhanced T1-weighted images.
3. There is at least one focal lesion with non-ischemic regional distribution in inversion recovery-prepared gadolinium-enhanced T1-weighted images ("late gadolinium enhancement").[39]

When two or more of the three criteria are positive, myocardial inflammation can be predicted with a sensitivity of 67%, specificity of 91% and diagnostic accuracy of 78%; if only late gadolinium enhancement imaging is performed, the diagnostic accuracy drops to 68%.[15, 39]

However, the utility of CMR in the diagnosis of chronic myocarditis and iCM is still limited. Lurz et al. reported that the diagnostic performance of CMR in suspected chronic myocarditis was unsatisfactory (sensitivity, 63%; specificity, 40%; and accuracy, 52%).[40] Furthermore, CMR has been found not to be accurate in patients with low-level or no inflammation.[35, 40, 41] CMR does not replace EMB in the diagnosis of myocarditis and should not delay EMB in life-threatening presentations.[3]

1.1.6.6. Endomyocardial biopsy

In patients fulfilling the diagnostic criteria for clinically suspected myocarditis, the Working Group on Myocardial and Pericardial Diseases of the ESC recommends selective coronary angiography and EMB. This recommendation also applies to patients with an acute coronary syndrome-like presentation (with or without ST segment elevation), increased cardiac troponins, preserved ventricular systolic function with or without features suggestive of myocarditis on CMR.[3]

EMBs can be obtained from the right ventricle, via the venous route through jugular, subclavian, or femoral veins, or from the left ventricle with transseptal puncture or by direct access through a peripheral artery, usually the femoral or brachial artery.

According to the recent Consensus statement on EMB from the Association for European Cardiovascular Pathology and the Society for Cardiovascular Pathology, multiple biopsy specimens from different sites should be taken in order to reduce the false-negative results.[8]

Histopathological diagnosis

Histopathological assessment is not only the gold standard for the diagnosis of myocarditis, but remains essential for the classification of myocarditis based upon histological criteria.[23]

Immunohistopathological diagnosis

Cardiac inflammation could be immunohistologically characterized by different markers of cell activation and enhanced expression of histocompatibility antigens and adhesion molecules (AMs). The sensitivity and specificity of monoclonal antibodies, directed against specific epitopes of immunocompetent cells, allow the identification, characterization and quantification of inflammatory cells infiltrating myocardial tissues.[11]

Molecular diagnosis

The molecular biological diagnosis of viral genomes comprises PCR for the qualitative evaluation, quantitative PCR for the determination of viral loads, and sequencing for the analysis of viral genotypes.[42] The development of molecular biological techniques, particularly amplification methods like PCR or nested-PCR, allows the detection of low copy viral genomes even from an extremely small amount of tissue such as in EMB specimens.

The main viruses to be considered when performing molecular pathology studies in the myocardium of patients with a suspicion of myocarditis are adenovirus, enteroviruses, CMV, EBV, hepatitis C virus, herpes simplex virus 1 and 2, HHV6, influenza viruses A and B, PVB19, and rhinovirus.

On the basis of recent study of Bock et al., it was suggested that PVB19 load of more than 500 genome equivalents (ge) per microgram of isolated nucleic acids of in EMB specimens is a clinically relevant threshold for the maintenance of myocardial inflammation.[23, 43]

Complications of EMB

Major complications of EMB included pericardial tamponade with need for pericardiocentesis, hemo- and pneumopericardium, permanent AV block requiring permanent pacemaker implantation, arteriovenous fistula, myocardial infarction, transient cerebral ischemic attack and stroke, infection, pneumothorax, pulmonary embolism during RV biopsy or systemic embolism during LV biopsy, severe valvular damage, and death. Minor complications included: hematoma, transient chest pain, transient ECG abnormalities, transient arrhythmias, transient hypotension, vasovagal reaction, and small pericardial effusions. The rate of major complication ranged from 0.12% to 0.84% in experienced centers, minor complication rate varied between 0.64% and 5.10%.[8, 44]

1.1.7. Prognosis

Outcome and prognosis of myocarditis depends on etiology, clinical presentation, and disease stage.[3,9 – 11] Acute myocarditis resolves in about 50% of cases in the first 2–4 weeks, but about 25% of the patients will develop persistent cardiac dysfunction with progressive impairment of LV function, another 12–25% may acutely deteriorate and either die or progress to end-stage DCM with a need for heart transplantation.[3] The progressive impairment of the LV function is often linked to chronic inflammation and viral persistence due to an inadequate immune response after AMC.[45] The persistence of enterovirus, adenovirus, PVB19, and HHV6 in the myocardium of patients with LV dysfunction was associated with a progressive impairment of left ventricular ejection fraction (LVEF), whereas spontaneous viral elimination was associated with a significant improvement in LV function.[46]

Patients with fulminant myocarditis who survive the acute phase have an excellent long-term prognosis compared with patients with acute myocarditis. The survival rates in giant-cell myocarditis in children and adults are markedly worse with a median survival of less than 6 months. These patients usually require cardiac transplantation. [3,15]

1.2. Speckle tracking echocardiography

1.2.1. Preamble

Speckle tracking echocardiography (STE) is a novel method, which can be applied to quantitatively characterize myocardial deformation in longitudinal, radial and circumferential directions. STE is especially suited for the assessment of global and regional systolic function in patients with apparently normal EF.

STE has several advantages compared to other modalities which are used for the diagnosis of iCM. STE is much more available, cost efficient, can be used "bedside", and has a shorter procedure and post-processing time in contrast to MRI. It is non-invasive and does not bear any risk for the patient in comparison with EMB.

There are only few reports about the diagnostic and prognostic importance of 2D STE in patients with myocarditis.[25, 32- 37]. No biopsy-controlled studies, in which the 3D STE is compared to immunohistological criteria of myocarditis, have been published to date.

Area tracking, expressed as global area strain (GAS) is a novel parameter, which is quantified by the percentage of deformation in the LV endocardial surface area using 3D STE. It is a parameter integrating longitudinal and circumferential deformation, therefore, it might decrease the tracking error and emphasize synergistically the magnitude of deformation and could provide a more global and comprehensive evaluation of LV systolic function.

1.2.2. Definitions

STE is a promising new, largely angle-independent imaging modality used for the evaluation of myocardial function. It is an offline technique that is applied to previously acquired 2D or 3D images and permits offline calculation of myocardial velocities and deformation parameters. It provides a quantitative regional and global LV assessment and is an independent supplement to wall motion analysis for evaluating LV mechanics.[47, 48]

STE has been validated for the assessment of myocardial deformation against sonomicrometry[49], tagged magnetic resonance imaging (MRI)[50, 51] and clinically against tissue Doppler imaging (TDI).[11, 49]

Strain describes the fractional change in the length of a myocardial segment. It quantitatively characterizes myocardial deformation in longitudinal, radial and circumferential directions. Strain is unitless and is expressed as a percentage. Strain can have positive or negative values, which reflect lengthening or shortening, respectively. In its simplest one-dimensional manifestation, a 10-cm string stretched to 12 cm would have 20% positive strain.[49] The so-called Langrangian strain (e) is mathematically defined as the change of myocardial fibre length during stress at end-systole compared to its original length in a relaxed state at end-diastole (figure 1).[48] Applied to a single segment of the heart, systolic strain is simply the standardized change in length in a segment. The change in length is standardized, or divided, by the end-diastolic length:

Strain = ((end-systolic length − end-diastolic length)/end-diastolic length) × 100.[52]

Strain rate is the rate of change in strain and is expressed as 1/sec or sec^{-1}.[49] It could also be defined as the speed at which deformation (i.e. strain) occurs. Mathematically, it is calculated as the change in velocity between 2 points divided by the distance between the 2 points with a unit s^{-1}. When acquired at the LV apex, normal ventricular myocardium has a negative SR in systole and a positive SR during diastole.[53] As a spatial derivative of velocity, SR provides increased spatial resolution for precise localization of diseased segments.[50]

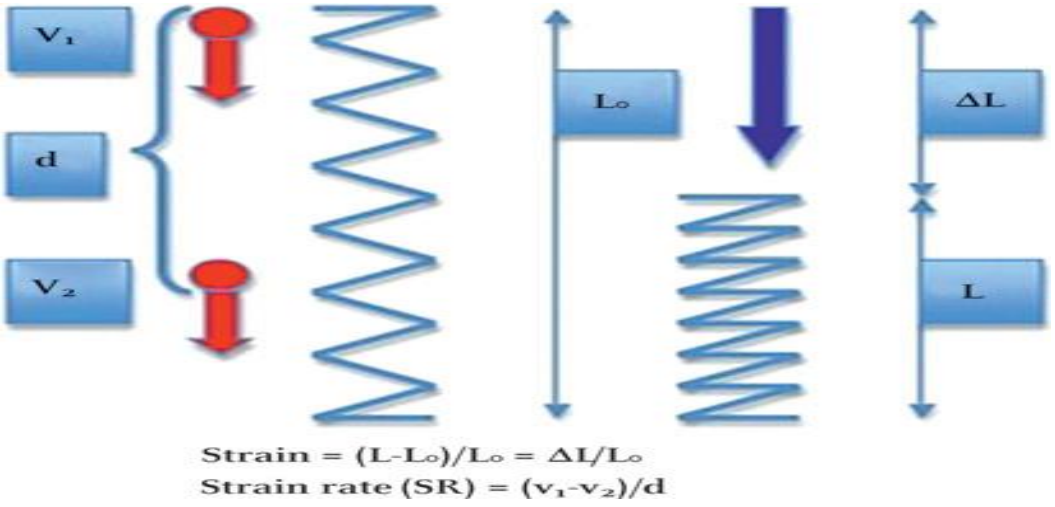

Figure 1. Elastic deformation properties. Strain=change of fibre length compared to original length, strain rate=difference of tissue velocities at two distinctive points relative to their distance. ΔL indicates change of length; L_o – unstressed original length; L – length at the end of contraction; blue arrow – direction of contraction; V1 – velocity point 1; V2 – velocity point 2; d – distance (modified after Blessberger, 2010).

Strain and SR can be obtained from either TD or STE. Because Doppler is velocity or distance divided by time, the initial measurement is strain rate. Integrating the strain rate gives strain.[47] The other way of recording strain uses the principle of speckle tracking. Since 2D echo is distance, the initial measurement is strain. The derivative of strain will give the strain rate.[47]

1.2.3. 3D speckle tracking echocardiography

3D STE was developed as a new application that can be used for regional wall motion analysis of the entire left ventricle and allows us to obtain real 3D indices and to assess 3D wall motion precisely.[54] 3D STE combines the measurement of all three strains (longitudinal, circumferential, and radial) as it tracks speckles in three dimensions. With this new technique, different components of myocardial deformation could be measured in one cardiac cycle, which should overcome the limitations of TDI and 2D STE.[55] 3D strain is clearly superior to other kinds of strain, as it is independent of geometric assumptions.[52]

1.2.4. Types of myocardial strains and strain rates

"Segmental strain" is the strain value for each myocardial wall segment, "territorial strain" is the strain for each of the theoretical vascular distribution areas.[49] Peak strain, peak systolic strain and SR are the more commonly used parameters. Peak strain is the maximum strain, which may occur during LV ejection (defined as the interval between aortic valve opening and closure) or after, whereas the peak systolic strain is the maximum strain that occurs during the LV ejection period only. End systolic strain (strain at the time of aortic valve closure), post-systolic thickening, and the post-systolic index (ratio of post-systolic increment to the end systolic strain) have also been used. Furthermore, timing of events can be obtained such as time to peak systolic strain.[53]

Depending on spatial resolution, selective analysis of epicardial, midwall, and endocardial function may be possible as well.[49]

Since contraction is three dimensional and myocardial fibres are oriented differently throughout the myocardial layers, deformation can also be described with respect to the different directional components of myocardial contraction.[48]

Three different components of contraction have been defined: longitudinal, radial and circumferential (figure 2):

- Longitudinal contraction represents motion from the base to the apex. Longitudinal strain is tangential to the endocardial contour and usually has negative values for the left ventricle.[48, 56] It is measured in apical long-axis views to capture the longitudinal movement of the heart. There is a progressive increase in longitudinal strain from base to apex.[52, 54]
- Radial contraction in the short axis is perpendicular to both long axis and epicardium. Thus, radial strain represents myocardial thickening and thinning. Normal radial strain is positive in ventricular systole and negative in ventricular diastole.[48, 56] It is estimated by measuring the radial change in length between endocardium and epicardium in short-axis views. Radial strain is analogous to percentage thickening in traditional regional wall motion analysis.[48] It decreases from subendocardium to subepicardium.[52]
- Circumferential contraction is defined as the change of the radius in the short axis, perpendicular to the radial and long axes. Circumferential strain is strain which is circumferential to the endocardial contour.[48, 56] It is measured in short-axis views by measuring the change in length along the circumference of myocardium. Normally it also increases from base to apex.[52, 54]

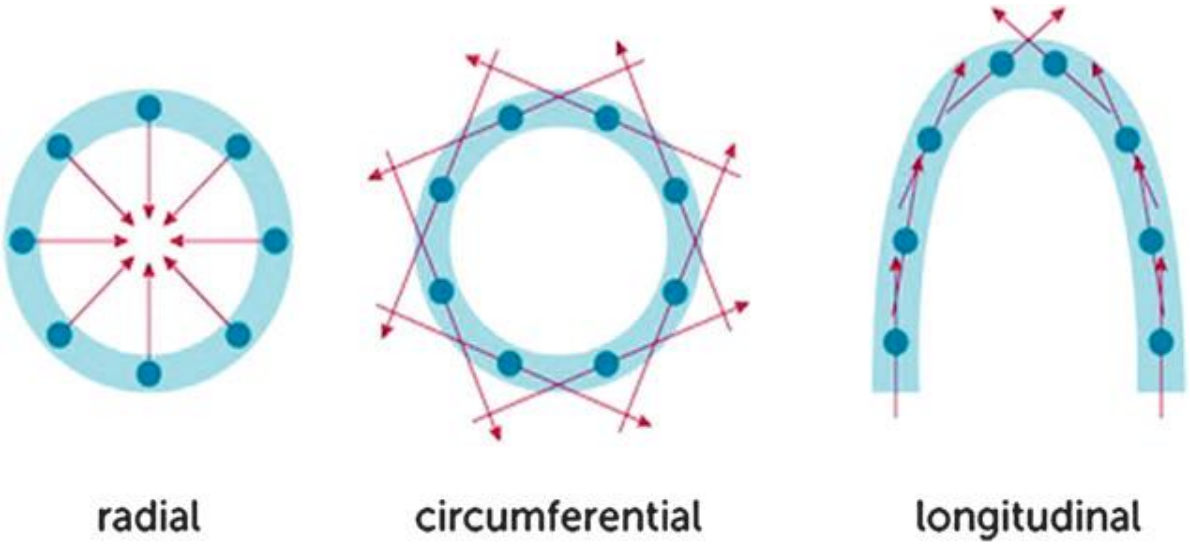

Figure 2. Longitudinal, circumferential and radial LV myocardial wall strains (modified after Blessberger, 2010).

The term "global longitudinal strain (GLS)", "global circumferential strain (GCS)" or "global radial strain (GRS)" refers to the average longitudinal, circumferential or radial component of strain in the entire myocardium, which can be approximated by the averaged segmental strain components in individual myocardial wall segments.

The general state of strain at a point in a body is composed of 3 components of normal strain (e_x, e_y, and e_z), and 3 components of shear strain (e_{xy}, e_{xz}, and e_{yz}). Therefore, for the left ventricle, 3 normal strains (longitudinal, circumferential, and radial) and 3 shear strains (circumferential-longitudinal, circumferential-radial, and longitudinal-radial) are used to describe LV deformation in 3 dimensions.[50]

The degree of shearing increases toward the subendocardium, therefore, higher velocities and strains are recorded at the subendocardium resulting in a subepicardial-to-subendocardial thickening strain gradient. Subendocardial strains are higher in magnitude than subepicardial strains.[50]

1.2.5. STE indexes – normal ranges

It is quite difficult to define normal values of STE-derived strain and strain rate, since several factors influenced the values obtained. Normal deformation values vary among publications and importantly depend on the brand of imaging equipment, which does not use the same algorithms to process measured data across vendors.[49] There is little information regarding the equivalency of the normal range of LV 2D strain comparing ultrasound systems from different vendors. Clear cut-offs for peak systolic strain to define pathologic conditions are still missing.[48] Until standardization is achieved, echocardiography labs should identify lab-specific normal values with each vendor analysis package and use the same software in serial studies.[57]

In the different studies performed in healthy individuals, the GLS values varied between -15.9% and -23.8%[48, 54, 58, 59] , peak systolic SR -1.1±0.01 s^{-1}, peak early diastolic SR 1.55±0.01 s^{-1} and peak late diastolic SR 1.02±0.01 s^{-1}.[48]

3D STE-derived LV deformation parameters are highly vendor-dependent.[51,60] The following 3D strain ranges in healthy subjects were obtained in the several studies performed: for GAS from -31%[61] to -43,1%[62], for GLS from -15.5% to -21%[54, 61], for GCS from -17%[61] to -31.6%[54] and for 3D GRS from 33.7% to 59%.[54, 58]

1.2.6. Factors affecting STE imaging parameters

A variety of parameters might potentially influence the measurement of strain and strain rate, including features specific to patients (age, gender, race, ethnicity, anthropometric variables), hemodynamic factors (heart rate, blood pressure), and cardiac factors (LV size, wall thickness).[58, 63] Speckle-tracking echocardiographic measurements are dependent on image quality[64, 65] and on excellent endocardial border detection.[65] All TD-derived data on wall motion and deformation are angle-dependent.[66] As described by a cosine function, the greater the insonation angle, the lower the detected Doppler shift and the lower the measured velocity.[53] The advantage of 2D speckle tracking-derived strain is that it tracks in two dimensions, along the direction of the wall, not along the ultrasound beam, and thus is angle-independent. This allows angle independent quantification of LV strain/ strain rate along all three orthogonal axes (circumferential, radial and longitudinal) that are obtainable only in limited LV segments by TDI. Furthermore, due to the automatic frame-by-frame tracking of the myocardium, translational movement due to respiration and tethering from adjacent myocardium would not affect the 2D speckle tracking measurements. According to some authors, both strain and displacement showed no significant age-related changes[53], however, other authors reported that velocities and deformation parameters, including strain were affected by age.[49] Loading conditions and heart rate need to be taken into account when interpreting all functional data.[49] Compared with strain rate, strain is more loading condition-dependent, increasing with increased preload and decreasing with increased afterload.[53]

In a meta-analysis, Yingchoncharoen found that systolic blood pressure is an important determinant of strain.[58] Another study found that female gender[67] is associated with lower GLS.[58]

Significant age dependency was observed for 3D longitudinal strain.[61, 68] Age could also influence 3D strains – it was reported that men had lower 3D longitudinal, area and radial strain than women. LV 3D strain parameters were also influenced by LV volumes and mass, image quality, and temporal resolution.[61]

The presence of some conditions like AH[69], CAD[70], cardiac amyloidosis, valvular heart disease (aortic stenosis[71]; mitral regurgitation[72]) HF, HCM, DCM[73], stress CM[74, 75], restrictive CM[76, 77], type 2 diabetes mellitus (DM)[78], decrease the value of the GLS.[57]

1.2.7. Advantages and disadvantages of STE

1.2.7.1. 2D STE versus TDI

STE has several important advantages compared to TD-derived strain imaging. In comparison to TDI, STE is insonation angle independent and does not require such high frame rates.[48] STE-derived strain, in contrast to TDI, reflects only active contraction, since the STE-derived deformation parameters are not influenced by passive traction of scar tissue by adjacent vital myocardium (tethering effect) or cardiac translation.[48, 79] The TD strain rate sample volume is fixed, while the myocardium is moving. Thus the sample volume may not stay within the myocardium throughout the cardiac cycle.[47] Color Doppler-derived strain and SR are noisy, and as a result, training and experience are needed for proper interpretation and recognition of artifacts.[49] Both TDI and STE measure motion against a fixed external point in space (i.e., the transducer). However, STE has the advantage of being able to measure this motion in any direction within the image plane, whereas TDI is limited to the velocity component toward or away from the probe. This property of STE allows measurement of circumferential and radial components irrespective of the direction of the beam.[49]

TD–derived strain variables faced a number of criticisms, not only in relation to angle dependency, noise interference, but also because of substantial intraobserver and interobserver variability.[50] Furthermore, it showed high inter-vendor variability. Therefore, for study purposes, the echocardiographic investigations are performed on one type of ultrasound machine.

Although STE-derived strain is superior to TD strain particularly with regard to noise and angle dependency, the accuracy of speckle tracking is dependent on 2D image quality and frame rates. Low frame rates result in unstable speckle patterns, whereas high frame rates reduce scan-line density and reduce image resolution.[50]

STE, however, is not completely angle independent, because ultrasound images normally have better resolution along the ultrasound beam compared with the perpendicular direction. Therefore, in principle, speckle tracking works better for measurements of motion and deformation in the direction along the ultrasound beam than in other directions. Because speckle tracking relies on sufficiently high temporal resolution, TDI may prove advantageous when evaluating patients with higher heart rates (e.g., during stress echocardiography) or if short-lived events need to be tracked (isovolumic phases, diastole, etc.).[49]

Speckle tracking strain results correlate significantly with TD–derived measurements. In comparison with TDI, ROC curve analysis has shown that longitudinal and radial strain measured using STE has a significantly greater area under the curve (AUC) than TDI strain in differentiating normal and dysfunctional segments.[50]

Overall, STE proved to be highly robust and reproducible.[80] Intra- as well as inter-observer variability in 2D STE between skilled echo examiners was negligible.[80] However, some studies have suggested underestimation of longitudinal strain with STE.[50]

1.2.7.2. Limitations of 2D STE

Similar to other 2D imaging techniques, 2D STE relies on good image quality. 2D STE is sensitive to acoustic shadowing or reverberations, which can result in underestimation of the true deformation.[49] The accurate estimation of strain is limited by frame rate and heart rate. With variable heart rates, the bulls-eye recording may not be generated.[47] Another limitation of STE is its poor inter-vendor agreement. [49] It is unclear how values from different scanners and software versions could be compared.[48] Suboptimal tracking of the endocardial border is one of the major limitations of 2D STE. In addition, assessment of strain and SR also requires definition of the epicardial borders. In most software versions, a uniform thickness of the myocardium is assumed - an assumption which is not true.[48] Global strain might be inaccurate if too many segmental strain values are discarded because of suboptimal tracking. This is particularly true in localized myocardial diseases, where strain values are unevenly distributed. A further limitation, encountered in large ventricles, is that it is often difficult to image the entire myocardium, especially the apical segments.[48] Ventricular remodelling and wall thinning of myocardial segments may affect the accuracy of strain measurements.[50]

1.2.7.3. 2D versus 3D STE

Although 2D STE is a useful technique, it has the intrinsic limitations of 2D imaging, such as the use of foreshortened views that affect the accuracy of the quantification of individual components of myocardial motion. In addition, the assumption that speckles remain within the 2D imaging plane and can be adequately tracked throughout the cardiac cycle may not always be valid,

because of the complex 3D motion of the heart chambers. The inability of 2D STE to measure one of the three components of the local displacement vector is an important limitation, which affects the accuracy of the derived indices of local dynamics. This shortcoming could be overcome by the use of 3D STE.[48]

3D STE is a promising tool for an objective, accurate, comprehensive and reproducible quantification of regional and global LV function. Technical developments in 3D speckle tracking with superior temporal and spatial resolution could theoretically circumvent the limitations of out-of-plane motion inherent in 2D imaging. Another advantage of 3D STE is the evaluation of the motion of all myocardial segments in a single analysis step, which significantly reduces analysis time.[50]

With the addition of the third component of motion vector, which is "invisible" to TDI or 2D STE, 3D STE promises to allow accurate assessment of regional ventricular dynamics. Nevertheless, it still requires rigorous validation and testing. The major pitfall of 3D STE is its dependency on good apical acoustic window, image quality and a regular cardiac rhythm. Random noise and relatively low temporal and spatial resolution affect its ability to define the endocardial and epicardial boundaries. These issues likely affect the frame-to-frame correlation of local image features and contribute to suboptimal myocardial tracking.[49]

Another limitation of 3D STE is the lack of a truely non-invasive "gold standard" technique that can be used in humans to validate regional ventricular function in three dimensions. As a result, most of the literature on this topic represents feasibility studies and potential advantages of 3D STE, but does not establish the accuracy of the method. The clinical value of this new technology in a wide variety of clinical scenarios such as chamber volume measurements, evaluation of global and regional WMAs, and others remains to be determined in future studies. Extensive clinical research to test the accuracy and prognostic value of 3D strain against reference standard is needed. [49]

2. Aim

The aim of our study was to perform myocardial deformation analysis using both 2D and 3D speckle tracking imaging in patients with suspected iCM in order to test the utility, reliability and diagnostic accuracy of these STE parameters. We aimed to:

1) search for STE parameters with a sufficient sensitivity and specificity to allow reliable recognition of myocardial inflammation and could help us in the selection of patients, who would need further invasive diagnostic work-up;
2) test the relation between 2D and 3D STE parameters and the myocardial inflammation as defined by immunohistology;
3) compare and search for correlations between 2D and 3D STE parameters and conventional echocardiographic parameters in order to evaluate the usefulness of deformation analysis in patients with iCM.

3. Materials and methods

3.1. Patient population

Three hundred and fifteen patients admitted to our department in the period from July 2012 to July 2013 with a clinical diagnosis of suspected iCM in whom endomyocardial biopsies (EMBs) were taken were screened. The clinical diagnosis of suspected iCM was based on the following criteria: 1. history of a former myocarditis; 2. one of the following clinical symptoms: fatigue, dyspnea, peripheral edema, chest pain, viral prodrome, presyncope, syncope, palpitations; 3. presence of ST/T wave abnormalities and/or increased TnT/TnI levels, and/or elevated inflammation markers (CRP); 4. echocardiographic data for diastolic and/ or systolic cardiac dysfunction. Patients with severe heart valve disease, severe AH, HCM, cardiac amyloidosis or sarcoidosis, significant CAD and lung disease, severe metabolic and endocrine diseases (DM) were excluded from the study based on echocardiography, laboratory values, angiography, chest X-ray and EMB results. EMB was performed within the first three days after the patient had been admitted to our department. Echocardiographic examinations were performed 1 to 24 hours prior to EMB. Antihypertensive and/or antidiabetic medical treatment was not stopped. All patients gave written informed consents for invasive diagnostic procedures.

A total of 255 patients fulfilled the above-mentioned criteria and were included in the study.

3.2. Echocardiography

3.2.1. Conventional echocardiography

One to 24 hours before performing EMB, transthoracic echocardiography was performed using GE VingMed Vivid 7 or VIVID E9 ultrasound machine (Horten, Norway). LVEF was measured from 2D apical images according to the Simpson's method. Measurements of chamber dimensions, including LV end-diastolic and end-systolic diameters, septal and posterior wall (PW) thicknesses, left and right atrial size were performed. Regional wall motion analysis was carried out. In the parasternal long-axis view, the thickness of the interventricular septum (IVS) and the LV PW thickness were measured at end-diastole, while LV diameters were measured at both end-diastole

and end-systole. For the assessment of diastolic function, the early (E) and late (A) diastolic peak velocities of mitral inflow were recorded and measured using pulsed-wave Doppler in apical 4-chamber view. The E/A ratio was calculated. TDI of the mitral annulus movements was obtained from the apical 4-chamber view. A 1.5 mm sample volume was placed sequentially at the lateral and the septal sites. Analysis was performed by pulsed wave Doppler for early diastolic septal (E'sep), early diastolic lateral (E'lat) peak tissue velocities, late diastolic septal (A'sep) and late diastolic lateral (A'lat) peak tissue velocities. The LV filling indices (E/E') for septal and lateral sites, calculated by the ratio of transmitral flow velocity to annular velocity, were determined.

3.2.2. 2D speckle tracking echocardiography

For myocardial deformation analysis, 2D grey scale cine-loop clips were selected from three apical views (4-, 2- and 3-chamber views) obtained by VIVID 7 or VIVID 9 ultrasound system (GE Vingmed, Horten, Norway) using a 2.5 MHz transducer probe. A sector scan angle of 30^{o} to 60^{o} was chosen, and frame rates of 50 to 70 Hz were used. Electrocardiograms were recorded simultaneously during the examinations. Data were stored and then transferred to a workstation for offline analysis. Post-acquisition 2D speckle-tracking analysis was performed using the software for echocardiographic quantification at the EchoPAC PC Workstation (GE Vingmed Ultrasound AS, Horten, Norway). Endomyocardial borders of the left ventricle were manually traced at the end-systolic frame. Six to 10 points were placed, starting from the mitral annulus. Epicardial tracing was automatically performed by the computer algorithm and, when necessary, manually adjusted to cover the whole myocardial wall. Along the cardiac cycle, visual assessment and adjustment of the tracing was performed until optimal tracking was obtained. The left ventricle was automatically divided into six equally distributed segments (septal, lateral, anterior, inferior, anteroseptal and posterior) and each segment was subdivided into three segments (basal, medial and apical). The basal, middle and apical segments of the septal and lateral walls were analyzed in 4-chamber view, the anterior and inferior walls in 2-chamber view, and the posterior and anteroseptal walls in 3-chamber view. GLS, GLSR, global longitudinal early diastolic strain rate (GLESR), and global longitudinal late diastolic strain rate (GLASR) were determined by averaging all 18 wall segments analyzed from the 3 apical views. All the echocardiographic investigations were performed prior to obtaining the results from EMB analyses.

3.2.3. 3D speckle tracking echocardiography

In 57 patients, full-volume 3D datasets were obtained with a commercially available ultrasound system Vivid 9 (GE Vingmed; Horten, Norway) with a 3.5-MHz matrix array transducer. Electrocardiograms were recorded simultaneously during the examinations. Optimal transducer position and angle were adjusted using the 3-plane imaging mode. A 3D dataset was obtained by scanning multiple sectors from the cardiac apex, which were integrated into a wide-angle pyramidal data image covering the entire left ventricle. It has been already established that low frame rate results in higher speckle decorrelation between subsequent frames, whereas too high frame rate results in a loss of spatial resolution and an associated coarser speckle pattern[81], therefore, images were acquired at a frame rate of 20 to 40 Hz. The 3D datasets were displayed as conventional apical and short-axis views on a single screen. When optimal endocardium delineation was achieved, the patient was asked to hold the breath as long as possible in order to record the best imaging planes in which all regions of interest of the LV walls could be well visualized. A full-volume electrocardiography-gated data set through 4 to 6 cardiac cycles was sampled during apnea. Care was taken to optimize the temporal and spatial resolution of images by decreasing depth and sector width as much as possible while retaining the entire left ventricle within the pyramidal volume. Data were stored digitally and analyzed offline using EchoPAC Clinical Workstation software. Two orientation points were designated to the mitral valve level and the LV apex in end-diastole and end-systole. Endocardial contours, myocardial thickness and epicardial borders were detected automatically and adjusted manually if necessary. The motion of the 3D myocardium was tracked throughout the cardiac cycle and deformation parameters were calculated for each segment. Tracking was proved visually and, if not accurate, repeated after manual adjustment. The system automatically performed segmental strain analysis through an entire cardiac cycle and provided continuous values of global and segmental strain, including 3D global longitudinal strain (GLS), 3D global circumferential strain (GCS), 3D global area strain (GAS), and 3D global radial strain (GRS), for all 17 segments simultaneously. End-systolic and end-diastolic LV volume, mass, and sphericity index were generated automatically. LVEF was calculated from end-diastolic and end-systolic estimates of these virtual LV-cavity casts. Completing the analysis, a 17 segments bulls-eye with global results was displayed.

3.3. Endomyocardial biopsy

All patients underwent heart catheterization for evaluation of their coronary status. After angiographic exclusion of CAD and other possible causes of LV dysfunction, EMBs were taken from the left and/ or right ventricle using a flexible bioptome (Westmed, St Ingbert, Germany) via femoral vein approach.[82] At least 6 biopsy samples were collected from 2 to 3 different sites of the ventricle. Three endomyocardial fragments were immediately fixed in 10% buffered formalin at room temperature for light microscopic examination. Additional tissues pieces were immediately snap-frozen in liquid nitrogen and stored at -80^{0}C until processing. Specimens were cut serially into cryosections of 5 μm thickness and placed in 10% poly-L-lysine-precoated slides, which were subsequently analyzed in a blinded fashion. A sample of peripheral blood in EDTA was also collected.

3.3.1 Histopathological assessment of the endomyocardial biopsies

The histological sections were paraffin-embedded and haematoxylin-eosin- stained and examined according to the Dallas criteria. They were analysed by light microscopy for evidence of myocardial necrosis and presence of fibrosis.[83] The distribution, type and extent of fibrosis were described.

3.3.2. Immunohistochemical analysis

Inflammatory infiltrates and cell adhesion molecules (CAMs) were characterized by immunohistochemistry. Immunohistological staining was carried out and the immunoreactivity was quantified by digital image analysis (unit: area fraction) at 200-fold magnification.[84, 85] A large panel of monoclonal and polyclonal antibodies (including anti-CD3, anti-CD8, anti-CD45RO, anti-CD54/ICAM-1, anti-CD68, anti-CD106/VCAM-1, anti-LFA1, anti HLA-I and anti-HLA-DR) was utilized for the identification and characterization of the inflammatory infiltrates and for the detection of HLA upregulation on EMB tissue sections.

3.3.3. Detection of viral genomes in the endomyocardial biopsy specimens

According to the published techniques[46], specimens were subjected to molecular biological investigation of cardiotropic viral genomes, performing nPCR/RT-PCR on RNA extracted from the biopsies for Enteroviruses (Coxsackieviruses and Echoviruses) and on DNA for EBV, PVB19 and HHV6. Analysis of the detected viral genotypes and determination of the viral loads was performed.

3.4. Definition of groups

According to the findings derived from the analysis of the EMB samples, patients were divided into three groups:

1. No inflammation group: infiltrating CD3 lymphocytes<7.0 cells/mm^2 (median cell count), infiltrating CD45RO lymphocytes<14.0 cells/mm^2 (median cell count), and macrophages<35.0 cells/mm^2 (median cell count), absence of myocyte lysis, and preserved LVEF.
2. Dilated cardiomyopathy (DCM) group: infiltrating CD3 lymphocytes<7.0 cells/mm^2 (median cell count), infiltrating CD45RO lymphocytes<14.0 cells/mm^2 (median cell count) and macrophages<35.0 cells/mm^2 (median cell count), absence of myocyte lysis, and reduced LVEF.
3. Inflammatory cardiomyopathy (iCM) group: infiltrating CD3 lymphocytes≥7.0 cells/mm^2 (median cell count), infiltrating CD45RO lymphocytes≥14.0 cells/mm^2 (median cell count) and macrophages≥35.0 cells/mm^2 (median cell count), and/ or presence of myocyte lysis, and/or detection of viral genomes.

3.5. Statistical analysis

The statistical analysis was performed using SPSS for Windows version 15.0. Descriptive statistics were obtained and a value for every parameter studied was achieved. Continuous variables were expressed as mean values ± standard deviation (SD), and categorical variables as the numbers of subjects and percentages. For univariate analysis, a 2-sample t test was used for continuous values, and the chi-square test or the Fisher exact test was used for categorical ones. The normality of distribution was evaluated using the Kolmogorov-Smirnov test. Comparisons between groups were provided using ANOVA if variables were normally distributed, the Mann-Whitney U test was performed if the data were not normally distributed. Correlations between the variables were calculated using the Pearson method. ROC curves analysis was used and an AUC were measured. Cut-off values for 2D and 3D STE parameters with the best sensitivity and specificity were determined. A value of $p<0.05$ was considered statistically significant in all analyses.

4. Results

4.1. Patients' characteristics

The study included 255 subjects with suspected iCM. According to the histological and immunohistological findings from EMB analyses, the study population was divided into three groups: 57 patients (22.4%) showed no myocardial inflammation, 60 patients (23.5%) were with DCM and 138 patients (54.1%) had iCM.

4.1.1. Age and gender

One hundred fifty six of the 255 patients included in study were men (61.2%), the rest 99 (38.8%) were women. The sex distribution of the patients included in the study is presented in table 1. The men in the DCM group and in the iCM group were proportionally more than the women compared to the no inflammation group (table 1). The mean age of all patients included in the study was 49 ± 13 years (range from 18 to 79). The mean age of the women was 51 ± 14 years and the mean age of the men was 49 ± 13 years. The mean age in the no inflammation group was 47 ± 14 years, in the DCM group – 52 ± 13 years and 49 ± 13 years in the iCM group (table 2). The patients were divided into three age groups – younger than 40 years of age, older than 60 years of age and aged between 40 and 60 years. In all groups, the middle-aged group – between 40 and 60 years of age was predominant (table 3).

According to the body mass index (BMI), the patients from all three groups were slightly overweight (table 4). There were no significant differences in respect to the BMI between the three groups (p=0.06).

Table 1. Distribution of patients by gender in the groups studied

Groups / Gender	Group 1, n=57		Group 2, n=60		Group 3, n=138	
	N	%	N	%	N	%
Men	25	43.86	45	75.00	86	62.32
Women	32	56.14	15	25.00	52	37.68
Men:women ratio	1:1.28		3:1		1.65:1	

Group 1=no myocardial inflammation group; group 2=DCM group; group 3=iCM group.

Overall Chi-square test=12.10; p=0.02. Group1 vs Group2 – Fisher's exact test p=0.0007;

Group1 vs Group3 – Fisher's exact test p=0.025; Group2 vs Group3 – Fisher's exact test p=0.10.

Table 2. Distribution of patients by age and gender in the groups studied

Groups / Age	Group 1, n=57	Group 2, n=60	Group 3, n=138	F	P value
Men's age, years, mean ± SD	44.31 ±14.17	50.31 ±12.24	49.07 ±13.24	1.88	0.158
Women's age, years, mean ± SD	49.29 ±13.33	56.94 ±13.03	49.75 ±13.89	1.78	0.172
Overall age, years, mean ± SD	47.1 ±13.81	51.97 ±12.67	49.33 ±13.44	1.95	0.144

SD indicates standard deviation.

Table 3. Distribution of patients from the groups studied into age groups

Patients's groups / Age groups	Group 1, n=57	Group 2, n=60	Group 3, n=138	Total, n=255	P value
<40 years, n (%)	14 (24.6)	8 (13.3)	32 (23.2)	54 (21.2)	0.478
40-60 years, n (%)	33 (57.9)	37 (61.7)	75 (54.3)	145 (56.9)	
≥ 60 years, n (%)	10 (17.5)	15 (25)	31 (22.5)	56 (21.9)	

Table 4. Distribution of patients by BMI in the groups studied

Groups / BMI	Group 1, n=57	Group 2, n=60	Group 3, n=138	F	P value
Male BMI, kg/m^2, mean ± SD	26.53 ± 4.80	27.99 ± 5.65	27.41 ±4.48	0.631	0.534
Female BMI, kg/m^2, mean ± SD	25.62 ± 5.75	29.57 ± 6.85	26.08 ± 6.01	2.675	0.075
Overall BMI, kg/m^2, mean ± SD	26.01 ±5,33	28.38 ±5.94	26.66 ±5.05	2.855	0.060

4.1.2. Clinical symptoms

Dyspnea was the prevalent clinical symptom – 54.9% of all patients presented with dyspnea. This symptom was most common among the patients from the DCM-group – 60% of these patients had dyspnea, followed by the patients from the iCM group – 53.6% of them presented with this symptom and the patients from the no-inflammation group – 52.6% of them complained of dyspnea. The patients with moderate and severe HF symptoms (III and IV functional class according to the NYHA classification) were equally distributed among the three groups without any statistically significant difference (p=0.352). The second most common clinical symptom was palpitation. Upon their admission to the clinic, 28.2% all patients complained of palpitation. Other frequently observed clinical symptoms were angina pectoris (AP) (21.6%) and fatigue (21.2%). Dizziness and syncope occurred in 6.7% and 5.5% of the patients, respectively, prior to hospitalization. The sum of the clinical symptoms exceeded 100%, because some of the patients presented with more than one symptom. No significant difference was observed among the three groups regarding the distribution of the clinical symptoms (table 5, figure 3).

Table 5. Clinical symptoms in the groups studied

Groups / Symptoms	Group 1, n=57	Group 2, n=60	Group 3, n=138	P value			
				1:2	1:3	2:3	Overall
AP, n (%)	17 (29.8)	7 (11.7)	31 (22.5)	0.015*	0.278	0.076	0.054
Fatigue, n (%)	13 (22.8)	15 (25)	26 (18.8)	0.781	0.529	0.326	0.586
Dyspnea, n (%)	30 (52.6)	36 (60)	74 (53.6)	0.422	0.900	0.407	0.657
Peripheral edema, n (%)	4 (7)	6 (10)	10 (7.2)	0.564	0.955	0.514	0.776
NYHA III and IV functional class of HF, n (%)	15 (26.3)	14 (23.3)	31 (22.5)	0.619	0.790	0.765	0.872
Palpitations, n (%)	13 (22.8)	16 (26.7)	43 (31.2)	0.629	0.241	0.525	0.476
Dizziness, n (%)	4 (7)	3 (5)	10 (7.2)	0.646	0.955	0.558	0.838
Syncope, n (%)	3 (5.3)	0 (0)	11 (8)	0.072	0.505	0.024*	0.077

Asterisk indicates statistically significant difference in the frequency of symptom in a definite group. AP indicates angina pectoris; HF – heart failure; NYHA – New York Heart Association.

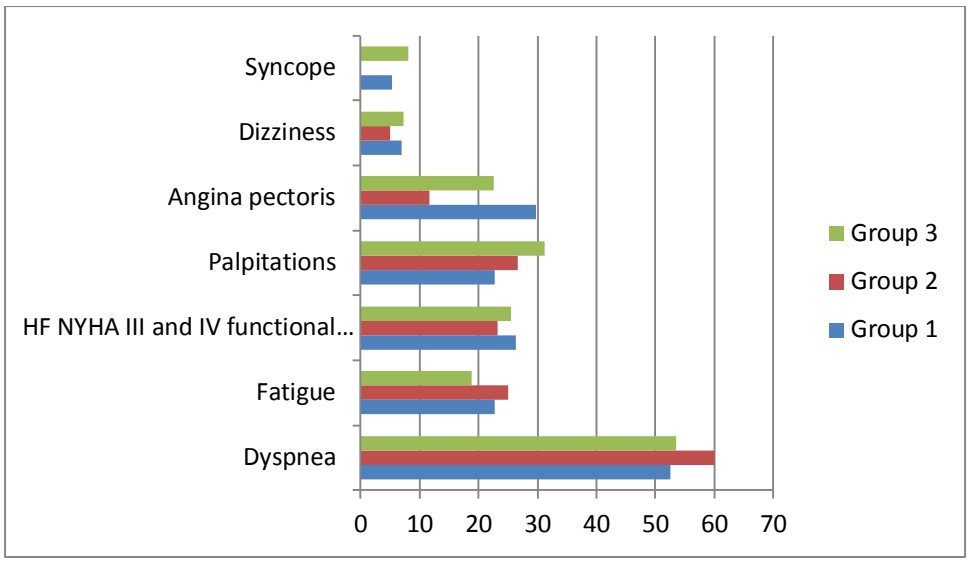

Figure 3. Incidence of symptoms in the groups studied. (Group 1- no myocardial inflammation group, group 2- DCM group, group 3- iCM group)

4.1.3. Concomitant diseases and risk factors

Arterial hypertension was the most common concomitant disease – 35% of the patients had AH. The highest proportion of patients with AH was observed in the DCM group (43%), followed by the iCM group (33%) and the no-inflammation group (30%) (table 6). The second most frequent concomitant cardiovascular disease was atrial fibrillation (AF). Persistent or permanent AF was observed in 7.1% of the patients from the three groups. Among the non-cardiovascular diseases, anemia was most frequent- it was detected in 22% of the patients, most of them had mild anemia. Chronic obstructive pulmonary disease (COPD) was present in 6.3% of all patients. Diabetes mellitus was the most common disease among the endocrine disorders – 8.2% of all patients were affected, followed by hypothyroidism – 4.7% and hyperthyroidism – 1.6% (table 7).

According to the glomerular filtration rate (GFR), calculated with the MDRD equation, the patients were classified as having preserved renal function- GFR> 90ml/min/1.73m^2; mildly impaired renal function- GFR: 60-89 ml/min/1.73m^2; moderately impaired renal function- GFR: 30-59 ml/min/1.73 m^2 and severely impaired renal function- GFR<30 ml/min/1.73 m^2. Most of the patients had mild or more severe renal impairment- 56.1% of the no inflammation group, 71.7% of the DCM group and 68.8% of the iCM group (table 8). The patients with preserved renal function

and those with different stages of renal dysfunction were equally distributed between the study groups.

The most common cardiovascular risk factor among the patients from the groups studied was dyslipidemia – it was present in 21.2% of all patients. Most often it was found in the iCM group – 23.9% (table 9). Eighteen percent of all patients were smokers, 3.5% had alcohol abuse. With respect to concomitant diseases and risk factors, no significant differences were determined between the three subgroups (tables 6-9).

Table 6. Concomitant cardiovascular diseases in the groups studied

Groups / Concomitant diseases	Group 1, n=57	Group 2, n=60	Group 3, n=138	P value			
				1:2	1:3	2:3	Overall
AH, n (%)	17 (29.8)	26 (43.3)	46 (33.3)	0.130	0.634	0.179	0.263
Persistent or permanent AF, n (%)	6 (10.5)	3 (5)	9 (6.5)	0.262	0.340	0.680	0.474

AF indicates atrial fibrillation.

Table 7. Concomitant non-cardiovascular diseases in the groups studied

Groups / Concomitant diseases	Group 1, n=57	Group 2, n=60	Group 3, n=138	P value			
				1:2	1:3	2:3	Overall
Anemia, n (%)	11 (19.3)	14 (23.3)	31 (22.5)	0.595	0.614	0.907	0.848
COPD, n (%)	2 (3.5)	5 (8.3)	9 (6.5)	0.271	0.407	0.648	0.552
DM, n (%)	5 (8.8)	7 (11.7)	9 (6.5)	0.606	0.580	0.222	0.474
Hyperthyreoidism, n (%)	2 (3.5)	0 (0)	2 (1.4)	0.130	0.330	0.344	0.281
Hypothyreoidism, n (%)	2 (3.5)	2 (3.3)	8 (5.8)	0.877	0.590	0.459	0.703

COPD indicates chronic obstructive pulmonary disease, DM indicated diabetes mellitus.

Table 8. Presence of renal dysfunction in the groups studied

Groups / Renal dysfunction	Group 1, n=57	Group 2, n=60	Group 3, n=138	P value
Patients with preserved renal function, n (% within the group)	25 (43.9)	17 (28.3)	43 (31.2)	0.160
Patients with mildly impaired renal function, n (% within the group)	26 (45.6)	29 (48.4)	75 (54.3)	
Patients with moderately and severely impaired renal function, n (% within the group)	6 (10.5)	14 (23.3)	20 (14.5)	

Patients were classified according to the glomerular filtration rate (GFR), calculated with the MDRD equation as follows: preserved renal function – GFR≥90 ml/min/1.73m^2; mildly impaired renal function – GFR: 60-89 ml/min/1.73m^2; moderately impaired renal function – GFR: 30-59 ml/min/1.73m^2 and severely impaired renal function – GFR<30 ml/min/1.73m^2.

Table 9. Cardiovascular risk factors in the groups studied

Groups / Risk factors	Group 1, n=57	Group 2, n=60	Group 3, n=138	P value			
				1:2	1:3	2:3	Overall
Dyslipidemia, n (%)	10 (17.5)	11 (18.3)	33 (23.9)	0.911	0.329	0.385	0.507
Smoking, n (%)	10 (17.5)	13 (21.7)	23 (16.7)	0.575	0.882	0.402	0.651
Alcohol abuse, n (%)	2 (3.5)	3 (5)	4 (2.9)	0.690	0.822	0.462	0.765

4.1.4 ECG changes

The most common conduction disorder was the left bundle branch block (LBBB). It was present in 16.47% of the patients. It was significantly more frequent in the DCM group (32%) in comparison with the iCM (13%) group and the no inflammation group (9%) (p=0.001) (table 10). AV-block (first and second degree) was the second most common conduction disorder- 6.27% of all patients had AV-block. Right bundle branch block (RBBB) was detected in 3.92% of the patients. There was no statistically significant difference in the incidence of AV-block and RBBB between the three groups studied.

Table 10. Distribution of conduction disorders in the groups studied

	Group 1, n=57	Group 2, n=60	Group 3, n=138	P value
AV-block, n (%)	4 (7)	2 (3)	10 (7)	0.561
LBBB, n (%)	5 (9)	19 (32)	18 (13)	0.001*
RBBB, n (%)	1 (2)	1 (2)	8 (6)	0.246

Asterisk indicates statistical significance.

Among the repolarization abnormalities, negative T-waves were most commonly observed among the patients (table 11). These ECG changes were observed in 25.49% of the patients. ST-segment depression was present in 7.8% of all patients, it was most frequently found in patients from the iCM group – 11%. Elevation of the ST-segment was detected upon admission in 7.06% of all patients; it was most common in patients from the iCM group- 9%. ECG diagnostic criteria for LV hypertrophy were present in 3.92% of all patients. There was no statistically significant difference between the three groups in relation to the incidence of repolarization abnormalities, or to the electrocardiographic signs of LV hypertrophy (table 11).

Table 11. Repolarization abnormalities and signs of LV hypertrophy in the groups studied

	Group 1, n=57	Group 2, n=60	Group 3, n=138	P value
ST-segment depression, n (%)	1 (2)	4 (7)	15 (11)	0.091
ST-segment elevation, n (%)	4 (7)	2 (3)	12 (9)	0.400
Negative T-waves, n (%)	13 (23)	17 (28)	35 (25)	0.790
ECG signs for LV hypertrophy, n (%)	2 (4)	4 (7)	4 (3)	0.447

LV indicates left ventricular.

4.1.5. Laboratory tests

The complete blood count results of all patients are presented in table 12. The leukocyte count was highest in the iCM group (8.4 x 10^9/L), followed by the DCM group (8.16 x 10^9/L) and lowest in the no inflammation group (6.75 x 10^9/L) (table 12) Leukocytosis was defined as leukocyte count greater than 11.00 x 10^9/L. We found that leukocytosis was significantly more frequently detected in the iCM group compared to the other two groups (p=0.003) (table 13). The CRP level was considered elevated when it was more than 5 mg/L. Elevation of the CRP level was

significantly more frequently observed among the patients from the iCM group compared to the other two groups. (p=0.046) (table 14).

Table 12. Complete blood count

Groups / CBC Parameters	Group 1, n=57	Group 2, n=60	Group 3, n=138	P value			
				1:2	1:3	2:3	Overall
Hemoglobin, (mean±SD) g/dL	13.82 (±1.62)	14.73 (±1.42)	14.16 (±1.66)	0.007*	0.544	0.060	0.007*
Hematocrit, (mean±SD) L/L	0.41 (±0.04)	0.43 (±0.04)	0.42 (±0.04)	0.001*	0.333	0.023*	0.001*
Erythrocytes count x 10^{12}/L (mean±SD)	4.59 (±0.48)	4.97 (±0.47)	4.76 (±0.51)	<0.001*	0.082	0.024*	<0.001*
Leukocyte count x 10^{9}/L, (mean±SD)	6.75 (±2.32)	8.16 (±2.03)	8.4 (±2.44)	0.004*	<0.001*	1.000	<0.001*
Thrombocytes count x 10^{9}/L, (mean±SD)	235.23 (±51.84)	236.60 (±62.09)	261.55 (±92.85)	1.000	0.104	0.124	0.036*

Asterisk indicates statistical significance.

Table 13. Prevalence of leukocytosis in the groups studied

Groups / Leu count	Group 1, n=57	Group 2, n=60	Group 3, n=138	Total, n=255	P value
NLC, n (%)	54 (94.7)	48 (80.0)	101 (73.2)	203 (79.6)	0.003*
Leukocytosis, n (%)	3 (5.3)	12 (20)	37 (26.8)	52 (20.4)	

Leu indicates leukocytes, NLC indicates normal leukocyte count. Asterisk indicates statistical significance.

Table 14. Prevalence of elevation of CRP in the groups studied

Groups / CRP level	Group 1, n=57	Group 2, n=60	Group 3, n=138	Total, n=255	P value
Normal CRP level, n (%)	50 (87.7)	51 (85.0)	102 (73.9)	203 (79.6)	0.046*
High CRP level, n (%)	7 (12.3)	9 (15.0)	36 (26.1)	52 (20.4)	

Asterisk indicates statistical significance.

The cardiac biomarker levels were not significantly different in the three groups, excluding the N-terminal pro B-type natriuretic peptide (NTproBNP) level (table 15). The level of the latter biomarker was significantly higher in the iCM group compared to the other two groups (table 15).

Table 15. Level of cardiac biomarkers in the groups studied

Groups / Cardiac biomarkers	Group 1		Group 2		Group 3		P value
	n	Value mean (±SD)	n	Value mean (±SD)	n	Value mean (±SD)	
CK, U/L	47	124.5 (±111.5)	46	143.9 (±273.3)	114	129.4 (±150.2)	0.857
CK – MB fraction, U/L	39	17.61 (±15.11)	38	17.47 (±10.21)	94	16.27 (±9.35)	0.757
Troponin T high sensitive, μg/L	11	0.011 (±0.005)	9	0.038 (±0.047)	40	0.074 (±0.14)	0.269
NTproBNP, pg/mL	17	267 (±254)	19	1052 (±915)	52	1509 (±2220)	0.046*

Asterisk denotes statistical significance, n indicates the number of patients from each group who were tested. CK indicates creatine kinase.

The cholesterol levels were tested in less than half of the patients. The total cholesterol, LDL-cholesterol and triglyceride levels were not significantly different between the three groups. Only the HDL-cholesterol levels differ significantly between the three groups, being highest in the no inflammation group – 59.77 mg/dL and lowest in the DCM group – 48.35 mg/dL (p=0.011) (table 16). The patients from the three groups did not differ significantly in relation to their creatinine level (p=0.079) (table 16).

Table 16. Cholesterol and creatinine levels in the groups studied

Groups / Cholesterol levels	Group 1		Group 2		Group 3		P value
	n	Value mean (±SD)	n	Value mean (±SD)	n	Value mean (±SD)	
Total cholesterol, mg/dL	24	190.54 (±45.92)	23	194.17 (±33.94)	61	197.84 (±52.31)	0.809
LDL-cholesterol, mg/dL	27	112.48 (±39.2)	23	117.13 (±29.35)	60	125.5 (±47.51)	0.381
HDL-cholesterol, mg/dL	26	59.77 (±14.94)	23	48.35 (±17.25)	60	49.1 (±15.47)	0.011*
Triglyceride, mg/dL	26	130.08 (±85.29)	23	189.48 (±160.32)	59	151.36 (±83.91)	0.139
Creatinine, mg/dL	57	0.94 (±0.31)	60	1.08 (±0.25)	138	1.05 (±0.41)	0.079

Asterisk denotes statistical significance, n indicates the number of patients from each group who were tested.

4.2. Endomyocardial biopsy

4.2.1. Site of endomyocardial biopsy

Endomyocardial biopsies were performed in all 255 patients. Most of the patients underwent LV EMBs (n=207 – 81.18%), whereas selective right ventricular (RV) EMBs were performed in 43 patients (16.86%), and biventricular EMBs were performed in another 5 (1.96%) (table 17).

Table 17. Site of the EMB

	Group 1, n=57	Group 2, n=60	Group 3, n=138	Total
LV EMB, n (%)	51 (89.47)	46 (76.67)	110 (79.71)	207 (81.18)
RV EMB, n (%)	4 (7.02)	13 (21.67)	26 (18.84)	43 (16.86)
Biventricular EMB, n (%)	2 (3.51)	1 (1.66)	2 (1.45)	5 (1.96)

EMB denotes endomyocardial biopsy, LV indicates left ventricular, RV indicates right ventricular.

4.2.2. Detection of viral genomes

On the basis of the PCR analysis, 52 of the biopsied patients (20.8%) were virus-negative. PVB19 genomes were detected in 163 of the patients (63.9%). Since a PVB19 load of more than 500 ge per microgram of isolated nucleic acids in EMB specimen is a clinically relevant threshold for the maintenance of myocardial inflammation[43], we should note that in 104 of these 163 patients, the PVB19 load was less than 500 ge. More than 500 ge were found in 59 (23.1%) of the biopsied patients. HHV6 type B genomes were detected in 11 patients (4.3%). HHV6 type B and PVB19 genomes were found in 22 patients (8.6%). Genomes of both HHV6 type B and Hepatitis B virus were found in 1 patient (0.4%). Enterovirus genomes were detected in 2 patients (0.8%). Combined Enterovirus and PVB19 genomes were found in 1 patient. EBV genomes were detected in 1 patient and combined EBV and PVB19 – in 1 patient. The frequencies of viral genomes by PCR are detailed in table 18. Overall, 98 of the 255 biopsied patients (38.4%) were virus-positive; in 73 patients one virus was isolated and in 25 patients more than one virus was detected. PVB19 with more than 500 ge per microgram of isolated nucleic acids in an EMB specimen was most frequently detected – 29 patients from the iCM group (55.77% of all patients with detected virus within this group), 16 patients from the no inflammation group (64% of all patients with detected virus within this group) and 14 patients in the DCM group (66.67% of all patients with detected virus within this group). The PCR analyses revealed the presence of PVB19 and HHV6 type B in 14 patients from the iCM group, in 5 patients from the no inflammation group and in 3 patients from the DCM group. Single infection with HHV6 type B was detected in 6 patients from the iCM group, in 4 patients from the no inflammation group and in 1 patient from the DCM group. There was no statistically significant difference in the distribution of PCR-positive samples between the three groups ($p=0.511$) (table 19).

Table 18. Results of PCR analysis of the biopsied material

	Group 1, n=57	Group 2, n=60	Group 3, n=138	Total, n=255
No virus, n (%)	13 (22.8)	15 (25.0)	25 (18.1)	53 (20.8)
PVB19<500 ge, n (%)	19 (33.3)	24 (40.0)	61 (44.2)	104 (40.8)
PVB19>500 ge, n (%)	16 (28.1)	14 (23.3)	29 (21.0)	59 (23.1)
HHV6 type B, n (%)	4 (7.0)	1 (1.7)	6 (4.4)	11 (4.3)
HHV6 type B + PVB19, n (%)	5 (8.8)	3 (5.0)	14 (10.2)	22 (8.6)
HHV6 type B + HBV, n (%)	0	1 (1.7)	0	1 (0.4)
Enterovirus, n (%)	0	1 (1.7)	1 (0.7)	2 (0.8)
Enterovirus + PVB19, n (%)	0	0	1 (0.7)	1 (0.4)
EBV, n (%)	0	0	1 (0.7)	1 (0.4)
EBV + PVB19, n (%)	0	1 (1.7)	0	1 (0.4)

HBV indicates Hepatitis B virus.

Table 19. Patients from the groups studied with virus detected in the biopsied material

	Group 1, n=25	Group 2, n=21	Group 3, n=52	Total, n=98	P value
PVB19>500 ge, n (%)	16 (64.00)	14 (66.67)	29 (55.77)	59 (60.20)	
HHV6 type B, n (%)	4 (16.00)	1 (4.76)	6 (11.54)	11 (11.23)	
HHV6 type B + PVB19, n (%)	5 (20.00)	3 (14.29)	14 (26.93)	22 (22.45)	
HHV6 type B + HBV, n (%)	0	1 (4.76)	0	1 (1.02)	
Enterovirus, n (%)	0	1 (4.76)	1 (1.92)	2 (2.04)	0.511
Enterovirus + PVB19, n (%)	0	0	1 (1.92)	1 (1.02)	
EBV, n (%)	0	0	1 (1.92)	1 (1.02)	
EBV + PVB19, n (%)	0	1 (4.76)	0	1 (1.02)	
Total, n (%)	25 (100)	21 (100)	52 (100)	98 (100)	

n indicates the number of patients from each group, who have positive viral PCR test.

4.2.3. Histopathology and immunohistochemistry

Inflammatory cellular infiltrates were detected in 138 of 255 patients (54.1% of all patients) via immunohistological methods. Among the patients from the iCM group, the macrophageal infiltrates were most frequently detected, followed by CD45RO lymphocytic and CD3 lymphocytic infiltrates (table 20).

Table 20. Inflammatory cells detected in the biopsy specimens

Groups / Immune cells	Group 1, n=57	Group 2, n=60	Group 3, n=138	df	P value
Increased CD3 lymphocytes, n (%)	0 (0)	0 (0)	67 (48.6)	2	<0.001*
Increased CD45RO lymphocytes, n (%)	0 (0)	0 (0)	88 (63.8)	2	<0.001*
Increased macrophages, n (%)	0 (0)	0 (0)	100 (72.5)	2	<0.001*

Asterisk indicates statistical significance, df indicates degrees of freedom, n indicates the number of patients, who have increased inflammatory cells in the EMB specimen.

Semiquantitative immunohistochemical analysis was performed for detection of AMs – intercellular adhesion molecule 1 (ICAM-1) and vascular cell adhesion molecule 1 (VCAM-1) and HLA class I, in frozen sections of the EMBs. The frequency of high expression of ICAM-1 and VCAM-1 on the endothelial and interstitial cells, and of HLA class I on the cardiomyocytes was greater in the iCM group (95.7%, 26.8%, and 84.8%, respectively), compared to no inflammation group (84.2%, 19.3%, and 71.9%, respectively) and to the DCM group (66.7%, 10.0%, and 63.3%, respectively) (table 21). In addition, no statistically significant difference was detected in relation to the presence of interstitial or perivascular fibrosis in the three groups (table 22).

Table 21. Expression of AMs and HLA class I in EMBs

	Group 1, n=57	Group 2, n=60	Group 3, n=138	df	P value
Increased expression of HLA class I, n (%)	41 (71.9)	38 (63.3)	117 (84.8)	2	0.003*
Increased expression of ICAM-1, n (%)	48 (84.2)	40 (66.7)	132 (95.7)	2	<0.001*
Increased expression of VCAM-1, n (%)	11 (19.3)	6 (10.0)	37 (26.8)	2	0.027*

Asterisk denotes statistical significance.

Table 22. Presence of interstitial and perivascular fibrosis in the biopsied material

	Group 1, n=57	Group 2, n=60	Group 3, n=138	df	P value
Interstitial fibrosis, n (%)	23 (40.4)	30 (50.0)	54 (39.1)	2	0.349
Perivascular fibrosis, n (%)	44 (77.2)	38 (63.3)	95 (68.8)	2	0.260

Significant differences were found regarding the cardiomyocyte diameter among the three groups. More than the half of the patients from the DCM and from the iCM group had hypertrophied cardiomyocytes (table 23). The patients from the no inflammation group had the smallest cardiomyocyte diameters (20.63 ± 4,788 μm), and the patients from the DCM group – the largest (23.88 ± 4.41 μm) (p=0.001) (table 23).

Table 23. Cardiomyocyte diameter

	Group 1, n=57	Group 2, n=60	Group 3, n=138	df	P value
Hypertrophied cardiomyocytes, n (%)	19 (33.3)	40 (66.7)	74 (53.6)	4	0.003*
Atrophied cardiomyocytes, n (%)	14 (24.6)	7 (11.7)	32 (23.2)		
Normal cardiomyocyte diameter, n (%)	24 (42.1)	13 (21.6)	32 (23.2)		
Average cardiomyocyte diameter, mean (± SD), μm	20.63 (±4.78)	23.88 (±4.41)	21.74 (±4.81)	-	0.001*

Asterisk indicates statistical significance.

4.3. Echocardiographic parameters

4.3.1. Conventional echocardiography and tissue Doppler imaging

Results from conventional echocardiography are presented in tables 24-28. The LVEF was highest in the no inflammation group – 57.8%, followed by the iCM group – 46.8% and the DCM group 30.3% (table 24). However, significant difference was observed between the three groups in respect to the LV diameters and volumes (table 25).

No significant differences were observed in regard to the IVS thickness and the LV PW thickness between the three groups (p=0. 581 and p=0.518, resp.) (table 26). The left atrial diameter and volume did not differ significantly between the no inflammation and the iCM groups (p=0.317

and p=0.137, resp.), but appeared to be significantly higher in the DCM group compared to the no inflammation group (p=0.019 and p<0.001) (table 27).

Table 24. LV systolic function

Groups / Echo parameters	Group 1, n=57	Group 2, n=60	Group 3, n=138	P value			
				1:2	1:3	2:3	Overall
LVEF, mean (±SD) %	57.79 (±10.11)	30.32 (±8.12)	46.8 (±16.96)	<0.001*	<0.001*	<0.001*	<0.001*
LVSF, mean (±SD) %	32.97 (±8.72)	15.59 (±5.16)	27.47 (±10.82)	<0.001*	0.007*	<0.001*	<0.001*

Asterisk denotes statistical significance; LVEF indicates LV ejection fraction; LVSF indicates LV shortening fraction.

Table 25. LV dimensions and volumes in the groups studied

Groups / Echo parameters	Group 1	Group 2	Group 3	P value			
				1:2	1:3	2:3	Overall
LVEDV, mean (±SD) ml	122.98 (±37.89)	203.17 (±55.73)	154.66 (±62.62)	<0.001*	0.004*	<0.001*	<0.001*
LVESV, mean (±SD) ml	55.19 (±24.05)	141.71 (±45.06)	89.57 (±57.98)	<0.001*	<0.001*	<0.001*	<0.001*
LVEDD, mean (±SD) mm	51.43 (±7.48)	64.77 (±7.47)	55.92 (±9.3)	<0.001*	0.004*	<0.001*	<0.001*
LVESD, mean (±SD) mm	35.05 (±8.38)	55.93 (±7.51)	41.5 (±12.24)	<0.001*	0.005*	<0.001*	<0.001*

Asterisk indicates statistical significance; LVEDD indicates LV end-diastolic dimension; LVEDV indicates LV end-diastolic volume; LVESD indicates LV end-systolic dimension; LVESV indicates LV end-systolic volume.

Table 26. LV wall thickness of the patients in the groups studied

Groups / Echoparameters	Group 1, n=57	Group 2, n=60	Group 3, n=138	P value			
				1:2	1:3	2:3	Overall
IVS, mean (±SD) mm	10.50 (±1.55)	10.55 (±1.66)	10.78 (±2.11)	1.000	1.000	1.000	0.581
PW, mean (±SD) mm	10.24 (±1.37)	10.30 (±1.66)	10.52 (±1.80)	1.000	0.923	1.000	0.518

Table 27. Left and right atrial dimensions of the patients in the groups studied

Groups / Echoparameters	Group 1	Group 2	Group 3	P value			
				1:2	1:3	2:3	Overall
LA diameter, mean (±SD) mm	37.14 (±6.52)	41.59 (±8.00)	39.43 (±8.32)	0.019*	0.317	0.292	0.024*
LA volume, mean (±SD) ml	57.17 (±24.12)	81.52 (±22.52)	66.64 (±30.53)	<0.001*	0.137	0.005*	<0.001*
RA volume, mean (±SD) ml	45.61 (±25.74)	58.87 (±22.69)	52.40 (±25.95)	0.056	0.437	0.563	0.062

Asterisk denotes statistical significance; LA indicates left atrial, RA indicates right atrial.

RV diameter, tricuspid annular plane systolic excursion (TAPSE) and PAP did not differ significantly between the three groups studied (p=0.809; p=0.381 and p=0.139, respectively) (table 28). The systolic PAP was significantly higher in the DCM and in the iCM group compared to the no inflammation group (table 28).

Table 28. RV functional echocardiographic parameters and pulmonary artery pressures

Groups / Echo parameters	Group 1		Group 2		Group 3		P value			
							1:2	1:3	2:3	Overall
	n	Mean value (±SD)	n	Mean value (±SD)	n	Mean value (±SD)				
RV diameter, mm	19	22.21 (±6.65)	14	27.29 (±5.76)	38	26.11 (±7.51)	1.000	1.000	1.000	0.809
TAPSE, mm	52	24.96 (±4.54)	55	21.84 (±4.02)	129	22.78 (±5.22)	1.000	0.563	1.000	0.381
Systolic PAP, mmHg	39	27.56 (±6.57)	30	36.33 (±12.02)	73	31.62 (±9.96)	0.038*	0.014*	1.000	0.011*

Asterisk indicates statistical significance; n indicates the number of patient from each group in whom the echocardiographic parameter was measured.

The transmitral E and A wave velocities and the ratio of transmitral E and A wave velocities (E/A) did not differ significantly between the three groups (p=0.378, p=0.310 and p=0.284 resp.) (table 29). The early diastolic mitral annulus velocity from the lateral annulus (E'lat) was significantly higher in the no inflammation group in comparison with the DCM group and the iCM

group (p=0.04). The early diastolic mitral annulus velocity from the septal annulus (E'sep) differed significantly between the three groups (p<0.001). The septal filling index (E/E'sep) and the lateral filling index (E/E'lat) were significantly lower in the no inflammation group compared to the DCM group (p=0.002 and p=0.001, resp.), but not in comparison to the iCM group (p=0.221 and p=1.000, resp.) (table 29).

Table 29. Conventional Doppler and TD echocardiographic parameters

Groups / Echo parameters	Group 1		Group 2		Group 3		P value			
							1:2	1:3	2:3	Overall
	n	Mean value (±SD)	n	Mean value (±SD)	n	Mean value (±SD)				
E, m/s	53	0.83 (±0.20)	54	0.80 (±0.22)	133	0.78 (±0.21)	1.000	0.502	1.000	0.378
A, m/s	46	0.70 (±0.23)	49	0.64 (±0.26)	123	0.69 (±0.23)	0.511	1.000	0.526	0.310
E/A	46	1.37 (±0.80)	49	1.56 (±1.07)	123	1.33 (±0.78)	0.872	1.000	0.344	0.284
E' sep, m/s	49	0.09 (±0.03)	38	0.07 (±0.02)	108	0.08 (±0.03)	<0.001*	0.022*	0.074	<0.001*
E' lat, m/s	48	0.15 (±0.26)	44	0.09 (±0.04)	108	0.10 (±0.04)	0.069	0.078	1.000	0.040*
E/E' sept	49	9.49 (±3.30)	38	12.88 (±4.61)	95	10.89 (±4.84)	0.002*	0.221	0.062	0.002*
E/E' lat	48	7.72 (±2.90)	44	11.32 (±7.82)	108	8.32 (±3.53)	0.001*	1.000	0.001*	<0.001*

Asterisk denotes statistical significance. E indicates early diastolic mitral inflow velocity, A indicates late diastolic mitral inflow velocity, E' sep indicates early diastolic mitral annulus velocity from the septal annulus, E' lat indicates early diastolic mitral annulus velocity from the lateral annulus.

Pericardial effusion was present in 44 patients (17.3%). There was no significant difference in the frequency of detection of pericardial effusion between the three groups (p=0.297) (table 30).

Table 30. Pericardial effusion

	Group 1, n=57	Group 2, n=60	Group 3, n=138	df	P value
Presence of pericardial effusion, n (%)	13 (22.8)	7 (11.7)	24 (17.4)	2	0.297

Assessment of diastolic function of the left ventricle showed that most of the patients from each group had diastolic dysfunction. Diastolic function abnormalities were divided into mild diastolic dysfunction (impaired relaxation), moderate diastolic dysfunction (pseudonormalization) and severe diastolic dysfunction (restrictive filling – reversible and fixed). Mild diastolic dysfunction was detected in 114 patients, 18 patients had moderate diastolic dysfunction and 9 patients – severe diastolic dysfunction (table 31).

Table 31. Types of diastolic dysfunction

Groups / Types of diastolic dysfunction	Group 1, n=57	Group 2, n=60	Group 3, n=138	df	P value
Impaired relaxation, n (%)	25 (44.9)	29 (48.3)	60 (43.5)	6	0.297
Pseudonormalization, n (%)	2 (3.5)	5 (8.3)	11 (8.0)		
Restriction, n (%)	0 (0)	3 (5)	6 (4.3)		

4.3.2. Speckle tracking echocardiography

4.3.2.1. 2D global longitudinal strain and strain rate parameters

Systolic and diastolic indices provided by 2D STE are presented in table 32. Patients with iCM showed reduced GLS in comparison to those without myocardial inflammation (-14.50±5.40% vs. -18.39±4.05%, $p<0.001$). Representative images are shown in figures 4-6. GLSR and GLESR were also significantly reduced in the iCM group compared to the no inflammation group (-0.92±0.32 s^{-1}, vs. -1.11±0.26 s^{-1}, $p<0.001$; and 1.16±0.45 s^{-1} vs. 1.53±0.41 s^{-1}, $p<0.001$, resp.). However, there was no significant difference in GLASR between the iCM group and no inflammation group (0.82±0.32 s^{-1}, vs. 0.89±0.29 $p=0.509$). The patients with DCM had

significantly lower GLS, GLSR, GLESR and GLASR compared to those without myocardial inflammation ($p<0.001$ for all).

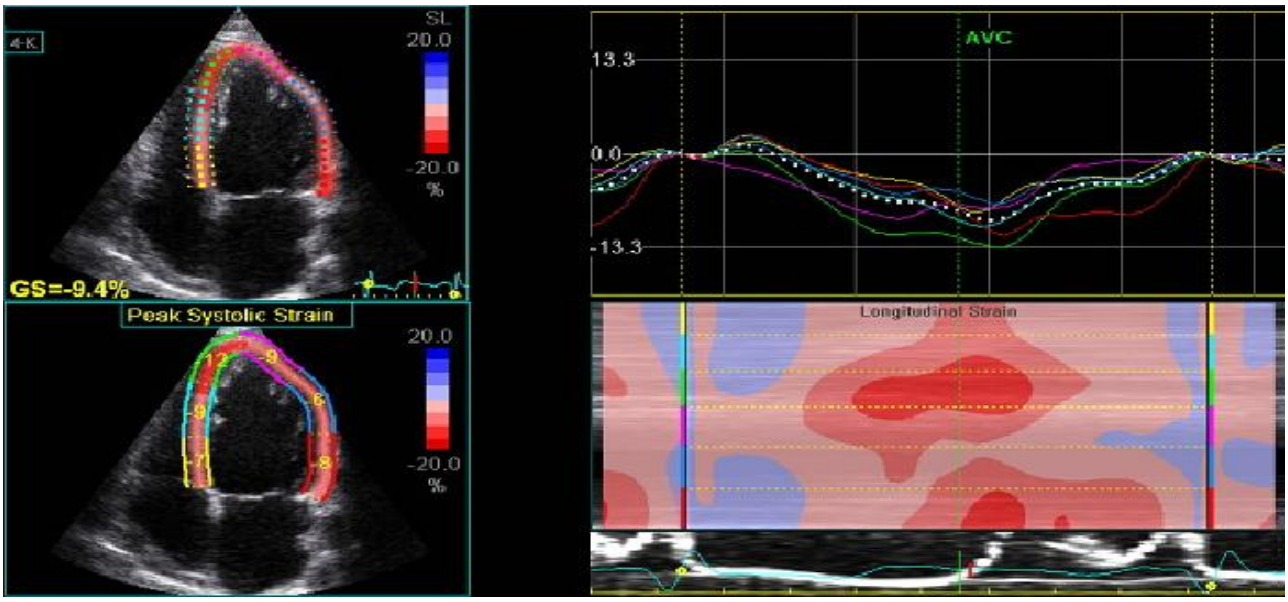

(a)

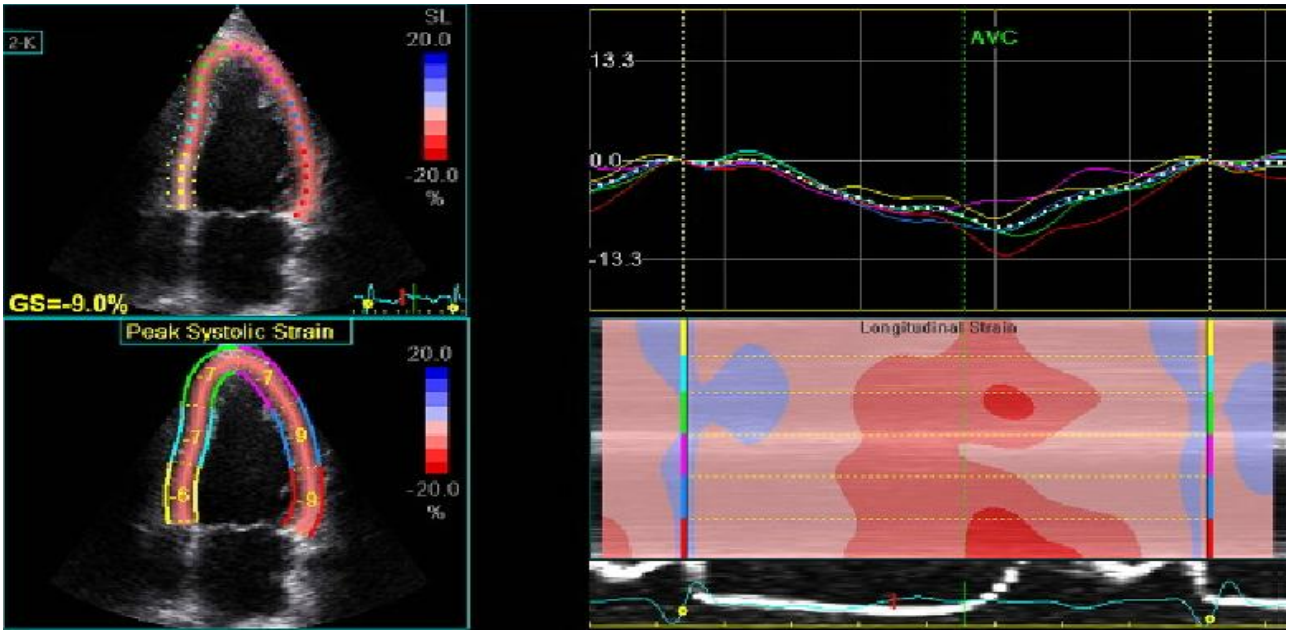

(b)

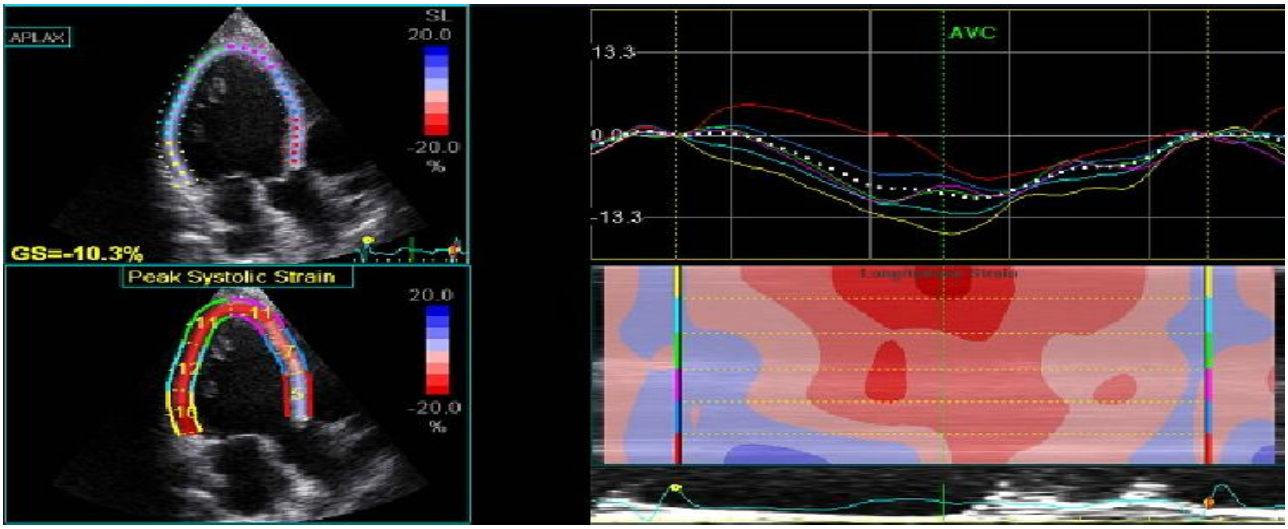

(c)

Figure 4. 2D STE-derived left ventricular longitudinal strain showing parametric image and segmental strain values/curves in a patient with iCM in a (a) 4-chamber view, (b) 2-chamber view and (c) 3-chamber view.

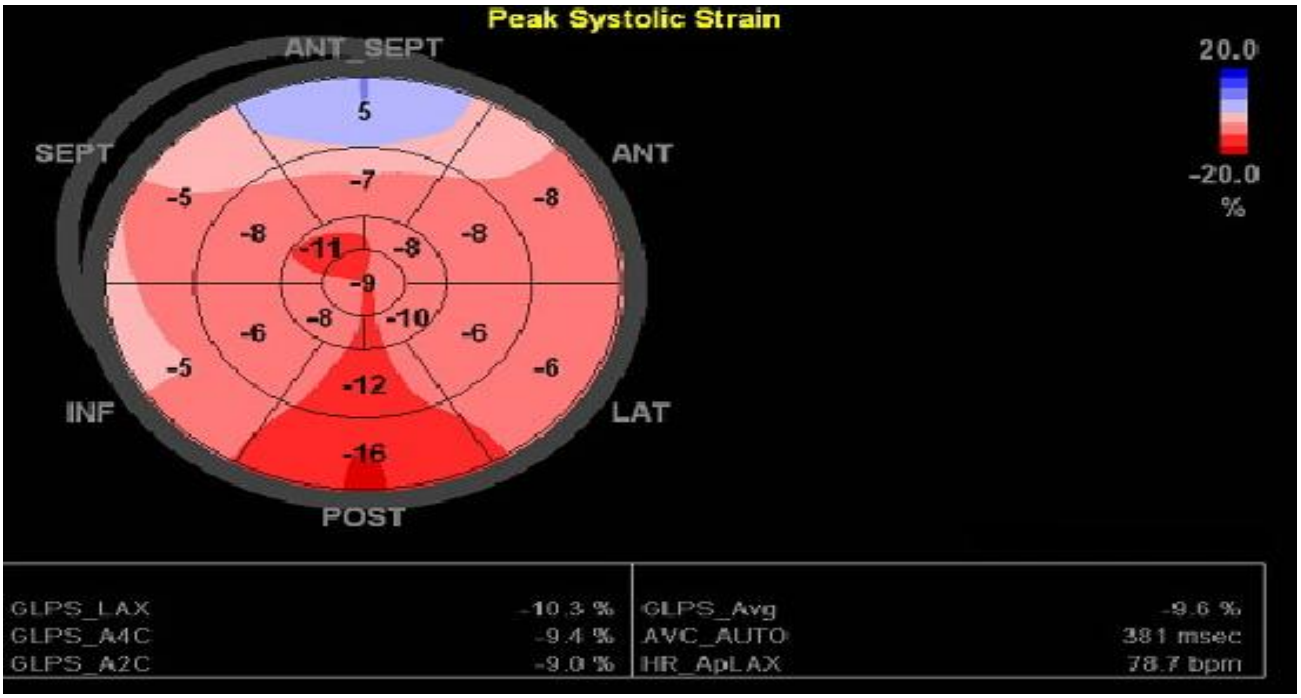

Figure 5. Bull's eye display of 2D STE-derived LV longitudinal strain of the same patient as in Fig. 4. The percent values of longitudinal strain for the individual segments are presented and color coded. Different shades of red represent negative strain. Slightly to moderately attenuated longitudinal strain is present in the anteroseptal, anterior, septal, inferior and lateral segments.

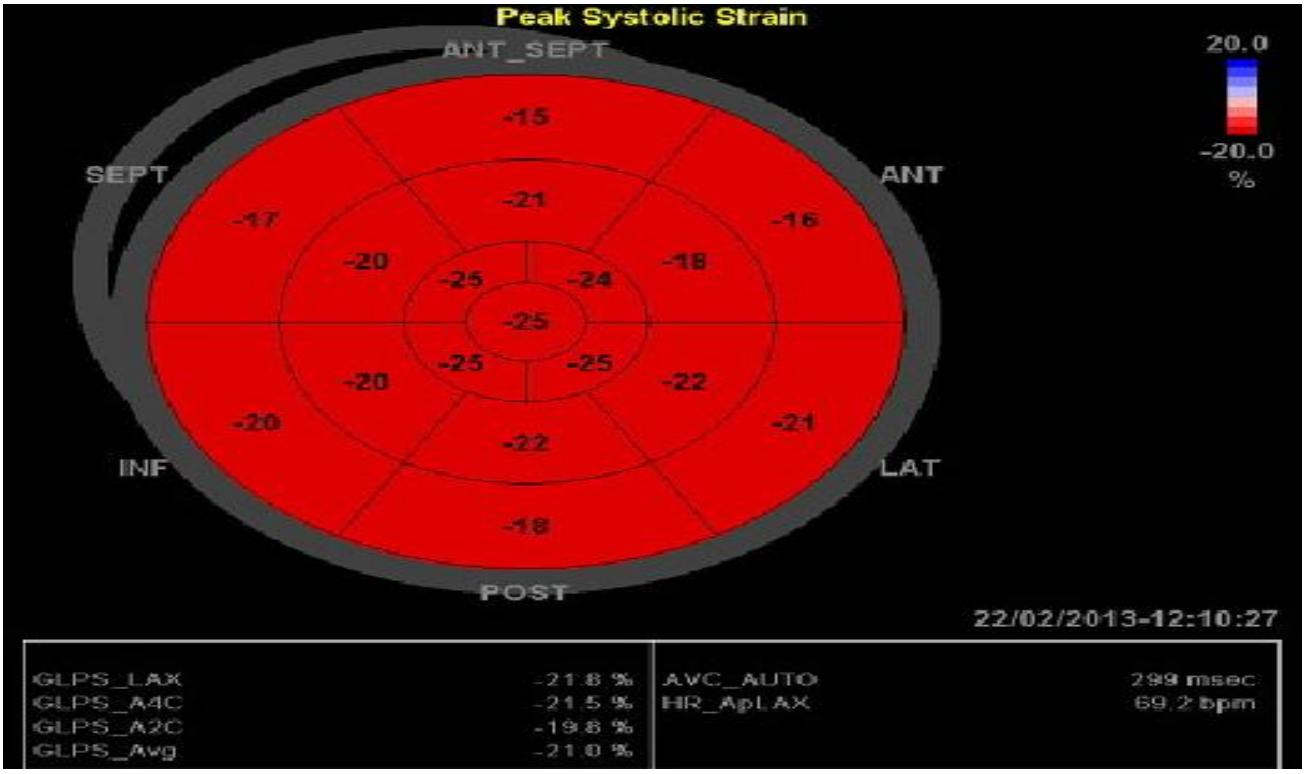

Figure 6. Bull's eye display of 2D longitudinal strain of a patient without myocardial inflammation.

Table 32. 2D GLS, GLSR, SLESR and GLASR among the groups studied

Groups / 2D strain parameters	Group 1, n=57	Group 2, n=60	Group 3, n=138	P value			
				1:2	1:3	2:3	Overall
2D GLS, %	-18.39 (±4.05)	-11.52 (±3.49)	-14.50 (±5.40)	<0.001*	<0.001*	0.001*	<0.001*
2D GLSR, s^{-1}	-1.11 (±0.26)	-0.74 (±0.17)	-0.92 (±0.32)	<0.001*	<0.001*	<0.001*	<0.001*
2D GLESR, s^{-1}	1.53 (±0.41)	0.89 (±0.27)	1.16 (±0.45)	<0.001*	<0.001*	<0.001*	<0.001*
2D GLASR, s^{-1}	0.89 (±0.29)	0.65 (±0.30)	0.82 (±0.32)	<0.001*	0.509	0.005*	<0.001*

Variables are expressed as mean (± SD). Asterisk indicates statistical significance.

An independent sample t-test was conducted to compare the 2D GLS, GLSR, GLESR and GLASR between different subgroups of patients with iCM.

Primarily, we compared the 2D longitudinal strain and strain rate parameters in female and male patients from the iCM group. Although 2D longitudinal strain and strain rates were higher in women than in men, the difference did not reach statistical significance for the strain or any of the strain rates (tables 33, 34).

Table 33. 2D GLS and GLSR in male and female patients from the iCM group

	2D GLS, %				2D GLSR, s^{-1}			
Gender	n	mean±SD	t	P value	n	mean±SD	t	P value
Women	40	-15.09±5.52	-0.840	0.403	40	-0.95±0.35	-0.771	0.443
Men	78	-14.20±5.35			78	-0.90±0.31		

Table 34. 2D GLESR and GLASR in male and female patients with iCM

	2D GLESR, s^{-1}				2D GLASR, s^{-1}			
Gender	n	mean±SD	t	P value	n	mean±SD	t	P value
Women	40	1.25±0.52	1.450	0.152	38	0.84±0.31	0.466	0.642
Men	78	1.11±0.40			71	0.81±0.32		

We compared the 2D strain and strain rates parameters in patients with iCM and preserved or reduced LVEF and found that the patients with preserved LVEF had higher 2D GLS (-18.78±4.38% vs. -11.57±3.87%, p<0.001), GLSR (-1.19±0.28 s^{-1} vs. -0.74±0.21 s^{-1}, p<0.001), GLESR (1.47±0.44 s^{-1} vs. 0.94±0.31 s^{-1}, p<0.001) and GLASR (1.02±0.29 s^{-1} vs. 0.66±0.25 s^{-1}, p<0.001) (tables 35, 36). 2D GLSR was significantly impaired in patients with LV hypertrophy in comparison to those without LV hypertrophy (-0.82±0.23 s^{-1} vs. -0.95±0.34 s^{-1}, p=0.030). The patients with LV hypertrophy also had lower 2D GLESR (0.95±0.33 s^{-1} vs. 1.22±0.46 s^{-1}, p=0.009) (table 36). 2D GLS and GLSR were significantly impaired in patients with WMAs, detected by transthoracic echocardiography, in comparison to patients without WMAs (p=0.031, and p=0.013, resp.) (table 35).

Table 35. 2D GLS and GLSR in different subgroups of patients with iCM

	2D GLS, %				2D GLSR, s^{-1}			
	n	mean±SD	t	P value	n	mean±SD	t	P value
LVEF								
Preserved	48	-18.78±4.38	-9.428	<0.001*	48	-1.19±0.28	-10.063	<0.001*
Reduced	70	-11.57±3.87			70	-0.74±0.21		
Pericardial effusion								
Not present	99	-14.52±5.27	-0.060	0.952	99	-0.92±0.31	-0.004	0.997
Present	19	-14.44±6.18			19	-0.92±0.37		
LV hypertrophy								
Not present	91	-14.90±5.55	-1.475	0.143	91	-0.95±0.34	-2.237	0.030*
Present	24	-13.07±4.77			24	-0.82±0.23		
WMAs								
Not present	68	-15.68±5.69	-2.188	0.031*	68	-1.00±0.35	-2.537	0.013*
Present	39	-13.33±4.68			39	-0.84±0.26		

Asterisk indicates statistical significance.

Table 36. 2D GLESR and GLASR in different subgroups of patients with iCM

	2D GLESR, s^{-1}				2D GLASR, s^{-1}			
	n	mean±SD	t	P value	n	mean±SD	t	P value
LVEF								
Preserved	48	1.47±0.44	7.337	<0.001*	48	1.02±0.29	6.896	<0.001*
Reduced	70	0.94±0.31			61	0.66±0.25		
Pericardial effusion								
Not present	99	1.15±0.44	-0.207	0.837	93	0.83±0.32	0.612	0.542
Present	19	1.18±0.49			16	0.78±0.31		
LV hypertrophy								
Not present	91	1.22±0.46	2.659	0.009*	83	0.82±0.33	-0.130	0.897
Present	24	0.95±0.33			23	0.83±0.31		
WMAs								
Not present	68	1.24±0.49	1.708	0.091	65	0.85±0.34	0.724	0.471
Present	39	1.08±0.38			35	0.80±0.29		

Asterisk denotes statistical significance.

2D GLS was significantly reduced in patients with iCM, who had mitral regurgitation (mild or moderate) in comparison to those without mitral regurgitation ($p<0.001$) (table 37). The same tendency was observed for 2D GLSR ($p<0.001$), 2D GLESR ($p<0.001$) and 2D GLASR ($p=0.005$) (tables 37, 38). The patients with the iCM who had tricuspid regurgitation (mild or moderate) had

significantly impaired 2D GLS, GLSR, GLESR and GLASR compared to the patients without tricuspid regurgitation ($p<0.001$; $p<0.001$; $p=0.033$ and $p=0.004$, resp.) (tables 37, 38). No statistically significant differences in global longitudinal strain or strain rate parameters were detected in patients with and without aortic vitium (tables 37, 38).

Table 37. 2D GLS and GLSR in subgroups of patients with iCM in relation to the presence of valvular heart disease

	2D GLS, %				2D GLSR, s^{-1}			
	n	mean±SD	t	P value	N	mean±SD	t	P value
AR or AS No ARor AS	107	-14.69±5.50	-0.708	0.480	107	-0.93±0.33	-0.644	0.521
AR or AS	7	-13.18±5.03			7	-0.85±0.29		
MR No MR	57	-17.07±4.88	-5.411	<0.001*	57	-1.08±0.31	-5.815	<0.001*
MR	57	-12.12±4.96			57	-0.77±0.27		
TR No TR	74	-15.91±4.80	-3.670	<0.001*	74	-1.01±0.30	-4.014	<0.001*
TR	40	-12.18±5.84			40	-0.77±0.31		
PR No PR	110	-14.78±5.39	-1.832	0.070	110	-0.94±0.32	-1.935	0.055
PR	4	-9.74±5.84			4	-0.62±0.31		

Asterisk indicates statistical significance. AR indicates aortic regurgitation, AS indicates aortic stenosis, MR indicates mitral regurgitation, TR indicates tricuspid regurgitation, PR indicates pulmonary regurgitation.

Table 38. 2D GLESR and GLASR in subgroups of patients with iCM in relation to the presence of valvular heart disease

	2D GLESR, s^{-1}				2D GLASR, s^{-1}			
	n	mean±SD	t	P value	n	mean±SD	t	P value
AR or AS								
No ARor AS	107	1.17±0.46	0.479	0.633	100	0.81±0.32	-1.148	0.253
AR or AS	7	1.09±0.33			5	0.98±0.33		
MR								
No MR	57	1.34±0.46	4.439	<0.001*	55	0.91±0.29	2.904	0.005*
MR	57	1.00±0.38			50	0.73±0.33		
TR								
No TR	74	1.24±0.43	2.157	0.033*	70	0.89±0.29	2.914	0.004*
TR	40	1.05±0.47			35	0.70±0.34		
PR								
No PR	110	1.18±0.45	0.930	0.354	102	0.83±0.32	1.995	0.049*
PR	4	0.96±0.44			3	0.46±0.18		

Asterisk denotes statistical significance. AR indicates aortic regurgitation, AS indicates aortic stenosis, MR indicates mitral regurgitation, TR indicates tricuspid regurgitation, PR indicates pulmonary regurgitation.

No statistically significant differences in the values of 2D longitudinal strain and strain rates were detected between the patients with and without conduction or repolarization abnormalities (tables 39, 40).

Table 39. 2D GLS and GLSR in subgroups of patients with iCM in relation to the presence of conduction or repolarization disorders

	2D GLS, %				2D GLSR, s^{-1}			
	n	mean±SD	t	P value	n	mean±SD	t	P value
LBBB								
Not present	101	-14.70±5.53	-0.942	0.348	101	-0.93±0.34	-1.542	0.132
Present	17	-13.36±4.54			17	-0.84±0.20		
RBBB								
Not present	111	-14.68±5.27	-1.422	0.158	111	-0.93±0.32	-1.185	0.238
Present	7	-11.70±7.11			7	-0.78±0.42		
AV block								
Not present	108	-14.44±5.46	0.415	0.653	108	-0.92±0.33	0.136	0.892
Present	10	-15.24±4.85			10	-0.93±0.30		
ST-segment depression								
Not present	104	-14.63±5.50	-0.695	0.488	104	-0.93±0.33	-0.876	0.383
Present	14	-13.56±4.68			14	-0.85±0.30		
ST-segment elevation								
Not present	107	-14.35±5,46	0.988	0.325	107	-0.92±0.33	0.533	0.595
Present	11	-16.04±4.71			11	-0.97±0.30		
Negative T-waves								
Not present	87	-14.81±5.58	-1.021	0.309	87	-0.94±0.32	-0.955	0.341
Present	31	-13.65±4.84			31	-0.87±0.33		

Table 40. 2D GLESR and GLASR in subgroups of patients with iCM in relation to the presence of conduction and repolarization disorders

	2D GLESR, s^{-1}				2D GLASR, s^{-1}			
	n	mean±SD	t	P value	n	mean±SD	t	P value
LBBB								
Not present	101	1.18±0.46	1.203	0.232	93	0.82±0.33	0.327	0.745
Present	17	1.04±0.37			16	0.80±0.28		
RBBB								
Not present	111	1.17±0.45	1.059	0.292	103	0.83±0.31	1.417	0.159
Present	7	0.98±0.41			6	0.64±0.39		
AV block								
Not present	108	1.16±0.46	0.011	0.991	100	0.82±0.32	-0.291	0.772
Present	10	1.16±0.36			9	0.85±0.32		
ST-segment depression								
Not present	104	1.17±0.47	0.982	0.337	96	0.83±0.32	1.129	0.262
Present	14	1.07±0.31			13	0.73±0.33		
ST-segment elevation								
Not present	107	1.14±0,45	-1.143	0.255	98	0.81±0.32	-0.550	0.583
Present	11	1.30±0.43			11	0.87±0.34		
Negative T-waves								
Not present	87	1.18±0.47	0.942	0.348	79	0.84±0.32	1.102	0.273
Present	31	1.09±0.40			30	0.77±0.28		

2D GLS was significantly lower in patients with elevated LV end-diastolic pressure (LVEDP) (measured during LV catheterization) compared to patients with normal LVEDP (p=0.014) (table 41).

Table 41. 2D GLS and GLSR in patients with iCM in relation to the LVEDP measured during LV catheterization

	2D GLS, %				2D GLS, s^{-1}			
	n	mean±SD	t	P value	n	mean±SD	t	P value
LVEDP								
Normal	80	-15.54±5.01	-2.502	0.014*	80	-0.97±0.30	-1.871	0.073
Elevated	21	-12.36±5.79			21	-0.79±0.41		

Asterisk indicates statistical significance. LVEDP indicates left ventricular end-diastolic pressure

Table 42. 2D GLESR and GLASR in patients with iCM in relation to the LVEDP measured during LV catheterization

	2D GLESR, s^{-1}				2D GLASR, s^{-1}			
	n	mean±SD	t	P value	n	mean±SD	t	P value
LVEDP								
Normal	80	1.21±0.43	1.119	0.266	75	0.88±0.29	-0.604	0.547
Elevated	21	1.08±0.54			18	0.63±0.29		

LVEDP indicates left ventricular end-diastolic pressure

The presence of myocardial scar, intramyocardial fibrosis or the expression of AMs detected with immunohistological analysis of the EMB specimens did not influence significantly the 2D longiutudinal strain and strain rates values in patients with iCM (tables 43, 44).

Table 43. 2D GLS and GLSR in different subgroups of patients with iCM in relation to the detection of fibrosis, myocardial scar or expression of AMs in the EMB specimens

	2D GLS, %				2D GLS, s^{-1}			
	n	mean±SD	t	P value	N	mean±SD	t	P value
Expression of AM								
Normal	5	-14.92±3.87	-0.177	0.860	5	-0.97±0.25	-0.315	0.753
Enhanced	112	-14.48±5.49			112	-0.92±0.33		
Perivascular fibrosis								
Not present	38	-15.20±5.67	-0.861	0.391	38	-0.97±0.35	-0.991	0.324
Present	75	-14.26±5.35			75	-0.90±0.31		
Interstitial fibrosis								
Not present	72	-15.07±5.43	-1.015	0.312	72	-0.95±0.32	-1.109	0.270
Present	39	-13.96±5.53			39	-0.88±0.35		
Myocardial scar								
Not present	99	-14.77±5.20	-1.075	0.293	99	-0.93±0.30	-0.733	0.471
Present	19	-13.11±6.18			19	-0.86±0.42		

AM indicates adhesion molecules.

Table 44. 2D GLESR and GLASR in different subgroups of patients with iCM in relation to the detection of fibrosis, myocardial scar or expression of AMs in the EMB specimens

	2D GLESR, s^{-1}				2D GLASR, s^{-1}			
	n	mean±SD	t	P value	n	mean±SD	t	P value
Expression of AM								
Normal	5	1.10±0.18	-0.680	0.520	5	0.92±0.39	0.707	0.481
Enhanced	112	1.16±0.46			103	0.82±0.32		
Perivascular fibrosis								
Not present	38	1.20±0.43	0.647	0.519	36	0.84±0.35	0.442	0.660
Present	75	1.14±0.46			68	0.82±0.31		
Interstitial fibrosis								
Not present	72	1.18±0.46	0.584	0.560	68	0.85±0.33	1.123	0.264
Present	39	1.13±0.45			35	0.78±0.31		
Myocardial scar								
Not present	99	1.16±0.44	0.435	0.665	93	0.83±0.31	0.754	0.452
Present	19	1.12±0.49			16	0.76±0.39		

AM indicates adhesion molecules.

One-way analyses of variance were conducted to determine whether significant differences existed in relation to 2D GLS, GLSR, GLESR, GLASR values among the patients from the iCM group with different stages of interstitial and perivascular fibrosis. The results revealed that the patients with moderate interstitial fibrosis had significantly lower 2D GLS, GLSR and GLASR in comparison to those without or with mild interstitial fibrosis (table 45). No significant differences in relation to the GLS, GLSR, GLESR and GLASR were detected in patients with slight, moderate or without perivascular fibrosis (table 46).

Table 45. 2D GLS, GLSR, GLESR and GLASR in patients from the iCM group with different stages of interstitial fibrosis

	Interstitial fibrosis						P value			
	n	NIFib (1)	n	SIFib (2)	n	MIFib (3)	1:2	1:3	2:3	Overall
2D GLS, mean±SD, %	72	-15.07 ±5.43	33	-15.02 ±5.35	6	-8.16 ±1.15	1.000	0.008*	0.013*	0.010*
GLSR, mean±SD, s^{-1}	72	-0.95 ±0.32	33	-0.94 ±0.34	6	-0.54 ±0.14	1.000	0.010*	0.018*	0.012*
GLESR, mean±SD, s^{-1}	72	1.18 ±0.46	33	1.20 ±0.45	6	0.77 ±0.20	1.000	0.097	0.104	0.090
GLASR, mean±SD , s^{-1}	68	0.85 ±0.33	30	0.83 ±0.30	5	0.46 ±0.17	1.000	0.028*	0.056	0.033*

Asterisk denotes statistical significance. MIFib indicates moderate interstitial fibrosis, NIFib indicates no interstitial fibrosis, SIFib indicates slight interstitial fibrosis.

Table 46. 2D GLS, GLSR, GLESR and GLASR in patients from the iCM group with different stages of perivascular fibrosis

	Perivascular fibrosis						P value
	n	NPFib	n	SPFib	n	MPFib	
2D GLS, mean±SD, %	38	-15.20±5.67	68	-14.68±5.20	7	-10.19±5.48	0.079
2D GLSR, mean±SD, s^{-1}	38	-0.97±0.35	68	-0.92±0.30	7	-0.67±0.36	0.091
2D GLESR, mean±SD, s^{-1}	38	1.20±0.43	68	1.16±0.46	7	0.93±0.46	0.349
2D GLASR, mean±SD, s^{-1}	36	0.84±0.35	62	0.84±0.30	6	0.60±0.32	0.156

MPFib indicates moderate perivascular fibrosis NPFib indicates no perivascular fibrosis, SPFib indicates slight perivascular fibrosis.

Patients with iCM who had an increased level of NTproBNP showed sigificantly impaired 2D GLS, GLSR, GLESR and GLASR in comparison to patients with normal NTproBNP level ($p=0.001$; $p<0.001$; $p=0.022$ and $p<0.001$, resp.) (tables 47, 48).

Table 47. 2D GLS and GLSR in different subgroups of patients with iCM in relation to the level of inflammatory, cardiac and long-term glicemic control markers

	2D GLS, %				2D GLSR, s^{-1}			
	n	mean±SD	t	P value	n	mean±SD	t	P value
CRP level								
Not elevated	36	-15.11±5.77	-0.281	0.779	36	-0.96±0.34	-0.045	0.964
Elevated	30	-14.72±5.31			30	-0.96±0.33		
NTproBNP level								
Not elevated	12	-18.18±4.57	-3.744	0.001*	12	-1.20±0.26	-3.952	<0.001*
Elevated	34	-12.03±5.00			34	-0.79±0.32		
HbA1c level								
Normal	29	-15.23±5.31	-1.180	0.246	29	-0.98±0.33	-1.502	0.142
Elevated	8	-12.62±6.38			8	-0.79±0.26		

Asterisk indicates statistical sisgnificance. HbA1c – indicates glycated hemoglobin.

Table 48. 2D GLESR and GLASR in different subgroups of patients with iCM in relation to the level of inflammatory, cardiac and long-term glycemic control markers

	2D GLESR, s^{-1}				2D GLASR, s^{-1}			
	n	mean±SD	t	P value	n	mean±SD	t	P value
CRP level								
Not elevated	36	1.20±0.45	-0.078	0.938	33	0.93±0.34	1.266	0.210
Elevated	30	1.21±0.46			27	0.83±0.30		
NTproBNP level								
Not elevated	12	1.37±0.43	2.371	0.022*	12	1.08±0.21	4.045	<0.001*
Elevated	34	1.04±0.40			28	0.69±0.30		
HbA1c level								
Normal	29	1.19±0.44	0.728	0.471	27	0.89±0.34	0.331	0.743
Elevated	8	1.06±0.38			6	0.84±0.24		

Asterisk denotes statistical significance.

We found no significant difference in the level of 2D GLS, GLSR, GLESR and GLASR in the patients from the iCM group with or without AH, with and without DM, with or without dyslipidemia, with or without COPD (tables 49 and 50). The patients with iCM, who had former infections showed lower, although not significantly, 2D GLS, GLSR, GLESR and GLASR, compared to those who did not have a history of infections (tables 49 and 50). However, the patients with iCM and chronic kidney disease (CKD) (eGFR<90 ml/min./1,73 m^2) had significantly lower

2D GLS (-13.66±4.89 vs. -16.42±6.07, p=0.019), 2D GLSR (-0.87±0.29 vs. -1.03±0.37, p=0.017), and 2D GLESR (1.08±0.41 vs. 1.32±0.50, p=0.007), compaired to the patients without CKD (p= 0.019; p=0.017 and p=0.007) (tables 49 and 50).

Table 49. 2D GLS and GLSR in subgroups of patients with iCM according to the presence of former infections or concomitant diseases

	2D GLS, %				2D GLSR, s^{-1}			
	N	mean±SD	t	P value	n	mean±SD	t	P value
DM								
Not present	110	-14.59±5.37	-0.645	0.520	110	-0.93±0.33	-0.606	0.546
Present	8	-13.31±6.08			8	-0.85±0.27		
AH								
Not present	79	-15.14±5.65	-1.829	0.070	79	-0.94±0.35	-1.213	0.228
Present	39	-13.22±4.67			39	-0.87±0.27		
Dyslipidemia								
Not present	89	-14.57±5.70	-0.253	0.801	89	-0.93±0.35	-0.376	0.708
Present	29	-14.31±4.45			29	-0.90±0.24		
COPD								
Not present	110	-14.44±5.46	0.465	0.643	110	-0.92±0.32	0.185	0.853
Present	8	-15.36±4.72			8	-0.94±0.35		
Former infections								
Not present	83	-14.94±5.55	-1.355	0.178	83	-0.95±0.33	-1.298	0.197
Present	35	-13.47±4.96			35	-0.86±0.30		
CKD								
Not present	36	-16.42±6.07	-2.411	0.019*	36	-1.03±0.37	-2.412	0.017*
Present	82	-13.66±4.89			82	-0.87±0.29		

Asterisk indicates statistical significance. CKD indicates chronic kidney disease, COPD indicates chronic obstructive pulmonary disease, DM indicates diabetes mellitus.

Table 50. 2D GLESR and GLASR in subgroups of patients with iCM according to the presence of former infections or concomitant diseases

	2D GLESR, s^{-1}				2D GLASR, s^{-1}			
	n	mean±SD	T	P value	n	mean±SD	t	P value
DM								
Not present	110	1.17±0.45	1.047	0.297	102	0.82±0.32	-0.259	0.796
Present	8	1.00±0.40			7	0.85±0.27		
AH								
Not present	79	1.21±0.47	1.778	0.078	75	0.85±0.33	1.462	0.147
Present	39	1.05±0.39			34	0.75±0.29		
Dyslipidemia								
Not present	89	1.18±048	1.029	0.306	83	0.82±0.32	-0.097	0.923
Present	29	1.08±0.32			26	0.83±0.32		
COPD								
Not present	110	1.16±0.45	0.149	0.882	101	0.82±0.32	-0.002	0.998
Present	8	1.13±0.42			8	0.82±0.33		
Former infections								
Not present	83	1.19±0.47	1.223	0.224	76	0.84±0.33	0.804	0.423
Present	35	1.08±0.40			33	0.78±0.28		
CKD								
Not present	36	1.32±0.50	2.757	0.007*	35	0.86±0.31	0.973	0.333
Present	82	1.08±0.41			74	0.80±0.32		

Asterisk denotes statistical significance. CKD indicates chronic kidney disease, COPD indicates chronic ostructive pulmonary disease, DM indicates diabetes mellitus.

The patients with iCM, who had no symptoms of HF showed significantly higher 2D GLS compared to the patients with severe HF (NYHA functional class IV) (table 51). This relation was not observed for 2D GLSR, GLESR or GLASR (table 51).

Table 51. 2D GLS, GLSR, GLESR and GLASR in subgroups of patients with iCM, divided according to the presence and severity of symptoms of HF

	Symptoms of HF								
	n	No symptoms of HF	n	NYHA II class	N	NYHA III class	n	NYHA IV class	P value
GLS, mean±SD, %	73	-15.14 ± 5.18	17	-14.09 ±5.32	25	-13.93± 5.68	3	-6.10 ± 1.00	0.032*
GLSR, mean±SD, s^{-1}	73	-0.95 ± 0.32	17	-0.93 ±0.31	25	-0.87 ± 0.33	3	-0.51 ± 0.07	0.108
GLESR, mean±SD, s^{-1}	73	1.20 ± 0.44	17	1.12 ±0.42	25	1.07 ± 0.50	3	0.94 ± 0.19	0.503
GLASR, mean±SD, s^{-1}	67	0.86 ± 0.32	17	0.81 ±0.32	24	0.75 ± 0.31	1	0.27	0.160

Asterisk indicates statistical significance.

One-way analyses of variance were conducted to determine whether significant differences existed in relation to 2D GLS, GLSR, GLESR, GLASR values among the patients from the iCM group with different virus detected by EMB. The results revealed no statistically significant differences (tables 52 and 53).

Table 52. 2D GLS and GLSR in patients with iCM according to the presence and type of virus detected by EMB

	2D GLS, %				2D GLSR, s^{-1}			
	n	mean±SD	F	P value	n	mean±SD	F	P value
No virus	23	-14.46±6.05	1.191	0.314	23	-0.90±0.39	1.152	0.337
PVB19<500 DNA copies	51	-14.96±5.45			51	-0.95±0.34		
PVB19>500 DNA copies or mRNA copies	23	-14.94±5.21			23	-0.94±0.30		
HHV6 type B	6	-15.92±5.41			6	-1.05±0.16		
PVB19 + HHV6 type B	12	-11.35±3.50			12	-0.74±0.19		
Enterovirus	1	-12.78			1	-0.99		
Enterovirus + PVB19	1	-20.72			1	-1.21		
EBV	1	-7.26			1	-0.51		

mRNA indicates messenger ribonucleic acid

Table 53. 2D GLESR and GLASR in patients with iCM according to the presence and type of virus detected by EMB

	2D GLESR, s^{-1}				2D GLASR, s^{-1}			
	n	mean±SD	F	P value	n	mean±SD	F	P value
No virus	23	1.21±0.51	1.337	0.240	22	0.72±0.36	2.144	0.055
PVB19<500 DNA copies	51	1.16±0.44			46	0.89±0.28		
PVB19>500 DNA copies or mRNA copies	23	1.23±0.44			22	0.83±0.32		
HHV6 type B	6	1.20±0.45			6	0.99±0.38		
PVB19 + HHV6 type B	12	0.84±0.32			11	0.63±0.25		
Enterovirus	1	1.28			1	0.54		
Enterovirus + PVB19	1	1.81			1	1.21		
EBV	1	1.11			0	-		

The smokers from the iCM group did not show any significant differences in regard to 2D GLS, GLSR, GLESR and GLASR values, compared to the non-smokers (table 54).

Table 54. 2D GLS, GLSR, GLESR and GLASR in patients with iCM according to smoking habits

	Smoking habits						F	P value
	n	Non smoker	n	Former smoker	n	Smoker		
GLS, mean±SD, %	93	-14.46±5.41	5	-14.56±7.53	20	-14.67±5.08	0.013	0.988
GLSR, mean±SD, s^{-1}	93	-0.93±0.33	5	-0.89±0.43	20	-0.91±0.27	0.043	0.958
GLESR, mean±SD, s^{-1}	93	1.17±0.45	5	1.15±0.65	20	1.11±0.43	0.151	0.860
GLASR, mean±SD, s^{-1}	85	0.80±0.31	5	0.89±0.45	19	0.88±0.33	0.533	0.589

4.3.2.2. 3D speckle tracking parameters

The 3D STE parameters – GAS, GCS, GLS and GRS are presented in table 55. 3D data sets were acquired using a wide-angle pyramidal volume acquisition mode in which wedge-shaped subvolumes were obtained in four or six consecutive cardiac cycles. Representative images are shown on figure 7.

Compared to the no inflammation group, the patients from the iCM group showed significantly impaired 3D strains obtained from four consecutive cardiac cycles: GAS (-22.09±7.46% vs. -30.01± .12%, p=0.003), GCS (-13.22±4.53% vs. -17.39±3.84%, p=0.013), GLS (-12.73±4.58% vs. -17.88±4.34%, p=0.003), and GRS (32.89±14.14% vs. 49.18±14.01%, p=0.002) (table 55). The 3D strains of the patients from the iCM group, obtained from six consecutive cardiac cycles, were also significantly lower compared to the no inflammation group: GAS (-22.76±6.59% vs. -29.00%±5.49%, p=0.011), GCS (-13.17±3.74% vs. -16.23±2.65%, p=0.03), GLS (-12.89±4.05% vs. -16.78±3.62%, p=0.01), and GRS (33.71±12.03% vs. 45.87±11.29%, p=0.007) (table 55, figures 8-11).

Most impaired were the values of 3D GAS, GCS, GLS and GRS among the patients from the DCM group (table 55).

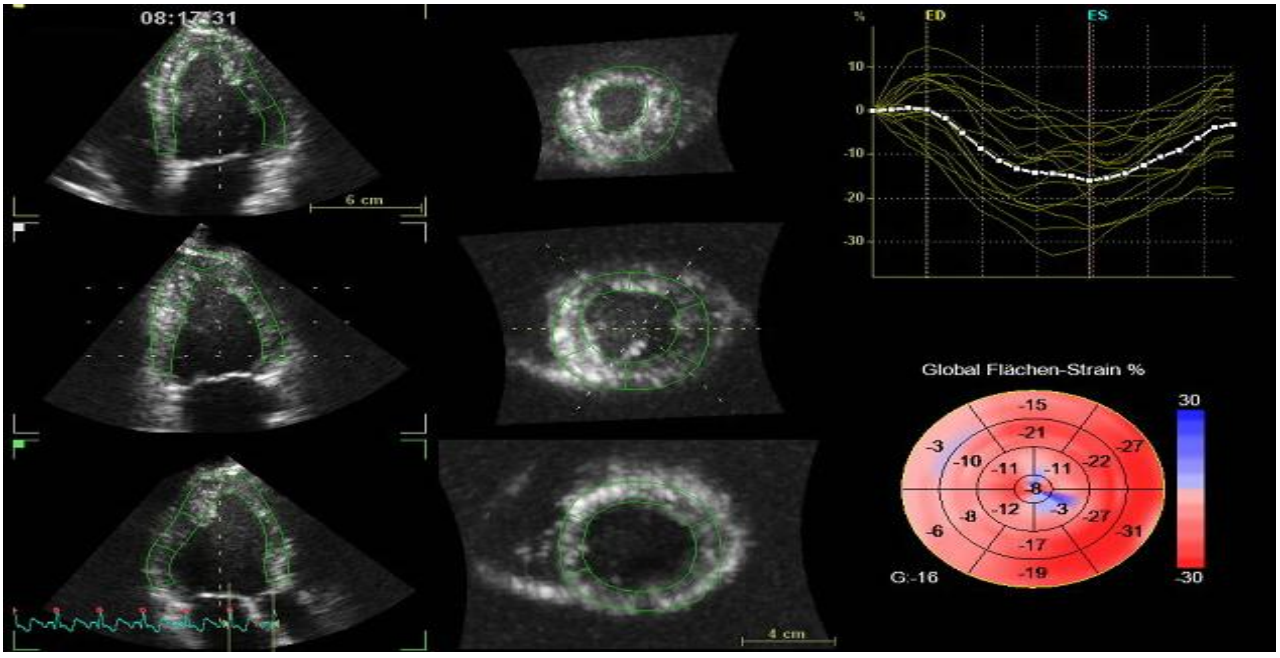

(a)

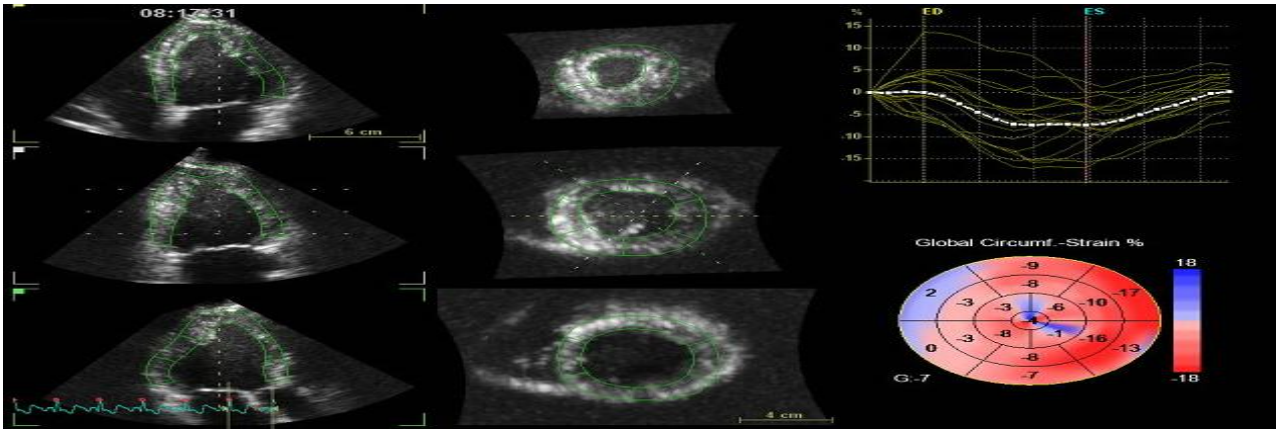

(b)

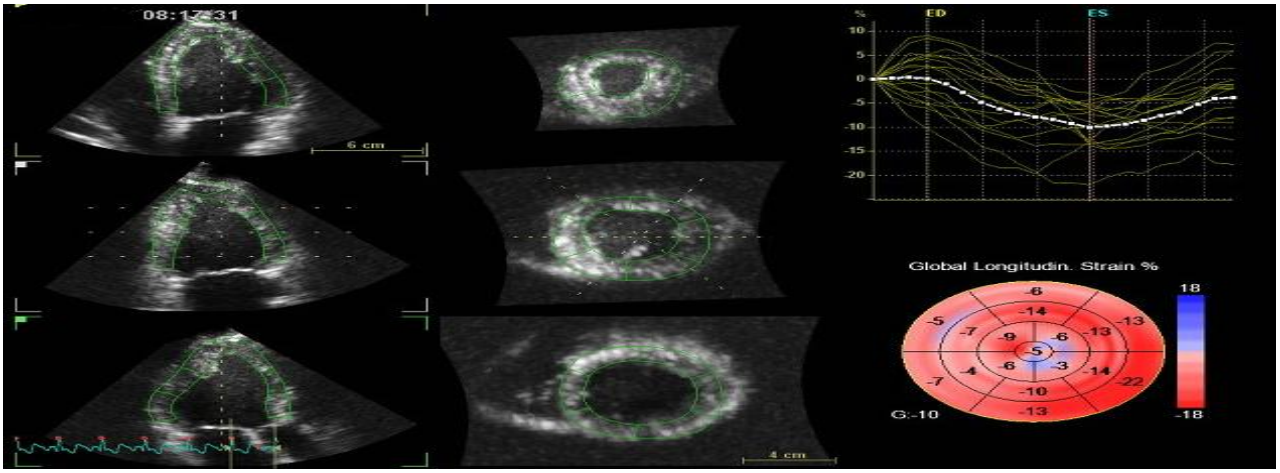

(c)

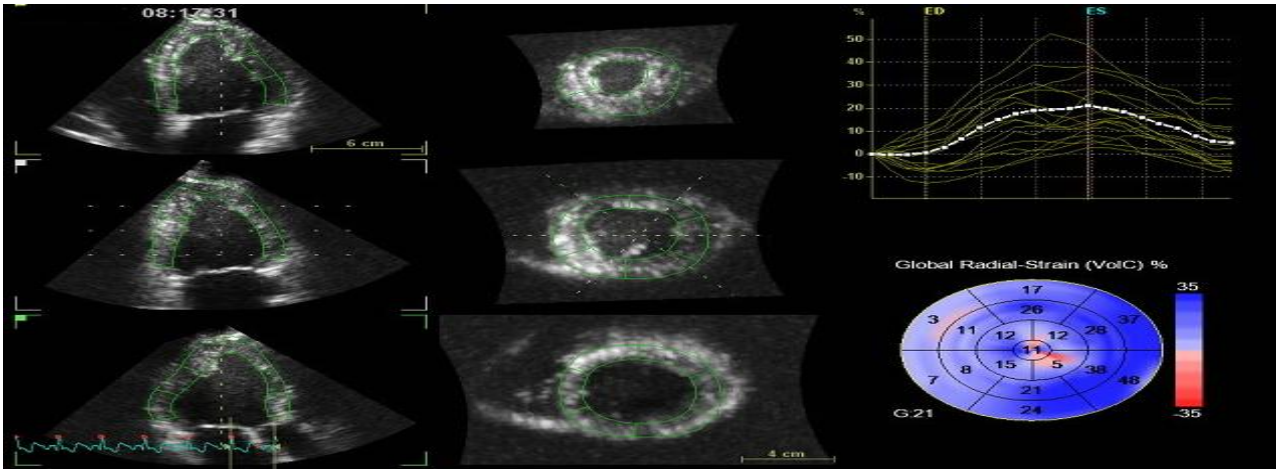

(d)

Figure 7. Impaired 3D strains: GAS (a), GCS (b), GLS (c) and GRS (d) in a patient with iCM. The 3D strains were measured in 6 consecutive cardiac cycles.

Table 55. 3D speckle tracking parameters among the groups studied (variable expressed as mean ± SD deviation)

Groups / 3D strain parameters	Group 1		Group 2		Group 3		P value			
							1:2	1:3	2:3	Overall
	n	Mean (±SD)	n	Mean (±SD)	n	Mean (±SD)				
GAS 4 cycles, %	15	-30.01 (±6.12)	9	-19.76 (±5.15)	20	-22.09 (±7.46)	0.002*	0.003*	1.000	0.001*
GCS 4 cycles, %	15	-17.39 (±3.84)	9	-10.80 (±3.02)	20	-13.22 (±4.53)	0.001*	0.013*	0.429	0.001*
GLS 4 cycles, %	15	-17.88 (±4.34)	9	-12.22 (±3.22)	20	-12.73 (±4.58)	0.009*	0.003*	1.000	0.001*
GRS 4 cycles, %	15	49.18 (±14.01)	9	28.17 (±8.44)	20	32.89 (±14.14)	0.001*	0.002*	1.000	<0.001*
GAS 6 cycles, %	13	-29.00 (±5.49)	11	-16.69 (±4.48)	24	-22.76 (±6.59)	<0.001*	0.011*	0.021*	<0.001*
GCS 6 cycles, %	13	-16.23 (±2.65)	11	-9.01 (±2.88)	24	-13.17 (±3.74)	<0.001*	0.030*	0.003*	<0.001*
GLS 6 cycles, %	13	-16.78 (±3.62)	11	-10.12 (±2.49)	24	-12.89 (±4.05)	<0.001*	0.010*	0.126	<0.001*
GRS 6 cycles, %	13	45.87 (±11.29)	11	22.34 (±6.96)	23	33.71 (±12.03)	<0.001*	0.007*	0.019*	<0.001*

Asterisk denotes statistical significance. 4 cycles indicates 3D strain parameters measured in 4 consecutive cardiac cycles, 6 cycles indicates 3D strain parameters measured in 6 consecutive cardiac cycles.

The 3D GLS measured in patients with iCM in four consecutive cardiac cycles were insignificantly lower (as an absolute value) than the 2D GLS measured in the same patients (-12.73± 4.58% vs. -13.41±4.91%, p=0.292) (table 56). The same situation was observed for 3D GLS measured in six cardiac cycles versus 2D GLS (-12.89±4.05% vs. -13.96±4.73%, p=0.089) (table 56). In the DCM group, no statistically significant difference was observed between 3D and 2D GLS. In the no inflammation group, the 3D GLS measured in 4 consecutive heart cycles was insignificantly lower than the 2D GLS (-17.88±4.34% vs. -19.59%±3.35%, p=0.221). However, statistically significant difference was detected between 3D GLS measured in 6 consecutive cardiac cycles and 2D GLS (-16.78±3.62% vs. -19.27±3.48%, p=0.042) (table 56).

Table 56. Comparison of 2D and 3D GLS in the population studied

	Group 1			Group 2			Group 3		
	n	Mean ± SD	P value	n	Mean ± SD	P value	n	Mean ± SD	P value
2D GLS	15	-19.59± 3.35	0.221	9	-12.12± 3.91	0.878	20	-13.41± 4.91	0.292
3D GLS 4 cycles	15	-17.88± 4.34		9	-12.22± 3.22		20	-12.73± 4.58	
2D GLS	13	-19.27± 3.48	0.042*	11	-11.67± 3.98	0.066	24	-13.96± 4.73	0.089
3D GLS 6 cycles	13	-16.78± 3.62		11	-10.12± 2.49		24	-12.89± 4.05	

Asterisk indicates statistical significance. 3D GLS 4 cycles indicates GLS measured with 3D speckle tracking in 4 consecutive cardiac cycles, 3D GLS 6 cycles indicates GLS measured with 3D speckle tracking in 6 consecutive cardiac cycles.

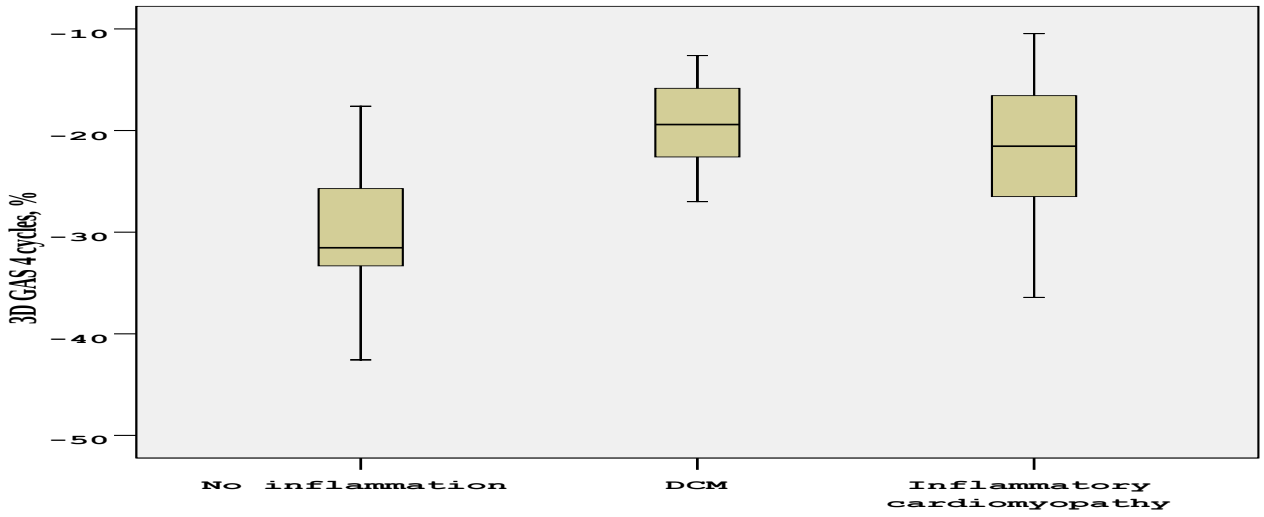

Figure 8. 3D GAS among the groups studied. 3D GAS 4 cycles indicates GAS measured with 3D speckle tracking in 4 consecutive cardiac cycles. DCM indicates dilated cardiomyopathy group. Inflammatory cardiomyopathy indicates iCM group. No inflammation indicates no inflammation group.

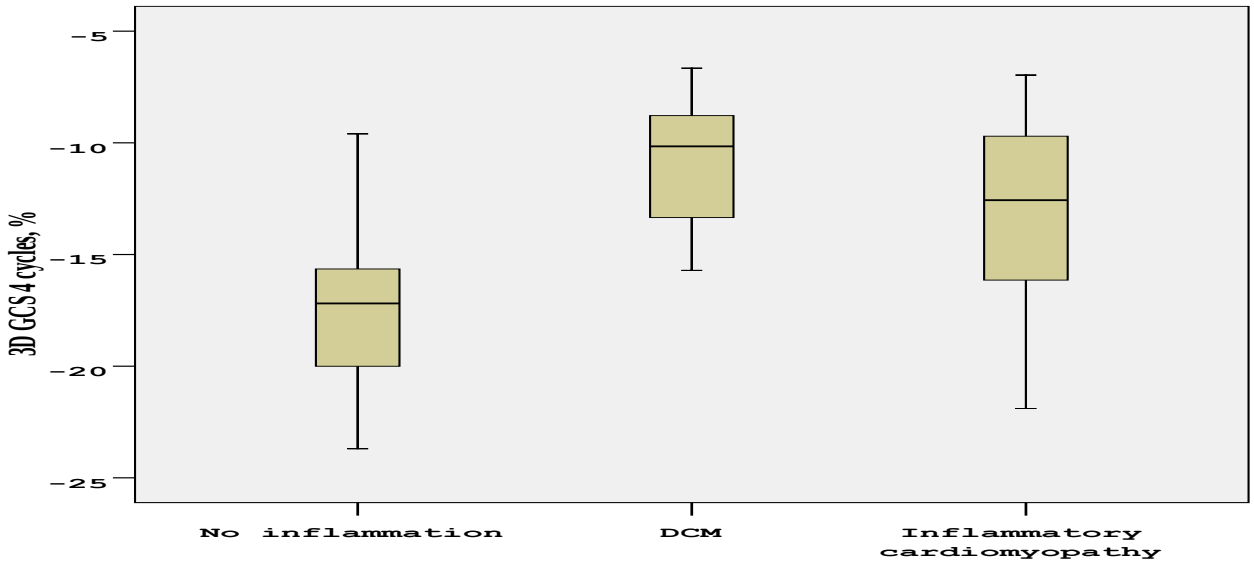

Figure 9. 3D GCS among the groups studied. 3D GCS 4 cycles indicates GCS measured with 3D speckle tracking in 4 consecutive cardiac cycles. DCM indicates dilated cardiomyopathy group. Inflammatory cardiomyopathy indicates iCM group. No inflammation indicates no inflammation group.

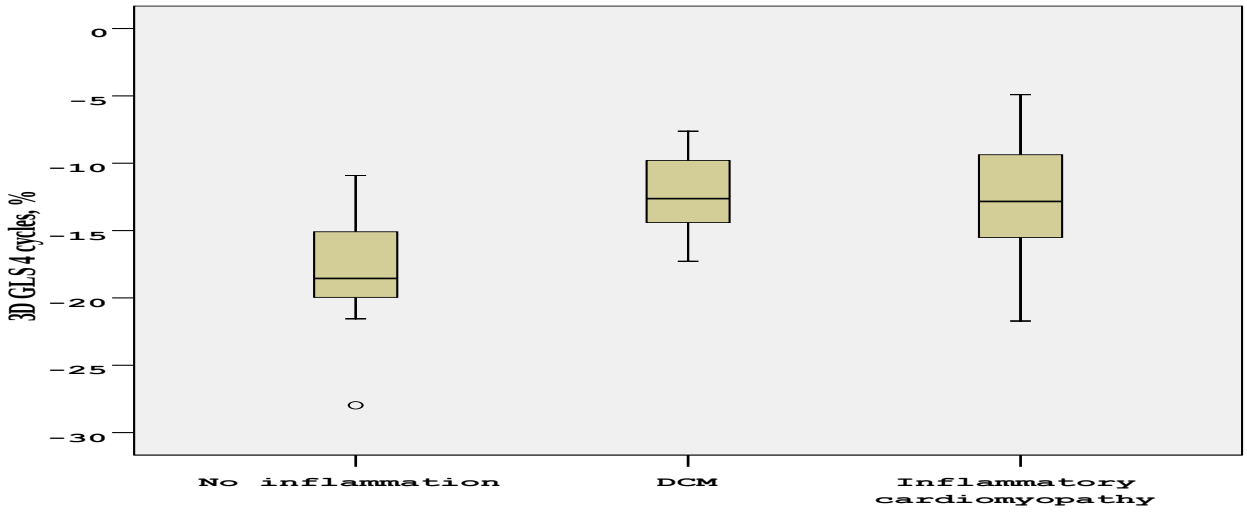

Figure 10. 3D GLS among the groups studied. 3D GLS 4 cycles indicates GLS measured with 3D speckle tracking in 4 consecutive cardiac cycles, DCM indicates dilated cardiomyopathy group, Inflammatory cardiomyopathy indicates iCM group, No inflammation indicates no inflammation group.

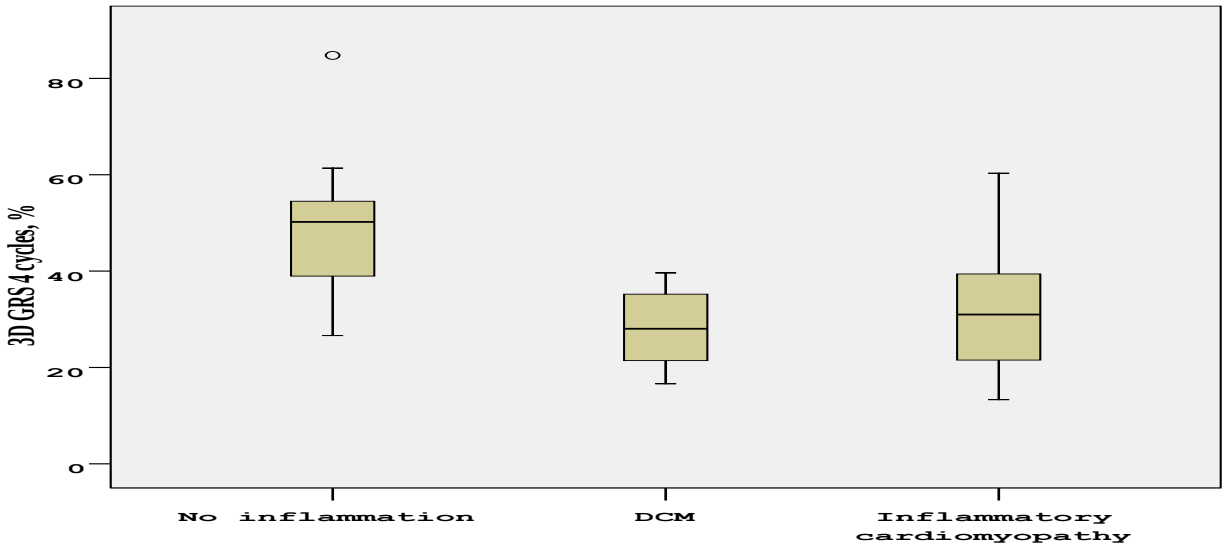

Figure 11. 3D GRS among the groups studied. 3D GRS 4 cycles indicates GRS measured with 3D speckle tracking in 4 consecutive cardiac cycles, DCM indicates dilated cardiomyopathy group, Inflammatory cardiomyopathy indicates iCM group, No inflammation indicates no inflammation group.

4.3.2.3. Correlations between 2D longitudinal strain, strain rate parameters and other quantitative indicators

2D and 3D STE parameters were further analyzed. To investigate the independent clinical determinants of 2D GLS, GLSR, GLESR and GLASR, bivariate correlation analysis was performed. The age, height, weight, BMI and some echocardiographic parameters were entered as covariates (tables 57-64). Significant and strong correlation was found between 2D GLS and LVEF (r=-0.789, p<0.001) (figure 12), LVSF (r=-0.744, p<0.001), LVESD (r=0.719, p<0.001), LVEDD (r=0.601, p<0.001), LVESV (r=0.674, p<0.001) (table 59). 2D GLSR correlated very strongly with LVEF (r=-0.829, p<0.001). Strong correlation was detected between 2D GLSR and LVSF (r=-0.779, p<0.001), LVESD (r=0.775, p<0.001), LVEDD (r=0.676, p<0.001), LVESV (r=0.725, p<0.001) and LVEDV (r=0.622, p<0.001) (table 59). Significantly strong correlation was found between 2D GLESR and LVEF (r=0.713, p<0.001), LVSF (r=0.712, p<0.001), LVESD (r=-0.711, p<0.001), LVEDD (r=0.616, p<0.001), LVESV (r=0.657, p<0.001) (table 60) and with early diastolic mitral

annulus velocity from the septal annulus (E'sep) (r=0.752, p<0.001) (table 64). Strong correlation was observed between GLASR and LVEF (r=-0.654, p<0.001), and LVESD (r=-0.607, p<0.001) (table 60).

Table 57. Correlations between 2D GLS, GLSR and age, height, weight, BMI, and BSA in patients with iCM

	2D GLS			2D GLSR		
	n	Pearson correlation coefficient, r	P value	n	Pearson correlation coefficient, r	P value
Age	118	0.040	0.665	118	0.001	0.992
Height	109	0.201*	0.036	109	0.181	0.060
Weight	111	0.167	0.079	111	0.207*	0.030
BMI	108	0.086	0.377	108	0.148	0.126
BSA	108	0.190*	0.049	108	0.215*	0.025

Asterisk denotes statistically significant correlation.

Table 58. Correlations between 2D GLESR, GLASR and age, height, weight, BMI and BSA in patients with iCM

	2D GLESR			2D GLASR		
	n	Pearson correlation coefficient, r	P value	n	Pearson correlation coefficient, r	P value
Age	118	-0.089	0.339	109	0.142	0.140
Height	109	-0.239*	0.012	100	-0.080	0.426
Weight	111	-0.290*	0.002	102	-0.133	0.183
BMI	108	-0.216*	0.025	99	-0.116	0.254
BSA	108	-0.297*	0.002	99	-0.120	0.237

Asterisk indicates statistically significant correlation.

Table 59. Correlations between 2D GLS, GLSR and echocardiographic markers for LV systolic function, LV dimensions and volumes, left atrial sizes and volumes, RV functional echocardiographic paramaters.

	2D GLS			2D GLSR		
	n	Pearson correlation coefficient, r	P value	n	Pearson correlation coefficient, r	P value
LVEF	118	**-0.789***	**<0.001**	118	**-0.829***	**<0.001**
LVSF	89	**-0.744***	**<0.001**	89	**-0.779***	**<0.001**
IVS thickness	115	0.117	0.214	115	0.116	0.218
PW thickness	114	0.096	0.310	114	0.117	0.217
LVEDD	**115**	**0.601***	**<0.001**	**115**	**0.676***	**<0.001**
LVESD	89	**0.719***	**<0.001**	89	**0.775***	**<0.001**
LVEDV	105	0.537*	<0.001	**105**	**0.622***	**<0.001**
LVESV	**105**	**0.674***	**<0.001**	**105**	**0.725***	**<0.001**
LA diameter	103	0.504*	<0.001	103	0.562*	<0.001
LA volume	102	0.492*	<0.001	102	0.542*	<0.001
TAPSE	112	-0.582*	<0.001	112	0.575*	<0.001

Asterisk denotes statistically significant correlation, Pearson correlation coefficients are bolded in the case of significant and strong or very strong correlation (r=0.60-0.79 indicates strong correlation, and r=0.80-1.00 indicates very strong correlation).

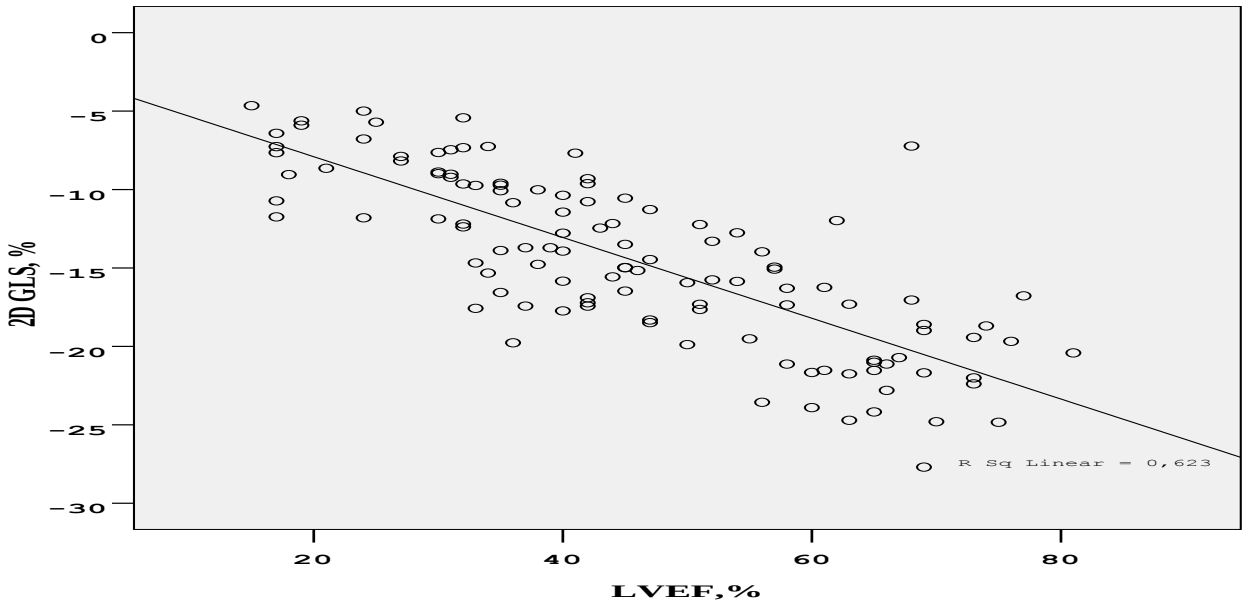

Figure 12. Negative correlation between left ventricular ejection fraction (LVEF) and two-dimensional (2D) global longitudinal strain (GLS) in patients with iCM (squared Pearson correlation coefficient – R^2=0.623, p<0.001). R Sq linear indicates squared Pearson correlation coefficient.

Table 60. Correlations between 2D GLESR, GLASR and echocardiographic markers for LV systolic function, LV dimensions and volumes, left atrial sizes and volumes, RV functional echocardiographic paramaters.

	2D GLESR			2D GLASR		
	n	Pearson correlation coefficient, r	P value	n	Pearson correlation coefficient, r	P value
LVEF	118	**0.713***	**<0.001**	**109**	**0.654***	**<0.001**
LVSF	89	**0.712***	**<0.001**	83	0.578*	<0.001
IVS thickness	115	-0.239*	0.010	106	0.044	0.657
PW thickness	114	-0.181	0.054	105	0.112	0.256
LVEDD	**115**	**-0.616***	**<0.001**	106	-0.552*	<0.001
LVESD	89	**-0.711***	**<0.001**	**83**	**-0.607***	**<0.001**
LVEDV	105	-0.576*	<0.001	97	-0.442*	<0.001
LVESV	**105**	**-0.657***	**<0.001**	97	-0.573*	<0.001
LA diameter	103	-0.488*	<0.001	96	-0.452*	<0.001
LA volume	102	-0.430*	<0.001	94	-0.475*	<0.001
TAPSE	112	0.471*	<0.001	103	0.506*	<0.001

Asterisk indicates statistically significant correlation, Pearson correlation coefficients are bolded in the case of significant and strong correlation (r=0.60-0.79 indicates strong correlation).

2D GLS correlated strongly with the maximal velocity across the LVOT (r=-0.642, p<0.001) (table 61), and with the early diastolic mitral annulus velocity from the septal annulus (E' septal) (r=-0.675, p<0.001) (table 63). GLSR correlated strongly with the maximal velocity across the LVOT (r=-0.671, p<0.001) (table 61), and with the early diastolic mitral annulus velocity from the septal annulus (E' septal) (r=-0.696, p<0.001) (table 63).

Table 61. Correlations between 2D GLS, GLSR and maximal LV outflow tract velocity (LVOT Vmax), and maximal velocity (Vmax) across the aortic, tricuspid and pulmonary valves

	2D GLS			2D GLSR		
	n	Pearson correlation coefficient, r	P value	n	Pearson correlation coefficient, r	P value
LVOT Vmax	**112**	**-0.642***	**<0.001**	**112**	**-0.671***	**<0.001**
AoV Vmax	109	-0.113	0.244	109	-0.113	0.244
TV Vmax	69	-0.225	0.063	69	-0.251*	0.037
PV Vmax	87	0.365*	0.001	87	-0.306*	0.004

Asterisk denotes statistically significant correlation. AoV indicates aortic valve, LVOT indicates left ventricular outflow tract, PV indicates pulmonary valve, TV indicates tricuspid valve, Vmax indicates maximal velocity across the valve/ outflow tract. Pearson correlation coefficients are bolded in the case of significant and strong correlation (r=0.60-0.79 indicates strong correlation).

Table 62. Correlations between 2D GLESR, GLASR and maximal LVOT velocity (LVOT Vmax), and maximal velocity (Vmax) across the aortic, tricuspid and pulmonary valves

	2D GLESR			2D GLASR		
	n	Pearson correlation coefficient, r	P value	n	Pearson correlation coefficient, r	P value
LVOT Vmax	112	0.560*	<0.001	104	0.569*	<0.001
AoV Vmax	109	0.059	0.544	101	0.290*	0.003
TV Vmax	69	0.267*	0.027	61	0.160	0.218
PV Vmax	87	0.215*	0.045	81	0.339*	0.002

Asterisk indicates statistically significant correlation.

Table 63. Correlations between 2D GLS, 2D GLSR, conventional Doppler and TD echocardiographic parameters

	2D GLS			2D GLSR		
	n	Pearson correlation coefficient, r	P value	n	Pearson correlation coefficient, r	P value
VE	115	0.083	0.379	115	0.042	0.655
VA	106	-0.196*	0.044	106	-0.190	0.051
E/A ratio	106	0.284*	0.003	106	0.265*	0.006
E' septal	**83**	**-0.657***	**<0.001**	**83**	**-0.696***	**<0.001**
E' lateral	93	-0.439*	<0.001	93	-0.410*	<0.001
E/E' septal ratio	83	0.580*	<0.001	83	0.571*	<0.001
E/E' lateral ratio	93	0.435*	<0.001	93	0.435*	<0.001

VE – indicates early diastolic mitral inflow velocity, VA indicates late diastolic mitral inflow velocity, E' sep indicates early diastolic mitral annulus velocity from the septal annulus, E' lat indicates early diastolic mitral annulus velocity from the lateral annulus. Pearson correlation coefficients are bolded in the case of significant and strong correlation (r=0.60-0.79 indicates strong correlation).

Table 64. Correlations between 2D GLESR, GLASR, conventional Doppler, and TD echocardiographic parameters

	2D GLESR			2D GLASR		
	n	Pearson correlation coefficient, r	P value	n	Pearson correlation coefficient, r	P value
VE	115	0.127	0.175	107	-0.296*	0.002
VA	106	0.001	0.993	104	0.465*	<0.001
E/A ratio	106	-0.029	0.765	104	-0.556*	<0.001
E' septal	**83**	**0.752***	**<0.001**	78	0.237*	0.037
E' lateral	93	0.564*	<0.001	88	0.051	0.637
E/E' septal ratio	83	-0.492*	<0.001	78	-0.410*	<0.001
E/E' lateral ratio	93	-0.394*	<0.001	88	-0.284*	0.007

Asterisk denotes statistically significant correlation, Pearson correlation coefficients are bolded in the case of significant and strong correlation (r=0.60-0.79 indicates strong correlation). VE – indicates early diastolic mitral inflow velocity, VA indicates late diastolic mitral inflow velocity, E' sep indicates early diastolic mitral annulus velocity from the septal annulus, E' lat indicates early diastolic mitral annulus velocity from the lateral annulus.

4.3.2.4. Correlations between 2D longitudinal strain, strain rate parameters and EMB quantitative indicators in patients with iCM

Bivariate correlation analysis was performed in order to detect the correlation between 2D GLS, GLSR, GLESR, GLASR and EMB quantitative markers in patients with iCM (tables 65, 66). Statistically significant correlation was detected between 2D GLSR, GLESR, GLASR and the cardiomyocyte diameter, although the strength of the Pearson correlation coefficient was moderate and weak, resp. ($r = 0.455$, $p<0.001$; $r = -0.456$, $p<0.001$; $r = -0.368$, $p<0.001$, resp.) (tables 65, 66).

Table 65. Correlations between 2D GLS, GLSR and EMB immunohistological findings in patients with iCM

	2D GLS			2D GLSR		
	n	Pearson correlation coefficient, r	P value	n	Pearson correlation coefficient, r	P value
CD3 lymphocyte count	112	0.110	0.247	112	0.133	0.163
Macrophage count	115	-0.013	0.891	115	-0.004	0.964
CD45 RO memory cell count	81	0.095	0.398	81	0.112	0.320
Cardiomyocyte diameter	115	-0.161	0.086	115	0.455*	<0.001

Asterisk indicates statistically significant correlation.

Table 66. Correlations between 2D GLESR, GLASR and EMB immunohistological findings in patients with iCM

	2D GLESR			2D GLASR		
	n	Pearson correlation coefficient, r	P value	n	Pearson correlation coefficient, r	P value
CD3 lymphocyte count	112	0.003	0.976	103	-0.039	0.692
Macrophage count	115	0.115	0.220	106	0.045	0.644
CD45 RO memory cell count	81	0.054	0.630	74	-0.021	0.859
Cardiomyocyte diameter	115	-0.456*	<0.001	106	-0.368*	<0.001

Asterisk denotes statistically significant correlation.

4.3.2.5. Correlations between 2D longitudinal strain, strain rate parameters and laboratory markers in patients with iCM

Significant correlations were detected between 2D GLS and troponin T level, NTproBNP level and HDL-cholesterol level (r=-0.330, p=0.046; r=0.582, p<0.001; r=-0.334, p=0.013, resp.) (table 67). 2D GLSR correlated significantly with NTproBNP level (r=-0.505, p<0.001) (table 68). 2D GLESR correlated significantly with troponin T level and NTproBNP level (r=0.328, p=0.047; r=-0.365, p=0.013) (table 68). 2D GLASR correlated significantly with NTproBNP level (r=-0.554, p<0.001) (table 68).

Table 67. Correlations between 2D GLS, GLSR, cardiac biomarkers and cholesterol levels in patients with iCM

	2D GLS			2D GLSR		
	n	Pearson correlation coefficient, r	P value	n	Pearson correlation coefficient, r	P value
Troponin T level	37	-0.330*	0.046	37	-0.219	0.192
CK level	96	-0.063	0.540	96	-0.048	0.646
CK MB fraction level	81	-0.092	0.416	81	-0.117	0.298
NTproBNP level	46	0.582*	<0.001	46	0.505*	<0.001
Total cholesterol level	55	-0.215	0.116	55	-0.125	0.364
LDL cholesterol level	54	-0.192	0.165	54	-0.110	0.431
HDL cholesterol level	54	-0.334*	0.013	54	-0.279*	0.041

Asterisk indicates statistically significant correlation.

Table 68. Correlations between 2D GLESR, GLASR, cardiac biomarkers and cholesterol levels in patients with iCM

		2D GLESR			2D GLASR	
	n	Pearson correlation coefficient, r	P value	n	Pearson correlation coefficient, r	P value
Troponin T level	37	0.328*	0.047	33	0.258	0.146
CK level	96	0.006	0.952	89	0.118	0.270
CK MB fraction level	81	0.089	0.430	75	0.109	0.351
NTproBNP level	46	-0.365*	0.013	40	-0.554*	<0.001
Total cholesterol level	55	0.070	0.611	51	0.184	0.195
LDL cholesterol level	54	0.076	0.587	50	0.149	0.302
HDL cholesterol level	54	0.291*	0.033	50	0.278*	0.050

Asterisk denotes statistically significant correlation.

4.3.2.6. Correlations between 3D strains and other quantitative indicators

To investigate the independent clinical determinants of 3D GAS, GCS, GLS and GRS correlation analysis was performed (tables 69-76). Strong correlations were observed between 3D GAS and the maximal velocity across the LVOT (r = -0.744, p<0.001) (table 73), LVEF (r=-0.623, p=0.003), LVEDD (r=0.642, p=0.003), LVESD (r=0.625, p=0.010), TAPSE (r=-0.622, p=0.006) (table 71) and early diastolic mitral annulus velocity from the septal annulus (r=-0.660, p=0.003) (table 75). 3D GCS correlated strongly with the maximal velocity across the LVOT (r = -0.748, P<0.001) (table 73), LVEF (r=-0.653, p=0.002), LVSF (r=-0.611, p=0.012), LVEDD (r=0.699, p=0.001), LVESD (r=0.680, p=0.004) (table 71), early diastolic mitral annulus velocity from the lateral annulus (r=-0.623, p=0.008) (table 75). 3D GLS and GRS correlated strongly and significantly with the maximal velocity across the LVOT (r = -0.700, p<0,001 and r = 0.756, p<0.001, resp.) (table 74). 3D GLS correlated strongly with early diastolic mitral annulus velocity from the septal annulus (E'sep) (r = -0.711, p<0.001) (table 76), with TAPSE (r=-0.648, p=0.004) (table 72). Strong correlation was detected between 3D GRS and LVEF (r=0.638, p=0.002), LVSF (r=0.634, p=0.008), LVEDD (r=-0.677, p=0.001), LVESD (r=-0.676, p=0.004), TAPSE (r=0.625, p=0.006) (table 72), and with early diastolic mitral annulus velocity from the septal and lateral annulus (r=0.686, p=0.002 and r=0.615, p=0.009, resp.) (table 76).

Table 69. Correlations between 3D GAS, 3D GCS (4 cycles) and age, height, weight, BMI and BSA in patients with iCM

	3D GAS			3D GCS		
	n	Pearson correlation coefficient, r	P value	N	Pearson correlation coefficient, r	P value
Age	20	0.286	0.221	20	0.241	0.306
Height	18	0.410	0.091	18	0.314	0.204
Weight	18	0.360	0.142	18	0.196	0.435
BMI	18	0.030	0.905	18	-0.069	0.786
BSA	18	0.434	0.072	18	0.274	0.271

Table 70. Correlations between 3D GLS, 3D GRS (4 cycles) and age, height, weight, BMI and BSA in patients with iCM

	3D GLS			3D GRS		
	n	Pearson correlation coefficient, r	P value	n	Pearson correlation coefficient, r	P value
Age	20	0.291	0.214	20	-0.302	0.196
Height	18	0.440	0.068	18	-0.427	0.077
Weight	18	0.483*	0.042	18	-0.403	0.097
BMI	18	0.144	0.569	18	-0.067	0.792
BSA	18	0.535*	0.022	18	-0.472*	0.048

Asterisk indicates statistically significant correlation.

Table 71. Correlations between 3D GAS, 3D GCS (4 cycles) and echocardiographic markers for LV systolic function, LV dimensions and volumes, left and right atrial sizes and volumes, RV functional echocardiographic paramaters, dimensions and PAP

	3D GAS			3D GCS		
	n	Pearson correlation coefficient, r	P value	n	Pearson correlation coefficient, r	P value
LVEF	**20**	**-0.623***	**0.003**	**20**	**-0.653***	**0.002**
LVSF	16	-0.578*	0.019	16	-0.611*	0.012
IVS thickness	19	0.362	0.128	19	0.318	0.184
PW thickness	19	0.354	0.137	19	0.269	0.266
LVEDD	**19**	**0.642***	**0.003**	**19**	**0.699***	**0.001**
LVESD	**16**	**0.625***	**0.010**	**16**	**0.680***	**0.004**
LVEDV	17	0.205	0.429	17	0.182	0.484
LVESV	17	0.465	0.060	17	0.470	0.057
Aortic root	18	0.561*	0.015	18	0.418	0.085
LA diameter	18	0.518*	0.028	18	0.465	0.052
LA volume	18	0.586*	0.011	18	0.556*	0.017
RA volume	14	0.363	0.202	14	0.211	0.468
RV diameter	9	0.237	0.540	9	0.230	0.551
TAPSE	**18**	**-0.622***	**0.006**	18	-0.578*	0.012
Systolic PAP	14	0.418	0.137	14	0.491	0.075
Mean PAP	14	0.427	0.128	14	0.495	0.072

Asterisk denotes statistically significant correlation. Pearson correlation coefficients are bolded in the case of significant and strong correlation (r=0.6-0.79 indicates strong correlation).

Table 72. Correlations between 3D GLS, 3D GRS (4 cycles) and echocardiographic markers for LV systolic function, LV dimensions and volumes, left and right atrial sizes and volumes, RV functional echocardiographic paramaters, dimensions and PAP

	3D GLS				3D GRS	
	n	Pearson correlation coefficient, r	P value	n	Pearson correlation coefficient, r	P value
LVEF	20	-0.590*	0.006	**20**	**0.638***	**0.002**
LVSF	16	-0.555*	0.026	**16**	**0.634***	**0.008**
IVS thickness	19	0.433	0.064	19	-0.404	0.086
PW thickness	19	0.472*	0.042	19	-0.391	0.098
LVEDD	19	0.580*	0.009	19	**-0.677***	**0.001**
LVESD	16	0.570*	0.021	16	**-0.676***	**0.004**
LVEDV	17	0.224	0.387	17	-0.244	0.346
LVESV	17	0.451	0.069	17	-0.495*	0.043
Aortic root	18	0.590*	0.010	18	-0.565*	0.015
LA diameter	18	0.546*	0.019	18	-0.523*	0.026
LA volume	18	0.581*	0.011	18	-0.578*	0.012
RA volume	14	0.458	0.099	14	-0.342	0.231
RV diameter	9	0.174	0.655	9	-0.237	0.538
TAPSE	**18**	**-0.648***	**0.004**	**18**	**0.625***	**0.006**
Systolic PAP	14	0.411	0.145	14	-0.402	0.154
Mean PAP	14	0.423	0.132	14	-0.413	0.142

Asterisk indicates statistically significant correlation. Pearson correlation coefficients are bolded in the case of significant and strong correlation (r=0.6-0.79 indicates strong correlation).

Table 73. Correlations between 3D GAS, 3D GCS (4 cycles) and Vmax across the LVOT, aortic, tricuspid and pulmonary valves

	3D GAS			3D GCS		
	n	Pearson correlation coefficient, r	P value	n	Pearson correlation coefficient, r	P value
LVOT Vmax	**20**	**-0.744***	**<0.001**	**20**	**-0.748***	**<0.001**
AV Vmax	18	-0.461	0.054	18	-0.361	0.141
TV Vmax	9	-0.441	0.235	9	-0.312	0.414
PV Vmax	14	-0.507	0.064	14	-0.422	0.133

Asterisk denotes statistically significant correlation, Pearson correlation coefficients are bolded in the case of significant and strong correlation (r=0.6-0.79 indicates strong correlation).

Table 74. Correlations between 3D GLS, 3D GRS (4 cycles) and Vmax across the LVOT, aortic, tricuspid and pulmonary valves

	3D GLS			3D GRS		
	n	Pearson correlation coefficient, r	P value	n	Pearson correlation coefficient, r	P value
LVOT Vmax	**20**	**-0.700***	**0.001**	**20**	**0.756***	**<0.001**
AV Vmax	18	-0.485*	0.041	18	0.453	0.059
TV Vmax	9	-0.507	0.164	9	0.402	0.284
PV Vmax	14	-0.539*	0.047	14	0.521	0.056

Asterisk indicates statistically significant correlation, Pearson correlation coefficients are bolded in the case of significant and strong correlation (r=0.6-0.79 indicates strong correlation).

Table 75. Correlations between 3D GAS, 3D GCS (4 cycles), conventional Doppler and TD echocardiographic parameters

	3D GAS			3D GCS		
	n	Pearson correlation coefficient, r	P value	n	Pearson correlation coefficient, r	P value
VE	20	-0.018	0.938	20	0.047	0.844
VA	19	-0.144	0.558	19	-0.064	0.796
E/A ratio	19	0.144	0.557	19	0.104	0.671
E' septal	**18**	**-0.660***	**0.003**	18	-0.587*	0.011
E' lateral	17	-0.584*	0.014	**17**	**-0.623***	**0.008**
E/E' septal ratio	18	0.409	0.092	18	0.394	0.106
E/E' lateral ratio	17	0.352	0.166	17	0.446	0.072

Asterisk denotes statistically significant correlation. Pearson correlation coefficients are bolded in the case of significant and strong correlation (r=0.6-0.79 indicates strong correlation). VE – indicates early diastolic mitral inflow velocity, VA indicates late diastolic mitral inflow velocity, E' sep indicates early diastolic mitral annulus velocity from the septal annulus, E' lat indicates early diastolic mitral annulus velocity from the lateral annulus.

Table 76. Correlations between 3D GLS, 3D GRS (4 cycles), conventional Doppler and TD echocardiographic parameters

	3D GLS			3D GRS		
	n	Pearson correlation coefficient, r	P value	n	Pearson correlation coefficient, r	P value
VE	20	-0.026	0.913	20	0.020	0.933
VA	19	-0.175	0.473	19	0.114	0.644
E/A ratio	19	0.175	0.473	19	-0.122	0.620
E' septal	18	**-0.711***	**0.001**	**18**	**0.686***	**0.002**
E' lateral	17	-0.591*	0.012	**17**	**0.615***	**0.009**
E/E' septal ratio	18	0.426	0.078	18	-0.409	0.092
E/E' lateral ratio	17	0.317	0.215	17	-0.377	0.136

Asterisk indicates statistically significant correlation, Pearson correlation coefficients are bolded in the case of significant and strong correlation (r=0.6-0.79 indicates strong correlation). VE – indicates early diastolic mitral inflow velocity, VA indicates late diastolic mitral inflow velocity, E' sep indicates early diastolic mitral annulus velocity from the septal annulus, E' lat indicates early diastolic mitral annulus velocity from the lateral annulus.

4.3.2.7. Correlations between 3D strains and EMB quantitative indicators in patients with iCM

No significant correlations were found between 3D GAS, GCS, GLS, GRS and EMB quantitative markers in patients with iCM (tables 77, 78).

Table 77. Correlations between 3D GAS, GCS and EMB immunohistological findings in patients with iCM

	3D GAS			3D GCS		
	n	Pearson correlation coefficient, r	P value	n	Pearson correlation coefficient, r	P value
CD3 lymphocyte count	19	0.003	0.991	19	-0.167	0.493
Macrophage count	20	0.038	0.874	20	-0.116	0.625
CD45 RO memory cell count	15	-0.064	0.821	15	-0.298	0.280
Cardiomyocyte diameter	20	0.287	0.220	20	0.255	0.341

Table 78. Correlations between 3D GLS, GRS and EMB immunohistological findings in patients with iCM

	3D GLS			3D GRS		
	n	Pearson correlation coefficient, r	P value	n	Pearson correlation coefficient, r	P value
CD3 lymphocyte count	19	0.134	0.585	19	0.006	0.980
Macrophage count	20	0.150	0.527	20	-0.023	0.924
CD45 RO memory cell count	15	0.136	0.628	15	0.101	0.721
Cardiomyocyte diameter	20	0.325	0.162	20	-0.306	0.189

4.3.2.8. Correlations between 3D strains and laboratory markers in patients with iCM

Significant correlations were detected between 3D GAS and creatinine level, GFR, HbA1c, TSH and with HDL-cholesterol level (r=0.484, p=0.030; r=-0.582, p=0.007; r=-0.875, p= 0.002; r=0.472, p=0.048 and r=-0.557, p=0.048, resp.) (table 79, 81). 3D GCS correlated significantly with creatinine level, GFR, HbA1c and with TSH level (r=0.466, p=0.038; r=-0.573, p=0.008; r=-0.807, p=0.009 and r=0.469, p=0.050, resp.) (table 79). 3D GLS correlated significantly with creatinine level, GFR, HbA1c level and with HDL-cholesterol level (r=0.446, p=0.049; r=-0.541, p=0.014; r=0.884, p=0.002 and r=-0.587, p=0.035, resp.) (table 80, 82). 3D GRS correlated significantly with creatinine level, GFR and with HbA1c level (r=-0.516, p=0.002; r=0.607, p=0.005 and r=0.873, p=0.002, resp.) (table 80).

Table 79. Correlations between 3D GAS, GCS (4 cycles), leukocyte count and some biochemical parameters in patients with iCM

	3D GAS			3D GCS		
	n	Pearson correlation coefficient, r	P value	n	Pearson correlation coefficient, r	P value
Leukocyte count	20	-0.008	0.973	20	-0.049	0.836
CRP level	15	0.091	0.747	15	0.173	0.538
Creatinine level	20	0.484*	0.030	20	0.466*	0.038
GFR MDRD	20	-0.582*	0.007	20	-0.573*	0.008
HbA1c	**9**	**0.875***	**0.002**	**9**	**0.807***	**0.009**
TSH level	18	0.472*	0.048	18	0.469*	0.050

Asterisk denotes statistically significant correlation, Pearson correlation coefficients are bolded in the case of significant and very strong correlation (r=0.80-1.00 indicates very strong correlation).

Table 80. Correlations between 3D GLS, GRS (4 cycles), leukocyte count and some biochemical parameters in patients with iCM

	3D GLS			3D GRS		
	n	Pearson correlation coefficient, r	P value	n	Pearson correlation coefficient, r	P value
Leukocyte count	20	0.006	0.980	20	0.016	0.948
CRP level	15	0.046	0.871	15	-0.071	0.800
Creatinine level	20	0.446*	0.049	20	-0.516*	0.020
GFR MDRD	20	-0.541*	0.014	20	**0.607***	**0.005**
HbA1c	**9**	**0.884***	**0.002**	**9**	**0.873***	**0.002**
TSH level	18	0.392	0.108	18	-0.442	0.066

Asterisk indicates statistically significant correlation, Pearson correlation coefficients are bolded in the case of significant and strong or very strong correlation (r=0.6-0.79 indicates strong correlation; r=0.80-1.00 indicates very strong correlation).

Table 81. Correlations between 3D GAS, GCS (4 cycles), cardiac biomarkers and cholesterol levels in patients with iCM

	3D GAS			3D GCS		
	N	Pearson correlation coefficient, r	P value	n	Pearson correlation coefficient, r	P value
Troponin T level	10	-0.104	0.775	10	0.076	0.836
CK level	18	0.165	0.514	18	0.270	0.279
CK MB fraction level	16	-0.141	0.603	16	0.096	0.722
NTproBNP level	10	0.494	0.147	10	0.432	0.212
Total cholesterol level	13	-0.361	0.225	13	-0.277	0.360
LDL cholesterol level	13	-0.234	0.442	13	-0.172	0.573
HDL cholesterol level	13	-0.557*	0.048	13	-0.433	0.139

Asterisk denotes statistically significant correlation.

Table 82. Correlations between 3D GLS, GRS (4 cycles), cardiac biomarkers and cholesterol levels in patients with iCM

		3D GLS			3D GRS	
	N	Pearson correlation coefficient, r	P value	n	Pearson correlation coefficient, r	P value
Troponin T level	10	-0.166	0.646	10	0.049	0.894
CK level	18	0.089	0.726	18	-0.187	0.458
CK MB fraction level	16	-0.234	0.383	16	0.035	0.899
NTproBNP level	10	0.452	0.190	10	-0.439	0.205
Total cholesterol level	13	-0.378	0.203	13	0.333	0.267
LDL cholesterol level	13	-0.266	0.380	13	0.219	0.471
HDL cholesterol level	13	-0.587*	0.035	13	0.512	0.074

Asterisk indicates statistically significant correlation.

4.3.2.9. Correlations between 2D GLS and 3D strains in patients with iCM

We evaluated the correlations between 2D GLS, 3D GLS and 3D GAS, since the latter presents the variation in the surface area defined by the longitudinal and circumferential strain vectors. Very strong correlation coefficients were found for both 3D strains. Interesting is the fact that the 3D GLS and GAS measured in 4 consecutive cardiac beats showed stronger correlation than those obtained in 6 consecutive cardiac beats. The strongest correlation coefficient was detected between 3D GAS, measured in 4 consecutive cardiac cycles and 2D GLS, followed by 3D GLS measured in 4 cardiac cycles and 2D GLS (table 83).

Table 83. Correlations between 2D GLS, 3D GLS and 3D GAS in patients with iCM

		2D GLS	
	n	Pearson correlation coefficient, r	P value
3D GLS (4 cycles)	20	0.829	<0.001
3D GLS (6 cycles)	24	0.784	<0.001
3D GAS (4 cycles)	20	0.834	<0.001
3D GAS (6 cycles)	24	0.780	<0.001

4.3.3. Predictive value of conventional echocardiography, 2D longitudinal strain, strain rates and 3D strains

4.3.3.1. Predictive value of conventional echocardiographic parameters for iCM

We selected the conventional echocardiographic parameters, that were found to differ significantly between the no inflammation group and iCM group. Then we used ROC curves to determine the diagnostic value of these parameters for iCM (table 84).

Table 84. The ROC analysis of conventional echocardiographic parameters for prediction of iCM (group1:3)

	AUC	95% CI	P value	Cut-off	Sensitivity(%)	Specificity(%)
LVEF, %	0.705	0.634-0.776	<0.001	52.5	63.2	62.3
LVSF, %	0.653	0.559-0.746	0.006	29.5	60.5	57.1
IVS, mm	0.525	0.439-0.612	0.589	10.5	52.3	53.7
PW, mm	0.522	0.434-0.610	0.635	10.5	41.2	53.7
LVEDD, mm	0.637	0.552-0.723	0.003	52.5	62.4	60.4
LVESD, mm	0.652	0.556-0.747	0.006	36.5	61.2	60.5
LVEDV, ml	0.647	0.560-0.735	0.003	128.5	60.9	55.3
LVESV, ml	0.675	0.593-0.756	<0.001	59.5	62.6	61.7

CI – confidence interval

The LVEF showed the highest AUC. However, the sensitivity and specificity were not quite satisfactory. The diagnostic accuracy of the other conventional echocardiographic parameters was poor (table 84).

4.3.3.2. Predictive value of 2D longitudinal strain and strain rates

ROC curves for all evaluated 2D longitudinal strain and strain rates were obtained to test their accuracy in diagnosing iCM. Sensitivity, specificity, 95% confidence interval (CI) were calculated for the chosen cut-off points (table 85).

The ROC analysis of the 2D STE-derived parameters showed that 2D GLS and 2D GLESR had a moderate predictive value (area under the ROC curve: 0.71, 95%CI: 0.63–0.79, p<0.001 and 0.73, 95%CI: 0.65–0.81, p<0.001, resp.). A 2D GLS cut-off value of –17.57% yielded the best result

in terms of a combined sensitivity (72%) and specificity (66%). When we chose a cut-off value of -17.90%, we observed a slightly greater sensitivity (73.7%), but a lower specificity (62%) and when we chose -17.39% as a cut-off value, we had a lower sensitivity (69.5%) and a greater specificity (68%). 2D GLESR cut-off point of 1.36 s^{-1} had a sensitivity of 67% and specificity of 63%. A cut-off point of 1.39 s^{-1} showed a sensitivity of 70.6% and specificity of 60.9%, and a cut-off value of 1.34 s^{-1} had a sensitivity of 66.1% and specificity of 69.6%. 2D GLSR also had relatively high predictive value with an AUC of 0.685 (95%CI: 0.60-0.77, p<0.001), a cut-off point of -1.06 s^{-1} showed a sensitivity of 69% and specificity of 64%. For GLASR, the p-value was above 0.05, therefore, we could conclude that this STE parameter did not have significant diagnostic value in patients with iCM and could not be used to distinguish these patients from the patients without myocardial inflammation. The results of ROC analyses with an AUC for the 2D longitudinal strain and strain rates are shown in figures 13-15 and table 85.

Table 85. ROC analysis of 2D GLS, GLSR, GLESR and GLASR for prediction of iCM

	AUC	95% CI	P value	Cut-off	Sensitivity (%)	Specificity (%)
2D GLS, %	0.713	0.633-0.793	<0.001	-17.90	73.7	62
				-17.57	72	66
				-17.39	69.5	68
2D GLSR, s^{-1}	0.685	0.603-0.767	<0.001	-1.09	71.2	60
				-1.08	70.3	62
				-1.06	68.6	64
2D GLESR, s^{-1}	0.727	0.647-0.807	<0.001	1.39	70.6	60.9
				1.36	67	63
				1.34	66.1	69.6
2D GLASR, s^{-1}	0.573	0.475-0.671	0.153	0.93	60.6	50
				0.89	56	56.5
				0.85	51.4	58.7

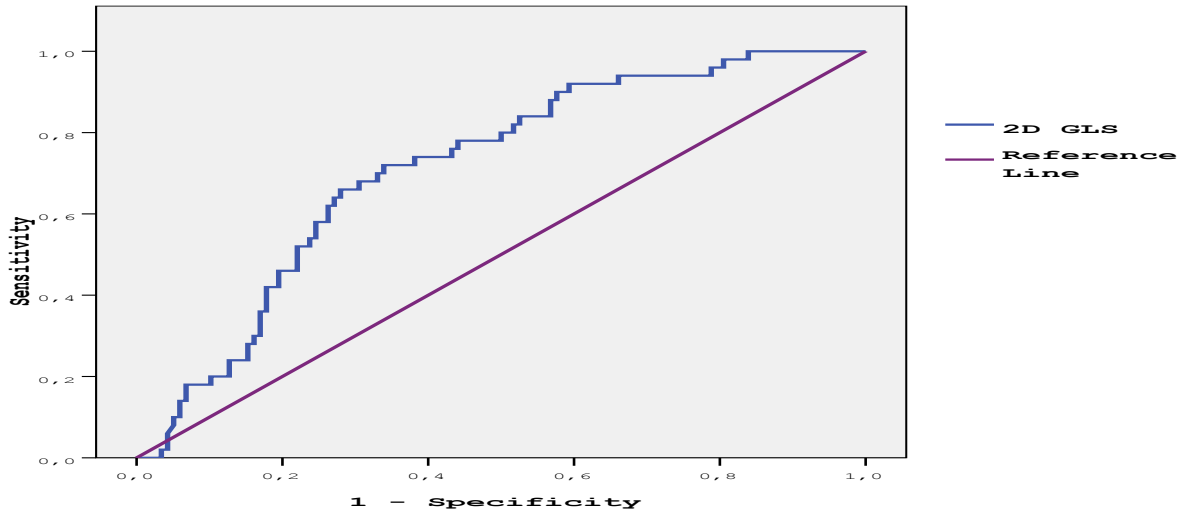

Figure 13. Receiver operating characteristic (ROC) curve of 2D GLS for prediction of iCM. The value of the area under the curve (AUC) indicates the significance of 2D GLS in identifying patients with iCM (AUC=0.713, p<0.001).

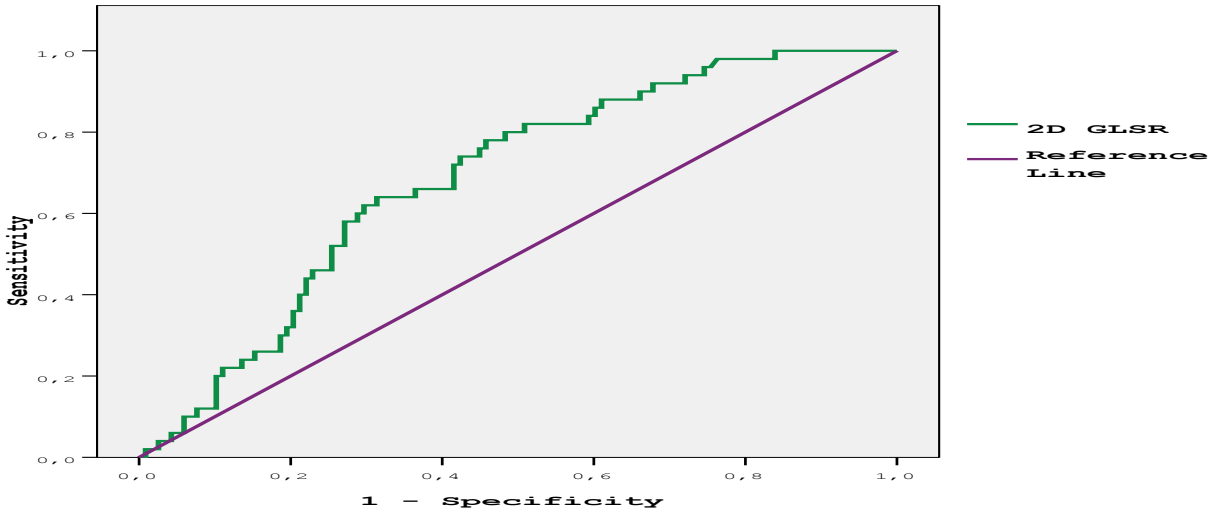

Figure 14. Receiver operating characteristic (ROC) curve of 2D GLSR for prediction of iCM. The value of the area under the curve (AUC) indicates the significance of 2D GLSR in identifying patients with iCM (AUC=0.685, p<0.001).

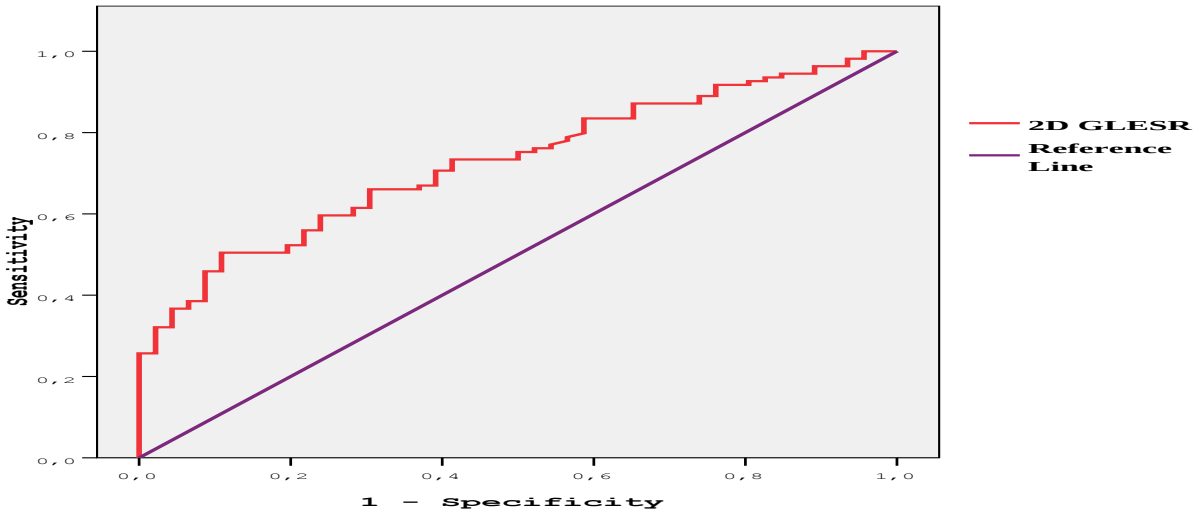

Figure 15. Receiver operating characteristic (ROC) curve of 2D GLESR for prediction of iCM. The value of the area under the curve (AUC) indicates the significance of 2D GLESR in identifying patients with iCM (AUC=0.727, p<0.001).

4.3.3.3. Predictive value of 3D strains

The ROC analysis showed that 3D strains could better predict the presence of iCM, compared to 2D longitudinal strain and strain rates (table 86).

The 3D strain parameters measured in 4 consecutive cardiac cycles showed better predictive value than those measured in 6 consecutive cardiac cycles. 3D GRS measured in 4 consecutive cardiac cycles showed the highest diagnostic value among the tested 3D strains, for prediction of iCM (AUC 0.790, 95%CI: 0.64–0.95, p=0.003) (table 86). 3D GRS cut-off point of 45.43% showed an optimal sensitivity of 80% and specificity of 66.7% in the detection of iCM. A cut-off value of 49.88% showed a better sensitivity – 85%, but a lower specificity – 60%, and the cut-off point of 38.19% showed a better specificity – 80%, but a lower sensitivity – 75%. The ROC curve is shown in figure 16.

3D GLS measured in 4 consecutive cardiac cycles also had a very high predictive value (AUC 0.790, 95%CI: 0.64–0.95, p=0.004), followed by 3D GAS and GCS measured in 4 consecutive cardiac cycles, which have equal predictive values (AUC 0.773, 95%CI: 0.62–0.93, p=0.006 for both). A cut-off point for 3D GLS of -15.79% showed a sensitivity of 80% and

specificity of 73.3%. When we chose -14.22% as a cut-off value, we observed a greater specificity – 87% and a lower sensitivity – 70%. The cut-off point of -16.87% showed a sensitivity of 85% and specificity of 67%. A cut-off point for 3D GCS of -16.10% showed an optimal sensitivity of 75% and specificity of 73% in the detection of iCM. The cut-off value of -16.31% demonstrated a better sensitivity – 80% and a lower specificity – 67%, and the cut-off value of -15.02% revealed a lower sensitivity – 65% and a better specificity – 80%. 3D GAS cut-off point of -28.77% showed a sensitivity of 80% and specificity of 67%, and a cut-off point of -25.09% demonstrated a sensitivity of 70% and specificity of 87% (table 86). The results of ROC analyses with an AUC are shown in figures 16-19.

Table 86. ROC analysis of 3D GAS, GCS, GLS and GRS for prediction of iCM

	AUC	95% CI	P value	Cut-off	Sensitivity (%)	Specificity (%)
4 cycles						
3D GAS, %	0.773	0.615-0.932	0.006	-28.77	80	66.7
				-25.09	70	86.7
3D GCS, %	0.773	0.617-0.930	0.006	-16.31	80	66.7
				-16.10	75	73.3
				-15.02	65	80
3D GLS, %	0.790	0.635-0.945	0.004	-16.87	85	66.7
				-15.79	80	73.3
				-14.22	70	86.7
3D GRS, %	0.793	0.641-0.946	0.003	49.88	85	60
				45.43	80	66.7
				38.19	75	80
6 cycles						
3D GAS, %	0.766	0.609-0.923	0.008	-28.47	79.2	69.2
				-24.92	66.7	76.9
3D GCS, %	0.750	0.587-0.913	0.013	-15.62	83.3	61.5
				-15.19	75	69.2
				-14.82	70.8	84.6
3D GLS, %	0.747	0.586-0.907	0.014	-16.03	75	69.2
				-13.84	66.7	84.6
3D GRS, %	0.772	0.618-0.927	0.007	42.73	79.2	69.2
				36.94	66.7	76.9

4 cycles indicates that the 3D strains were measured in 4 consecutive cardiac cycles, 6 cycles indicates that the 3D strains were measured in 6 consecutive cardiac cycles.

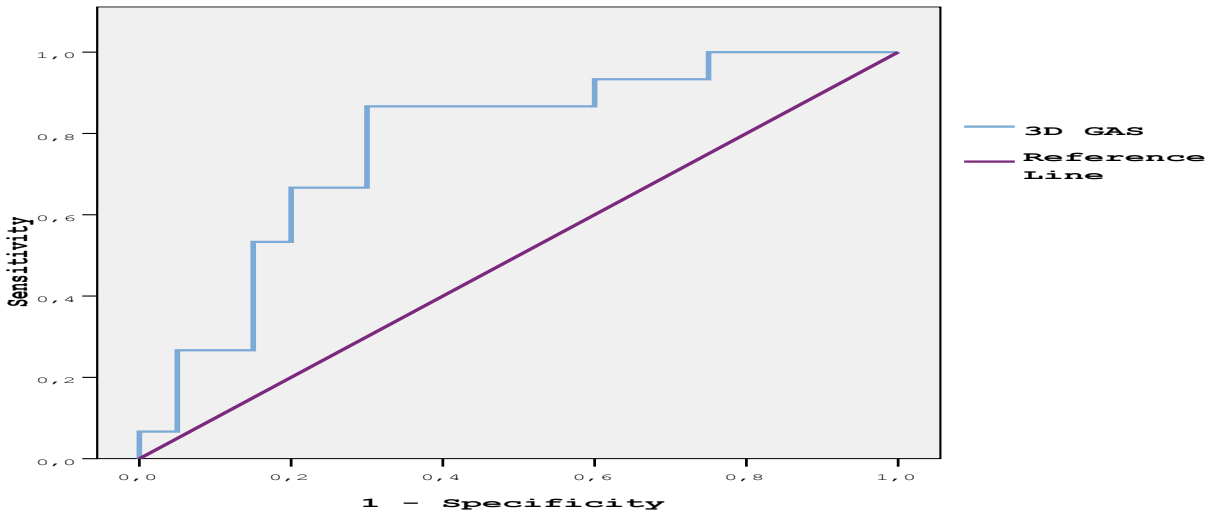

Figure 16. Receiver operating characteristic (ROC) curve of 3D GAS, measured in 4 consecutive cardiac cycles, for prediction of iCM. The high value for the area under the curve (AUC) indicates the value of 3D GAS in identifying patients with iCM (AUC=0.773, p=0.006).

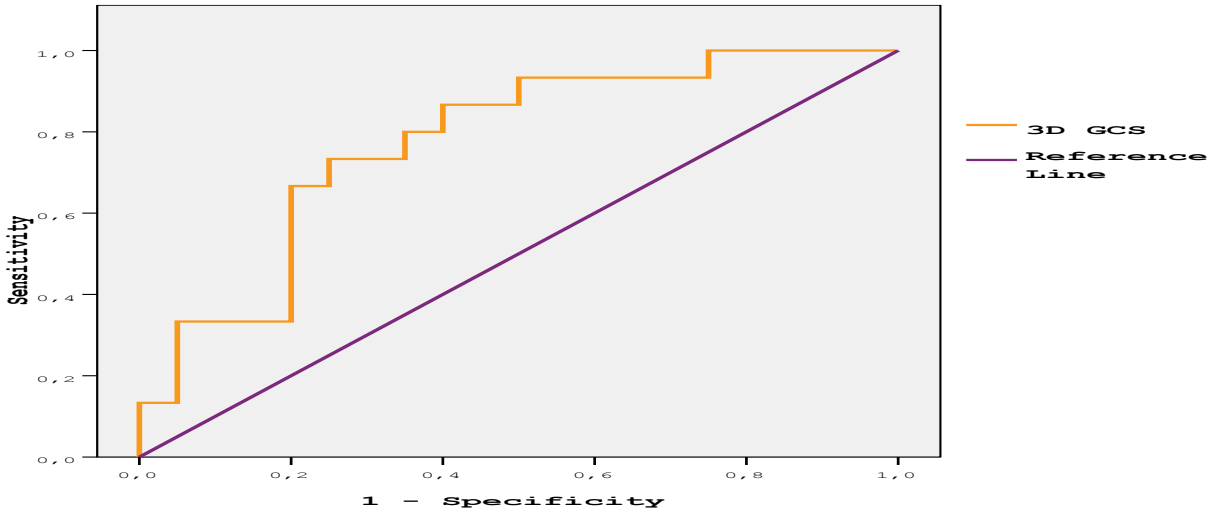

Figure 17. Receiver operating characteristic (ROC) curve of 3D GCS, measured in 4 consecutive cardiac cycles, for prediction of iCM. The high value for the area under the curve (AUC) indicates the value of 3D GCS in identifying patients with iCM (AUC=0.773, p=0.006).

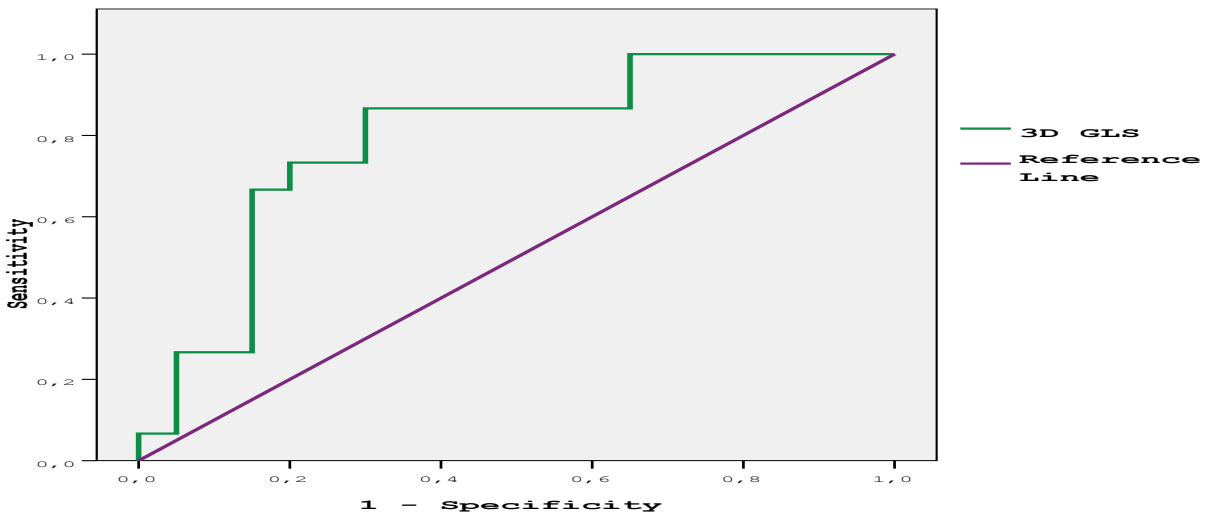

Figure 18. Receiver operating characteristic (ROC) curve of 3D GLS, measured in 4 consecutive cardiac cycles, for prediction of iCM. The high value for the area under the curve (AUC) indicates the value of 3D GLS in identifying patients with iCM (AUC=0.790, p=0.004).

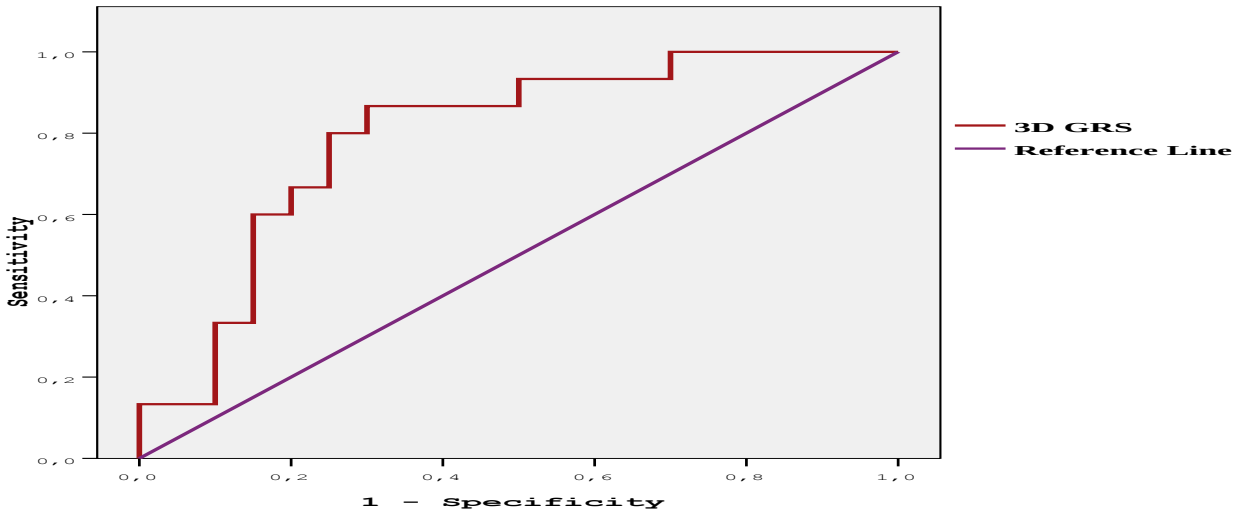

Figure 19. Receiver operating characteristic (ROC) curve of 3D GRS, measured in 4 consecutive cardiac cycles, for prediction of iCM. The high value for the area under the curve (AUC) indicates the value of 3D GRS in identifying patients with iCM (AUC=0.793, p=0.003).

5. Discussion

The aim of the study was to perform myocardial deformation analysis using both 2D and 3D STE in patients with suspected iCM and to test the diagnostic accuracy of these echocardiographic parameters. We aimed to search for parameters with a sufficient sensitivity and specificity to allow reliable recognition of myocardial inflammation and could help us to select patients, who would need further invasive diagnostic work-up.

The highly variable clinical manifestation, the unsatisfactory sensitivity and specificity of the non-invasive diagnostic methods and the reliance on myocardial biopsies for pathological confirmation lead to significant difficulties in establishing the diagnosis of iCM. EMB is still the gold standard for diagnosing iCM. However, it has a high specificity, but a low sensitivity, due to the patchy involvement of the myocardium and the high interobserver variability in interpretation.[30] Furthermore, it is not performed routinely due to many inherent risks[86] and fears of possible complications. The availability of new diagnostic modalities such as CMR imaging and echocardiographic strain and strain rate imaging will help to increase the appropriate identification of suspected cases. However, CMR has been found not to be accurate in patients with low-level or no inflammation[35] and in borderline myocarditis.[87]

Echocardiographic strain and strain rate imaging by 2D and 3D STE are novel methods, which quantitatively characterize myocardial deformation in longitudinal, radial and circumferential directions, which is not detectable by conventional echocardiography.

Cardiac strain imaging is less resource intensive, less expensive, portable, easily performed by a skilled operator, providing diagnostic quality images. 2D-STE is adopted by different vendors. Post-processing of 2D-STE is automated requiring minimal interpreter adjustment; however, the "normal" values vary between the vendors.[36]

Our study differed from other studies in this field in that it included patients with suspected iCM, because the latter include predominantly patients with acute myocarditis.

We should state the fact that all patients included in our study had suspected iCM, i.e. every patient had some symptoms or signs suggestive of iCM. The patients were divided into three groups according to the result of the EMB. Therefore, the individuals in the group with no inflammation are not the classic healthy controls. This is the explanation for having similar distribution of clinical

symptoms in the iCM group and the "no inflammation" group. Moreover some of the complaints, like AP, fatigue, etc. were more common in the no inflammation group.

Our results showed that such a highly available non-invasive imaging method as echocardiography might be a useful tool in diagnosing patients with iCM and could help in taking the decision who should undergo EMB. We found that 2D GLS and GLESR had high predictive value for iCM. Furthermore, 3D GAS, GLS, GCS and GAS showed even higher predictive values.

5.1. Patients' characteristics

It was found that there were significantly more male than female patients in the iCM group compared to the no inflammation group. The female to male ratio in the iCM group was 1:1.65. This result corresponds with the well-known fact that men are affected more often by myocarditis than women. According to recent trials and registries of myocarditis, the female to male ratio varies between 1:1.5 and 1:1.7.[12] A possible explanation for the male preponderance is the protective effect of hormonal influences on immune responses in women.[88]

No significant differences were detected between the three groups in respect to the mean age and BMI. The cardiovascular and the non-cardiovascular concomitant diseases, and the cardiovascular risk factors, the main clinical symptoms among the patients, were equally distributed between the groups. A statistically significant difference in the frequency of the LBBB between the three studied groups was found. It was most frequent in the DCM group – in 32% of the patients, followed by the iCM group – 13% and the no inflammation group – 9%. T-wave inversion was most common among the repolarization changes observed in the iCM group (25%), followed by ST-segment depression (11%) and ST-segment elevation (9%). However, no statistically significant differences were detected in regard to the remaining conduction disorders and repolarization abnormalities between the three groups. This corresponds with the literature data that none of the ECG abnormalities are pathognomonic for iCM. Furthermore, ECG has a low sensitivity in myocarditis.[9, 17]

The patients from the iCM group presented predominantly with symptoms of HF and AP. Considering the viral prevalence in the myocardium of these patients, we could conclude that our results are consistent with other reports demonstrating that HHV6 myocarditis, and combined

HHV6/PVB19 myocarditis, usually present with HF symptoms, and PVB19 myocarditis may mimic acute myocardial infarction.[89-92]

No significant differences were detected in regard to the level of hemoglobin and hematocrit, erythrocyte and thrombocyte counts between the no inflammation and the iCM groups. However, the leukocyte count was significantly higher in the iCM group compared to the no inflammation group. Furthermore, leukocytosis was more frequently observed among patients from the iCM group in comparison to the other two groups. However, the leukocyte count is not much increased in the iCM group. That could be explained by the fact that the leukocyte count rises briefly after an acute infection and in our study a long period of time has passed between the onset of the symptoms and the EMB and the blood tests. The CRP level, as an absolute value, was higher, although not significantly, in the iCM group in comparison to the no inflammation group. The lack of statistical significance could be due to lower percentage of patients tested in both groups (51.4% vs. 42.1%, resp.). Another probable explanation for the absence of statistical significance is the long time interval between the onset of the disease and the performance of the blood tests and the EMB. Since the level of CRP rises in acute inflammations, a possible explanation for its elevation is recent infection (i.e. bronchopulmonary). Therefore, this parameter has limited significance and could not be used for confirmation of the diagnosis of iCM. Nevertheless, we found that elevation of the CRP≥5 mg/L was significantly more frequently detected in the iCM group compared to the other two groups.

Among the cardiac biomarkers, only NTproBNP was significantly increased in the iCM group in comparison to the no inflammation group. The result corresponds with the symptoms of HF observed in the iCM group and could be useful in confirming or refuting the diagnosis of HF. Natriuretic peptide elevation may be partially caused by moderate to severe renal impairment. Such impairment was observed in 14.5% of the patients from the iCM group. In the study of Kasner et al., no statistically significant difference was detected between the patients from the acute myocarditis, the borderline myocarditis group and the no inflammation group in relation to the NTproBNP level.[35]

The level of troponin T was not significantly different between the three groups. The lack of statistically significant differences in the level of serum troponin is primarily due to the fact that few patients in the iCM group had acute myocarditis. Cardiac troponins are elevated mainly in patients with acute, early-onset myocarditis, who have ongoing myocardial necrosis. Another probable

explanation is the fact that the inflammatory process caused by myocarditis does not necessarily induce significant myocytolysis in all patients suffering from myocarditis.[37] Furthermore, the absence of increased levels does not exclude the presence of iCM; it usually suggests long-term presence of the disease. [3,9] Persistent elevations of cardiac enzymes in patients with myocarditis are indicative of ongoing necrosis.[21]

An interesting observation is the significantly lower level of HDL-cholesterol in patients with iCM compared to patients without inflammation. There is no special explanation for this finding. However, we should note that HDL-cholesterol was tested in 43.5% of the patients from the iCM group and in 45.6% of the patients from the no inflammation group. No statistically significant differences were detected in the level of the total cholesterol or other types of cholesterol.

5.2. Endomyocardial biopsy

5.2.1. Site of endomyocardial biopsy

In most of the cases, LV EMB was performed. Right-ventricular EMBs were performed in 18.84% of the patients from the iCM group and 7.02% of the patients from the no inflammation group. Only 1.45% of the patients from the iCM group and 3.51% of patients from the no inflammation group underwent biventricular EMBs.

A recent study found no significant difference in cardiac immune cell infiltration and CAMs between LV and RV EMB specimens. In respect to the viral persistence in the myocardium, the authors stated that only data of erythrovirus were reported owing to the low detection rate of HHV6 genomes in EMBs. No significant predominance was detected in erythrovirus prevalence between the left and right ventricle. However, morphological changes, like interstitial fibrosis, cardiac remodeling, and cardiomyocyte hypertrophy, were more frequently determined in LV EMBs. Pronounced or severe fibrosis was detected in LV EMB of 27.6% of the patients and in RV EMB of 4.6% of the patients. Furthermore, cardiac collagen type I protein expression was significantly elevated in LV compared to RV EMBs.[93]

Yilmaz et al. found that diagnostic EMB results were obtained significantly more often in patients with suspected myocarditis or nonischemic CM, who underwent biventricular EMBs as compared to those who underwent only selective LV or selective RV EMB. This finding could be

due to a significantly higher number of biopsy samples taken in patients undergoing biventricular EMB, thereby increasing the diagnostic yield of the procedure. Another observation from this study was that omitting the LV EMB would result in missing 18.7% of cases with myocardial inflammation, whereas by leaving out the RV EMB 7.9% of patients with inflammatory disease would be missed (p=0.002). The major complication rate was lowest for biventricular EMB (0.56%), followed by the LV EMB (0.64%), and was highest for the RV EMB (0.82%).[44]

5.2.2. Detection of viral genomes

No virus was detected in 18.1% of the patients from the iCM group, in 22.8% of the patients from the no inflammation group and in 25% of the patients from the DCM group. PVB19 with less than 500 ge were detected in 44.2% of the patients from the iCM group, in 33.3% of the patients from the no inflammation group and in 40% of the patients from the DCM group. Bock et al. suggested that PVB19 load of more than 500 ge per microgram in EMB specimens is a clinically relevant threshold for the maintenance of myocardial inflammation.[43] Considering the above-mentioned statement, we could conclude that 62.3% of the patients from the iCM group, 56.1% of the patients from the no inflammation group and 65% of the patients from the iCM group were virus negative.

PVB19 with more than 500 ge per microgram was found to be prevalent among all viruses detected in the biopsy specimens of the patients from the three group studied (table 19). The combination of PVB19 and HHV6 type B was the second most frequently observed intramyocardial viral infection, followed by HHV6 type B alone (table 19). Enteroviruses (including coxsackievirus), which were the most frequently identified intramyocardial viruses in patients with myocarditis during the second half of the 20th century, were detected in only two patients from the iCM. Adenoviruses, which were also very frequently identified in the EMB specimens during the second half of the 20th century in patients with myocarditis, were not detected in the myocardium of any patient from the groups studied. However, the PVB19 and other viruses could be detected also in healthy transplant donors, in autoptic samples without myocarditis or with borderline myocarditis and in patients undergoing EMB for other reasons. Furthermore, it should be underlined that the presence of viral genomes does not automatically imply a direct role of viruses in the pathogenesis of myocarditis, since an infective agent detected by PCR may be just an innocent bystander.[23]

Our results are in contrast to reports that enteroviruses and adenoviruses are the most frequently detected viruses in EMB specimens from patients with myocarditis.[94, 95] and may indicate a shift of the type of virus causing myocarditis.[90]

Our results partially correspond with those received from Kühl et al., who enrolled 172 consecutive patients in whom PCR analysis had detected viral genomes in the EMB sample at the initial clinical presentation. The authors found that in 36.6% of patients the EMBs were positive for PVB19, followed by enterovirus (32.6%). Dual infection with PVB19 and HHV6 was detected in 12.2% of the EMB specimens, 10.5% of the EMB specimens were positive for HHV6 and 8.1% for adenovirus. The mismatch in the percentage of enteroviruses and adenoviruses detected in the EMB samples of the patients in our study and study from Kühl et al could be due to the fact that the study of Kühl et al. was performed approximately 10 years before our study and the most commonly detected viral genomes in the myocardium could have changed.[46]

The distribution of viral prevalence in the myocardium in our study is largely in line to the findings reported by Mahrholdt et al. The latter group investigated 128 patients with clinical signs of myocarditis and found that PVB19 prevails in the EMB specimens, followed by HHV6 and combined PVB19/HHV6 infection. Coxsackie B viruses and EBV were detected only in one patient each.[90]

5.2.3. Histopathology and immunohistochemistry

The macrophages were the most frequently observed inflammatory cells in the intramyocardial inflammatory infiltrates. An increased number of macrophages was detected in 72.5% of the EMB specimens of the patients from the iCM group. Macrophages may be of great importance for the induction and progression of the inflammatory process caused when local release of cytokine activates the vascular endothelium and they are a prerequisite for the induction of AMs.[96-98] Since the activation of CAMs is related to the presence of inflammatory infiltrates, an evaluation of the expression of these molecules is another component of immunohistochemical diagnosis in myocardial inflammation.[99]

As expected, increased expression of endothelial CAMs from the immunoglobulin superfamily (HLA class I, ICAM-1 and VCAM-1) was significantly more frequently observed in the EMB specimens of the patents from the iCM group compared to the other two groups studied.

Increased expression of CAMs has previously been observed by other authors, who investigated patients with iCM.[85,96,97,99] The CAMs are considered independent pathogenic and diagnostic hallmarks of iCM.[85] The expression of endothelial CAMs constitutes an essential prerequisite for the adhesion of circulating immunocompetent cells to the endothelium of vessels and for the transendothelial migration of these cells in the myocardium. Therefore, in cases of myocardial inflammation, these immune mediators show an increased expression along with an elevation of T-lymphocytes in the myocardium. Vascular CAMs (VCAM-1) are expressed exclusively on activated endothelial cells, the tissue distribution of lymphocyte function antigen (LFA-3), ICAM-1, and HLA molecules comprises additionally interstitial cells (eg, immunocompetent infiltrates, histiocytes, dendritic cells, and fibroblasts).[99, 100]

The patients from the DCM group had a significantly increased cardiomyocyte diameter compared to the no inflammation and iCM group. Hypertrophied cardiomyocytes were significantly more frequently observed among the patients from the DCM group compared to the patients from the other two groups. Most often the patients from the no inflammation group had normal cardiomyocyte diameter. These results correspond with the fact that one of the characteristic markers of DCM at tissue level is cardiomyocyte hypertrophy.[101, 102] Cardiomyocyte hypertrophy has been found to be a determinant of clinical outcome in CM.[93] It was reported that the cardiomyocyte diameter was significantly increased in LV- in contrast to RV-EMBs.[93] In our study, 76.67% of the patients from the DCM group underwent LV EMBs.

5.3. Diagnostic value of conventional echocardiography and tissue Doppler imaging in iCM

Conventional echocardiography still represents the first-choice imaging modality in iCM. In patients with suspicion of iCM, echocardiography was mainly used to evaluate cardiac chamber size, wall thickness, systolic and diastolic dysfunction or to detect WMAs and to rule-out other causes of HF. Especially before an EMB procedure, echocardiography is needed to exclude pericardial effusion and intracavitary thrombi, which are present in some patients with iCM. Felker at al. found that patients with fulminant myocarditis presented with non-dilated, thickened and hypocontractile left ventricles, mainly due to the greater inflammatory response and acute myocardial, and interstitial edema. The patients with acute myocarditis had marked LV dilation,

normal LV thickness and decreased LV function.[27] However, there are no specific echocardiographic features of iCM.

One of the greatest disadvantages of the conventional transthoracic echocardiography is that it cannot identify the presence of a segmental myocardial dysfunction. [34]

No significant differences were detected in the thickness of IVS or PW between the no inflammation and the iCM group. The LVEF was higher in the no inflammation group – 57.8%, compared to the iCM group – 46.8%. However, the LV end-diastolic and end-systolic dimensions and volumes were significantly increased in the iCM group compared to no inflammation group. The echocardiographic findings of the patients from the iCM group correspond partially with the above-mentioned description of acute myocarditis by Felker et al. However, the patients in our study had iCM, but not acute myocarditis, and perhaps for this reason, no marked LV dilation was observed and the LV systolic function was not severely impaired.

The early diastolic mitral annulus velocity from the septal annulus was significantly lower in patients with iCM compared to those without inflammation. Left ventricular diastolic dysfunction was found in 55.8% of the patients from the iCM group. The proportion of patients from the no inflammation group with LV diastolic dysfunction was insignificantly lower in comparison to the iCM group. This could be explained by the fact that in a substantial part of the EMB specimens of the patients from both iCM and no inflammation group, interstitial and/ or perivascular fibrosis was detected (table 22). The correlation between the intramyocardial fibrosis and the diastolic dysfunction is well-known.

Our study showed that conventional echocardiography is less sensitive and specific in the prediction of iCM compared to 2D and 3D STE. The sensitivity and specificity of the conventional echocardiographic parameters for prediction of iCM varied from 41.2 to 63.2% and from 53.7 to 62.3%, respectively.

5.4. Diagnostic value of 2D STE longitudinal strain and strain rate

To assess the diagnostic value of 2D longitudinal strain and strain rates, we analyzed 4 longitudinal systolic and diastolic STE-derived parameters in apical 4-, 2- and 3-chamber view.

GLS was significantly reduced in patients with iCM compared to patients with no evidence of myocardial inflammation. GLSR and GLESR were also significantly reduced in patients with iCM compared to those with no myocardial inflammation.

To interpret these results, we should consider the following facts about the cardiac structure and mechanics: epicardial and endocardial oblique fibers are almost perpendicularly oriented toward each other. The midwall LV fibers have a circumferential course. Contraction of the midwall fibers is responsible for the circumferential shortening, whereas longitudinal shortening is the result of contraction of the oblique epicardial and endocardial fibers. Shortening of the epicardial fibers forces the endocardial fibers to passively reorder, with shortening along the epicardial fiber direction. The magnitude of this cross-fiber endocardial shortening exceeds the intrinsic endocardial fiber shortening. Although deformation is the largest in the inner part of the myocardium, this deformation is directed by the outer myocardial wall.24 Myocarditis predominantly starts from the subepicardial layer, which contains fibers with oblique orientation that determine longitudinal shortening and endocardial thickening. That may explain the reduced longitudinal strain in the patients with iCM.[103] Left ventricular function is usually preserved as long as the involvement of the myocardium is minimal, thus making it difficult to recognize regional WMAs in early myocarditis by traditional echocardiography alone.[36]

In contrast to longitudinal and circumferential strain, radial function was unaffected in isolated subepicardial damage because it strongly depends on the shortening of subendocardial longitudinal fibers.[32]

To our knowledge, our study is the first, which evaluates LV strain and strain rate in patients with iCM.

There are few studies in which the novel echocardiographic modalities such as TD, 2D or 3D STE strain and strain rates were evaluated in patients with myocarditis. The patients included in most of the studies had acute myocarditis. Therefore, we could not compare totally the results from these studies with ours. In most of the studies, the diagnosis of acute myocarditis was made with the

use of CMR, but not with EMB, which is still accepted as the gold diagnostic standard for myocarditis.

Smedema demonstrated in a case report the value of TD echocardiography and contrast-enhanced cardiac magnetic resonance (CMR) imaging in the diagnosis and management of patients with myocarditis.[28, 31]

A multimodality echocardiographic approach towards the diagnosis of myocarditis was first reported by Afonso et al. They presented a case of acute myocarditis wherein a multimodality echocardiographic approach was adopted. 2D strain was performed in the initial diagnostic workup and findings were later confirmed with CMR imaging. They found significantly attenuated longitudinal strain in the inferior, inferolateral segments, as well as in the apical segments compared with preserved longitudinal strain in the anterior septum. However, no EMB was performed for confirmation of the diagnosis of acute myocarditis.[25]

Leitman et al. measured longitudinal and circumferential strain in three myocardial layers (endocardial, midlayer and epicardial layer) with a modified 2D strain speckle tracking software in patients with perimyocarditis and in healthy controls. They found that patients with perimyocarditis had attenuated longitudinal strain in all three myocardial layers and at all three levels (basal, mid and apical), compared to healthy subjects. Circumferential strain was also significantly lower in patients with perimyocarditis than in normal subjects in all three myocardial layers, with the exception of apical epicardial strain.[103]

Di Bella et al. analyzed the myocardial deformation in 13 patients with acute myocarditis with evidence of subepicardial damage and preserved wall motion and LVEF. They showed that these patients had a significant global longitudinal LV strain decrease compared to healthy controls. The diagnosis of acute myocarditis was established with CMR; however, EMB was not performed. The average LVEF of the patients with myocarditis was significantly lower compared to the controls. Global circumferential strain and radial strain did not show any difference between the two groups. In fact the circumferential strain of the lateral LV wall was significantly decreased in patients with myocarditis.[32]

Hsiao et al. evaluated 2D LV longitudinal and circumferential strain and strain rate and its diagnostic and prognostic value in 45 patients with acute myocarditis (mean age: 39 ± 15 years). They found that the patients with acute myocarditis had impaired longitudinal and circumferential strain compared to healthy individuals. Longitudinal and circumferential strain rate values were also

decreased in the patients with acute myocarditis in comparison to the healthy controls. It should be noted that LVEF in the myocarditis group was significantly lower compared to the control group (49 ± 12% vs. 64 ± 4%, $p<0.001$), and LVEDD and LVESD were significantly increased in the patients with acute myocarditis compared to the control group. The patients with acute myocarditis and LVEF< 50% had significantly lower circumferential strain and strain rate compared to the patients with acute myocarditis and LVEF≥50%. The LV strain and strain rate were independently significant after adjusting for sex, IVS thickness, LVEF and stroke volume index. [33]

In 2013, Kasner et al. reported that 2D GLS and GLSR were significantly impaired in patients with acute and borderline myocarditis compared to patients without inflammation according to the EMB analysis. The GLASR was significantly lower in the borderline myocarditis group compared to the no inflammation group. The correlation of myocardial deformation imaging results with immunohistological findings as obtained by EMB in patients with myocardial inflammation was independent of conventional 2D echocardiographic parameters showing that strain rate and strain imaging is more sensitive in the detection of early changes or mild myocardial damage.[35]

Furthermore, Kasner at al. found that patients with proven myocarditis, who had revealed an impairment of longitudinal strain or strain rate at baseline, showed worse recovery of LV function and persistence of symptoms; recovered strain values at follow-up examination might indicate a better prognosis.[35]

Another study that confirmed the fact that the patients with acute myocarditis had decreased longitudinal strain and strain rate included 25 patients with clinically suspected acute myocarditis, proven with EMB analyses. Longitudinal strain and strain rate correlated significantly with lymphocytic infiltrates, but not with monocytes/ macrophages and CAMs.[34]

Uppu et al. evaluated 2D STE-derived longitudinal and circumferential strain in 10 adolescents (mean age 17.23±1.34 years) with clinically suspected myocarditis and in 19 age-controlled healthy subjects. The diagnosis was confirmed with CMR, no EMB was performed. The GLS was significantly attenuated in patients with myocarditis compared to healthy subjects. Longitudinal strain was significantly reduced in basal inferior, mid-inferior, mid-anterolateral, apical septal, apical inferior and apical lateral cardiac segments in the myocarditis group. The average circumferential strain was significantly reduced in the myocarditis group compared to the control group, as well. Circumferential strain was reduced in the inferior and inferoseptal segments at the levels of the papillary muscles. Moderate correlation between the overall number of LGE segments

detected by CMR and abnormal longitudinal strain was observed. It was observed that 90% of the patients with myocarditis were obese, as opposed to the patients in the control group who were not obese. Whether the reduced strain is related to obesity was not determined. GLS <-13.5% showed a sensitivity of 90%. It was found that 2D STE was better than CMR in identifying abnormalities in the apical regions. [36]

A recent study revealed reduced 2D GLS and circumferential strain in patients with acute myocarditis. Endocardial and epicardial longitudinal systolic strain were assessed in the same study and it was found that the epicardial layer had decreased strain compared to the endocardial layer. The same tendency was observed for epicardial and endocardial circumferential strain. According to the univariate analysis, 2D GLS correlated significantly with the amount of oedema assessed by CMR. However, no correlation was found between epicardial or endocardial strain and the amount of oedema.[37]

Interstitial edema may contribute to both thickened ventricular walls and decreased ventricular contractility in acute myocarditis. It is presumed that the decreased longitudinal strain, in the study of Escher et al. was the result of myocardial wall motion disturbance from the elevation of the LV mass index. Also, decreased longitudinal strain should be regarded as a myocardial functional disturbance in the myocarditis because elevation of the LV mass index is an index of geometric change in iCM.[34]

Comparison of 2D longitudinal strain and strain rate parameters, measured in the above-mentioned studies, is presented on table 87.

Table 87. Comparison of 2D longitudinal strain parameters in patients with myocarditis

Author and year*	Diagnosis	Method**	n	Mean age***, years	Mean EF, %	Vendor	Mean GLS, %	Mean GLSR, s^{-1}
Afonso L[25]; 2010	Acute myocarditis[a]	STE	1	17	35	Echo: GE SP: GE[d]	-11.4	-
Leitman M[103]; 2011	Peri-myocarditis[a]	STE	38	35	55.7	Echo: GE[e]	-18.3	-
Di Bella G[32]; 2010	Acute myocarditis[a]	STE	13	27±9	62±2	Echo: Esaote SP: XStrain[f]	-20.0±7.0	-
Hsiao JF[33]; 2013	Acute myocarditis[b]	STE	45	39±15	49±12	Echo: Siemens, GE, Philips Electronics SP: Siemens[g]	-11.7±4.0	-0.7±0.2
Kasner M[35]; 2013	Acute myocarditis[c]	STE	14	44±16	49±22	Echo: GE SP: GE[h]	-10.2±4.1	-0.8±0.3
Kasner M[35]; 2013	Borderline myocarditis[c]	STE	8	38±14	43±15	Echo: GE SP: GE[h]	-8.5±4.9	-0.7±0.3
Escher F[34]; 2013	Acute myocarditis[c]	STE	25	41±13	40±10	Echo: GE SP: GE[h]	-8.4±3.5	-0.5±0.3
Uppu SC[36]; 2015	Acute myocarditis[a]	STE	10	17±1	66	Echo: GE SP: GE[i]	-14.8±2.6	-
Logstrup BB[37]; 2015	Acute myocarditis[a]	STE	28	32±13	54±11	SP: GE[j]	-16.2±3.6	-
Our results	iCM[c]	STE	138	49±13	47±17	Echo: GE SP: GE[k]	-14.5±5.4	-0.9±0.3

n indicates number of patients included in the study, Echo indicates ultrasound system, GE indicates General Electric, SP indicates software package, STE indicates speckle tracking echocardiography, * - year of publication, ** - method used for assessment of strain and strain rate; *** - mean age of the patients with myocarditis; [a] – diagnosis was established with the use of CMR; [b] – the diagnosis was proved partially with CMR and partially with EMB; [c] – the diagnosis was proven with EMB analyses; [d] – ultrasound system: Vivid 7 (GE), SP: EchoPacPC (GE); [e] – ultrasound system: Vivid 7 or Vivid i; [f] – ultrasound system: My Lab 50 (Esaote), SP: XStrain; [g] – ultrasound system: Sequoia (Siemens), Vivid 7 (GE), iE33 (Philips Electronics), SP: Syngo Vector Imaging, version 2.0 (Siemens); [h] – ultrasound system: Vivid 7 (GE), SP: EchoPAC Version 7.0 (GE); [i] – ultrasound system: Vivid 7 scanner (GE), SP: EchoPAC version 108.1.4 (GE); [j] – SP: EchoPAC version 1.13.0 (GE); mean GLS of the patients with borderline myocarditis; [k] – ultrasound system: Vivid 7 and Vivid 9 (GE), SP: EchoPAC Version 7.0 (GE).

5.4.1. 2D GLS, GLSR, GLESR and GLASR in different subgroups of patients with iCM

No statistically significant difference was detected in the value of 2D GLS, GLSR, GLESR and GLASR between men and women from the iCM group.

The patients with iCM who had reduced LVEF showed significantly attenuated 2D GLS compared to the patients who had preserved LVEF. The GLSR, GLESR, GLASR were also significantly impaired in patients with reduced LVEF in comparison to those with preserved LVEF.

Similar results, but in patients with acute myocarditis, were announced by other authors, as well. Di Bella et al. reported that a patient with acute myocarditis and reduced LVEF had impairment of longitudinal, circumferential and radial strain in comparison with the patients with acute myocarditis and preserved LVEF.[32] In another study, it was found that patients with acute myocarditis, who had LVEF< 50%, had significantly lower longitudinal strain and systolic strain rate compared to the patients with acute myocarditis and LVEF≥50%.[33] Worse GLS was significantly associated with lower LVEF in patients with HFpEF ($p< 0.001$).[104]

The patients with LV hypertrophy had significantly reduced 2D GLSR and GLESR compared to the patients without LV hypertrophy. Well-known is the fact that in patients with myocarditis, interstitial oedema of the myocardium (caused by increased infiltration and vascular permeability) leads to a thickening of the ventricular wall and decreased ventricular contractility. Some authors believe that the increased thickness is likely due to a strong inflammatory response.[34] Therefore, we attribute the decreased 2D GLSR and GLESR in the patients with iCM to a stronger inflammatory response.

2D GLS and GLSR were significantly decreased in patients with regional WMAs. Leitman, et al. reported that longitudinal strain was significantly decreased in the apical segments of the left ventricle in patients with acute perimyocarditis and WMAs compared to those who had no WMAs.[103] However, Di Bella et al. found impaired 2D longitudinal strain in patients with acute myocarditis, although they had no WMAs.[32] Ha et al. also reported decreased longitudinal strain in a patient with myocarditis and lack of regional WMAs.[105]

The patients with mild or moderate mitral regurgitation (the patients with severe valve regurgitations were excluded from the study) had reduced 2D GLS, GLSR, GLESR and GLASR compared to patients without mitral regurgitation. The same observation was made for the patients

with mild or moderate tricuspid regurgitation in comparison to the patients without tricuspid regurgitation. The patients with mild aortic regurgitation or stenosis had no significantly different 2D strain and strain rates in comparison to those without aortic regurgitation. This could be due to the fact that only 7 of the patients with iCM had aortic regurgitation or stenosis, and in all of them, the AoV lesion was mild. In comparison, 42 of patients from the iCM group had mild mitral regurgitation and 15 – moderate mitral regurgitation; 32 – mild tricuspid regurgitation and 8 – moderate tricuspid regurgitation.

2D GLS was significantly impaired in patients with elevated LVEDP (measured during LV catheterization).

The patients with moderate interstitial fibrosis in the myocardium had significantly attenuated 2D GLS, GLSR and GLASR compared to patients without interstitial fibrosis (table 45). These findings correspond with the literature data that diastolic strain rate provides important information about interstitial fibrosis.[49] However, it has already been established that the amount of LV fibrosis is an independent predictor of GLS.[50] No statistically significant differences in 2D longitudinal strain and strain rates were detected in patients with different stages of perivascular fibrosis (table 46).

The patients from the iCM group with increased NTproBNP level had significantly attenuated 2D GLS, GLSR, GLESR and GLASR in comparison with the patients with normal NTproBNP levels. Close and strong correlation between LV longitudinal strain and BNP (NTproBNP) levels has already been found in patients with HF.[106-8] It was found that reduced longitudinal strain was moderately associated with higher NT-proBNP levels in patients with HFpEF.[104] A possible explanation is that the patients with an increased level of NTproBNP had more severe symptoms of HF.

No significant difference was found in GLS, GLSR, GLESR and GLASR in patients from the iCM group with DM, AH, dyslipidemia and COPD compared to those who do not have the above-mentioned concomitant diseases. The patients with former infections had insignificantly attenuated strain and strain rates compared to patients without former infections. The patients with CKD had significantly reduced GLS, GLSR, and GLESR in comparison to the patients without CKD. It was reported that LV longitudinal strain is significantly impaired in patients with CKD and HFpEF.[109] Edwards et al. showed that patients with CKD without a history of cardiovascular disease have abnormal strain parameters, including reduced longitudinal strain and strain rate in the setting

of normal LVEF and regional systolic tissue velocities, thereby demonstrating the increased sensitivity of strain parameters beyond tissue velocities and global LVEF in patients with CKD.[110] Hassanin et al. found that in patients with CKD the LV longitudinal strain, early and late diastolic strain rates were significantly impaired.[111] Furthermore, patients with CKD, with no history or symptoms of cardiovascular diseases and with preserved LVEF, showed decreased GLS, GLSR and GLESR.[112]

The patients with severe symptoms of HF (NYHA class IV) showed significantly attenuated GLS in comparison with the patients with no symptoms of HF or with less severe symptoms of HF (NYHA class II and III). It has already been reported that in hypertensive patients, the LV longitudinal systolic strain progressively deteriorates from NYHA I to IV.[113]

However, no significant differences were found in relation to the GLS, GLSR, GLESR and GLASR among the patients with different types of viruses detected by EMB. The patients who had intramyocardial co-infection with PVB19 and HHV6 type B presented with lower GLS, GLSR, GLESR, and GLASR, however, statistical significance was not reached. Our results correspond with those of Escher et al., who reported that none of the investigated echocardiographic findings seem to be able to detect viral genomes.[34]

5.4.2. Correlation between 2D GLS, GLSR, GLESR, GLASR and other quantitative indicators

We found strong negative correlation between 2D GLS, GLSR on the one hand, and LVEF and LVSF on the other. Both strain and LVEF measure LV function; however, there is a fundamental difference between the two: strain calculates the contractility of the myocardium, while LVEF is a surrogate parameter that describes myocardial pump function. STE is especially suited for the assessment of global and regional systolic function in patients with HFpEF.[114] STE-derived longitudinal strain and LVEF correlate well in healthy individuals; however, in ST elevation myocardial infarction (STEMI) survivors and HF patients, the correlation is weaker.[48] Strong correlation between longitudinal strain and LVEF was observed also in patients with acute STEMI and advanced ischemic HF.[115] In patients with HFpEF longitudinal strain was found to be related to LVEF.[104] Longitudinal strain and strain rate correlated significantly with LVEF in patients with

myocarditis, as well. However, the correlation between longitudinal strain and LVEF was found to be moderate, and the correlation between longitudinal strain rate and EF – weak. [34]

Strong positive correlation was detected between 2D GLS and LVESD. Strong positive correlation was found between 2D GLSR and LVESD and LVESV. Other authors showed that myocardial deformation parameters depended on ventricular size. They found that 2D GLS and GLSR correlated inversely with LVESD and LVEDD both in healthy people and in patients with mitral regurgitation, i.e. an increase in LV size would lead to a decrease in deformation.[116] Correlation between 2D GLESR, LVEF, LVSF and early diastolic septal (E'sep) peak tissue velocity was significantly positive. This is in conformity with the fact that GLESR is recognized as one of the markers of diastolic dysfunction. Strong negative correlation was detected between 2D GLESR and LVESD.

However, no correlation was found between myocardial deformation imaging parameters and immunohistological findings by EMB. Escher et al. also found that AMs and monocytes/ macrophages did not correlate with longitudinal strain and strain rate, but the latter myocardial deformation parameters correlated significantly with lymphocytic infiltrates. [34]

5.5. Diagnostic value of 3D STE parameters

The left ventricle is a 3D structure with complex 3D patterns of wall motion and the inability to quantify one of the 3 components of the local displacement vector is a major limitation. Therefore, 2D STE is intrinsically limited by its 2D nature, because it can only track motion occurring within the imaging plane, and motion in and out of plane manifests as features appearing and disappearing from the image, resulting in noise and interfering with tracking.[117]

Three-dimensional STE is one of the most advanced techniques in the evaluation of myocardial deformation.[118] There is general agreement that 3D STE is a simple, feasible, and reproducible method to measure the myocardial strains. Three-dimensional STE can be used for regional wall motion analysis of the entire LV and allows obtaining real 3D indices and to assess 3D wall motion precisely.[54] Subtle myocardial damage or deteriorated LV function could be detected at an earlier stage by using 3D STE in comparison with one-directional strain.[119]

The possibility of evaluating the deformation on a full-volume model avoids the errors associated with the use of 2D images.[118] However, the 3D STE overcomes the drawbacks of 2D STE, which is likely to be affected by both geometric assumptions and the use of foreshortened apical views for assessment of global and regional LV function.[120]

We assessed 3D LV GAS, GLS, GCS and GRS in four and/or six consecutive cardiac cycles in patients with iCM, DCM and in patients without myocardial inflammation. We found that the patients with iCM had significantly attenuated 3D STE indices, assessed in both four and six consecutive cardiac cycles compared to the patients with no myocardial inflammation (table 55). To the best of our knowledge, our study is the first to evaluate 3D STE indices in patients with iCM.

The 3D GLS measured in patients from the iCM group were more impaired compared to the 2D GLS measured in the same patients, although the mean difference did not reach statistical significance. In the DCM group, no statistically significant difference was observed between 3D and 2D GLS values. In the no inflammation group, the 3D GLS values measured in 4 consecutive heart cycles were insignificantly lower than the 2D GLS values. However, statistically significant difference was detected between the value of 3D GLS measured in 6 cycles and 2D GLS in the group without myocardial inflammation. The reduced values of 3D GLS could be attributed to the twisting cardiac motion, i.e. the length of the pair points in the end-systolic frame measured by 2D STE is shorter than measured by 3D STE. [54]

3D and 2D longitudinal strain values in the subjects from our study, who had no myocardial inflammation, correspond to values reported by Saito et al., who evaluated 3D GLS, GCS and GRS in 46 healthy individuals. The 3D longitudinal strain values in these healthy subjects were lower than the 2D GLS values and the difference was even more significant in comparison to our own study.[54]

Reant et al. assessed 3D STE strains in a group of 100 subjects, who included both healthy individuals and patients with DCM, ischemic DCM, myocarditis and other cardiovascular diseases. It was found that the mean 3D GLS was slightly more reduced than 2D GLS.[121]

Jasityte et al. investigated and compared the GLS obtained by 3D STE with those obtained with 2D STE in 24 subjects (12 healthy individuals and 12 patients with CAD). They found that GLS was more impaired on 3D STE compared to 2D STE. The investigators attributed this to the twisting of the heart and out-of-plane rotation of myocardial segments on 2D STE.[70]

Kleijn et al. investigated the 3D GAS in 56 healthy subjects and reported mean GAS of -35±10%. In our study the 3D GAS among the patients from no inflammatrion group were lower than those reported by Kleijn et al., which may be due to the different vendors, analysis software we used for assessment of 3D strains and to the fact that we investigated patients with suspected iCM, rather than healthy subjects.[62]

Another group of investigators evaluated and compared standard 2D GLS and 3D GLS in patients with and without myocardial infarction and found that in both groups the standard 2D GLS was significantly higher than the 3D GLS. This was explained as an effect of out-of-plane speckle patterns, as well as technical differences between the two methods.[122]

The orientation of myocardial fibers could explain the impairment of 3D speckle tracking indices in patients with iCM. The orientation of myocardial fibers changes from oblique at the subepicardium to circumferential at the mid-wall. Thus, cardiac motion actually involves 3D rotation, contraction, and shortening, which might cause the ‘‘disappearance’’ of some of the speckles from the 2D view by through-plane motion.[54] The inflammation in iCM usually affects the subepicardial and the mid-wall areas of the venricular wall. Subepicardial fibers play a major role in radial strain and longitudinal strain and mid-wall fibers – in circumferential strain.[51] Furthermore, 3D STE measures simultaneously the myocardial deformation in longitudinal, circumferential and radial directions, which is not possible with 2D STE.

5.5.1. Correlations of 3D strain indices in patients with iCM

We found statistically significant correlations between 3D GAS, GCS and LVEF, LVSF, LVEDD, LVESD, TAPSE, early diastolic septal (E’sep) and lateral (E’lat) peak tissue velocities at the level of the mitral valve. Strong correlations were detected between 3D GAS, GCS, GRS and LVOT Vmax. 3D GLS correlated significantly with LVOT Vmax and with early diastolic septal (E’sep) peak tissue velocities at the level of the mitral valve. Moderate correlation was detected between 3D GLS and LVEF, LVSF, LVEDD, LVESD, TAPSE, early diastolic lateral (E’lat) peak tissue velocities at the level of the mitral valve.

Our results are in line to those obtained by other investigators. Reant et al. investigated the correlation between 3D LVEF and 3D strain indices and found the highest correlation between 3D GAS and LVEF. 3D GLS correlated slightly weaker with 3D LVEF than 3D GCS and 3D GRS.[121]

Li et al. found strong correlation between 3D GAS and LVEF in 30 patients after repair of tetralogy of Fallot.[123] Kleijn et al. found an excellent correlation between 3D GAS and LVEF.[62] In the study of Seo et al. 3D GCS showed better correlation with LVEF than GLS and GRS. In patients with reduced LVEF, 3D GCS still demonstrated better correlation with LVEF than GLS and GRS. In patients with preserved LVEF, 3D GCS showed a moderate, but better correlation with LVEF than did GLS and GRS.[124]

Trache et al. found strong correlation between standard 2D GLS and LVEF, 3D GAS and LVEF and moderate correlation between 3D GRS and LVEF, 3D GLS and LVEF and between 3D GCS and LVEF.[122]

In our study 3D GAS, GLS, GCS and GRS correlated very strongly with HbA1c. Strong and moderate correlation existed between all 3D strains and GFR. 3D GAS and GLS correlated moderately with HDL cholesterol. Such correlations were not reported in other studies using 3D STE. Only Vitarelli et al. observed a significant correlation between longitudinal deformation and LDL cholesterol level in hypercholesterolemic and obese children and adolescent. Moreover, significantly higher correlation was found between 3D GAS and LDL cholesterol level.[119]

We investigated the correlation between 2D GLS, 3D GAS and 3D GLS among the patients from the iCM group. 3D GAS and GLS showed significantly strong correlation with 2D GLS (table 83). The strongest correlation was determined between 2D GLS and 3D GAS measured in 4 consecutive cardiac cycles, followed by the correlation between 2D GLS and 3D GLS measured in 4 consecutive cardiac cycles. Several studies reported strong correlations between 2D GLS and 3D GLS values.[119, 121, 122] Maffessanti et al. found moderate correlation between 2D and 3D longitudinal strain (r=0.49).[117]

5.6. Predictive value of 2D and 3D STE

5.6.1. Predictive value of 2D longitudinal strain and strain rates

The assessment of myocardial deformation may offer a better sensitivity and specificity than conventional echocardiography for the detection of subclinical LV dysfunction.[37] Therefore, we tested the diagnostic value of 2D global longitudinal strain and strain rates. Among the 2D STE parameters measured in our patients with iCM, the GLESR showed the best predictive value with an AUC of 0.73, followed by GLS with an AUC of 0.71 and GLSR with an AUC of 0.69. 2D GLS showed a very good sensitivity and specificity at a cut-off point of -17.57%. We believe that patients with suspected iCM, who have 2D GLS more attenuated than the above-mentioned (2D GLS > -17.57%) should undergo EMB.

There are few studies that address the usefulness of 2D longitudinal strain and strain rate imaging in the prediction of iCM. In fact, all the studies in this field assess the predictive value of 2D STE in patients with acute myocarditis, but not in iCM. Our study is the first which evaluates the predictive value of 2D STE parameters in patients with iCM.

Our results correspond to those of Di Bella et al., who found a moderate predictive value of 2D GLS in patients with acute myocarditis. However, our 2D GLS cut-off point of -17.57% showed a better sensitivity and specificity than the cut-off point of –21%, in the study of di Bella et al., which yielded a sensitivity of 69% and specificity of 65%.[32]

Hsiao et al. reported very high predictive value for 2D GLS and GLSR in patients with acute myocarditis. In their study, 2D GLS showed an AUC of 0.93, the cut-off value -15.1% revealed a sensitivity of 78% and specificity of 93%. The 2D GLSR also showed a large AUC of 0.91, the cut-off value -0.9 s^{-1} showed a sensitivity of 71% and specificity of 89%. The ROC curve analysis for the patients with acute myocarditis and EF≥50% revealed an AUC of 0.83 for 2D GLS and 0.82 for GLSR. The optimal cut-off value for 2D GLS in acute myocarditis patients with preserved LVEF was -16.9% with 84% sensitivity and 68% specificity. The optimal cut-off value for GLSR in myocarditis patients with preserved EF was -0.9 s^{-1}, which revealed 74% sensitivity and 70% specificity. [33]

We should mention that the number of study subjects included in each of the above-mentioned trials was smaller than that of patients with iCM, that we evaluated in our study. Thirteen patients with acute myocarditis and 13 healthy controls were included in the study of Di Bella et al.

In the study of Hsiao et al. 45 patients with acute myocarditis and 83 healthy controls were evaluated. The different vendors and post-processing software packages used in the above-mentioned studies could lead to differences in the deformation values and in the predictive value of this method. Moreover, we tested the sensitivity and specificity of 2D longitudinal strain and strain rates against EMB, which is still the gold diagnostic standard for myocarditis and iCM. However, the sensitivity and specificity of 2D GLS and GLSR in the study of Di Bella et al. were investigated against CMR, but not against EMB. In the study of Hsiao et al. the acute myocarditis was diagnosed on the basis of clinical symptoms, evidence of structural or functional abnormalities by conventional echocardiography, elevated cardiac biomarkers and absence of evidence of CAD. Only in 12 patients (26.7% of the patients from the acute myocarditis group) was EMB performed and 22 patients (48.8%) underwent CMR.

5.6.2. Predictive value of 3D STE

We found that 3D strains had even better predictive value in iCM. We detected that 3D strains measured in 4 consecutive cardiac cycles had better predictive value than those measured in 6 consecutive cardiac cycles. The 3D GRS showed the best predictive value, followed by 3D GLS, GAS and GCS. We determined cut-off points with an optimal sensitivity and specificity for every 3D strain index. We could conclude that patients with suspected iCM, who have 3D GAS>-25.09%, 3D GCS>-15.02%, 3D GLS>-14.22% and/ or 3D GRS<38.19% should undergo EMB.

To the best of our knowledge, this is the first study which investigates the predictive value of 3D deformation parameters in patients with iCM.

Few studies investigated the predictive value of 3D strains in other disease entities. In the study of Huttin et al., 3D GAS was found to be the best among all 3D strains for detecting non-viable segments with microvascular obstruction in patients with STEMI. 3D GAS showed an AUC of 0.867, the cut-off point -16.1% had a sensitivity of 78% and specificity of 81.1%.[125]

In the study of Nagata et al., 3D GLS was found to be the most powerful predictor for future major adverse cardiac events in asymptomatic patients with severe aortic stenosis. 3D GLS showed an AUC of 0.78, which was significantly greater than that of 2D GLS (0.62, p=0.0044) and 3D GRS (0.66, p=0.0069).[126] In another study, 3D GLS showed excellent predictive value (AUC 0.96), with a sensitivity of 92% and specificity of 91% at the cut-off value of -11.1% in identification of LV segments with functional improvement after acute myocardial infarction.[127]

6. Conclusion

In the present study, we report that 2D longitudinal deformation is impaired in patients with iCM. 2D GLS, GLSR and GLESR were found to be significantly impaired in iCM patients compared to the patients without myocardial inflammation. Furthermore, we found that 3D GLS, GAS, GCS and GRS were also significantly reduced in patients with iCM compared to those without myocardial inflammation.

We tested the predictive value of 2D and 3D STE in iCM. Among the 2D STE-derived strains and strain rates GLESR and GLS showed the highest predictive value, followed by 2D GLSR. Among the 3D strain parameters, the 3D GRS showed the best predictive value, followed by 3D GLS, GAS and GCS. Moreover, 3D strains showed even better predictive values than 2D strain and strain rates.

In the present work we found strong and significant correlations between 2D and 3D STE indexes and LVEF, LV dimensions and volumes, LVOT Vmax, TD parameters, etc. Moreover, very strong correlations were detected between 2D GLS and 3D strains.

In regard to presence of viruses, none of the 2D STE and 3D STE echocardiographic parameters seemed to be able to detect viral genomes.

In the present work, we are suggesting a basically new approach in the diagnosis of iCM. We proved for the first time that 2D and 3D STE are reliable echocardiographic methods in iCM. We believe that patients with definite values for GLS and 3D STE parameters should undergo EMB, since according to the ROC analysis, these patients had the highest chance of having iCM.

In conclusion we could say that 2D and 3D STE could be extremely valuable in the practice, since they represent a non-invasive diagnostic approach without radiation and provide online imaging allowing real-time assessment of myocardial deformation. Myocardial deformation analysis obtained by 2D and 3D STE appeared to be a very sensitive indicator for iCM. Left ventricular myocardial involvement in iCM can be identified by both 2D and 3D STE. The high predictive value of 2D and 3D STE-derived parameters shows that these parameters could serve as a useful additional noninvasive tool in the diagnosis of inflammation CM. The myocardial deformation imaging has the potential to facilitate early prediction of myocardial inflammation and therefore, could avoid unnecessary EMBs. Moreover, myocardial deformation analysis is likely to improve conventional diagnostic investigations in suspected iCM, especially in cases where access to EMB is

limited. 2D and 3D deformational imaging are very useful methods, as they allow a better understanding of iCM pathophysiology and throw light on the progress of this disease in individual patients. Further studies with larger sample size are required to obtain age-specific normative data that can be widely used, and across all vendor platforms.

7. References

1. Richardson P, McKenna W, Bristow M, Maisch B, Mautner B, O'Connell J, Olsen E, Thiene G, Goodwin J, Gyarfas I, Martin I, Nordet P. Report of the 1995 World Health Organization/ International Society and Federation of Cardiology Task Force on the Definition and Classification of cardiomyopathies. Circulation 1996;93:841-2.
2. Sagar S, Liu PP, Cooper LT Jr. Myocarditis. Lancet 2012;379:738-47.
3. Caforio AL, Pankuweit S, Arbustini E, Basso C, Gimeno-Blanes J, Felix SB, Fu M, Helio T, Heymans S, Jahns R, Klingel K, Linhart A, Maisch B, McKenna W, Mogensen J, Pinto YM, Ristic A, Schultheiss HP, Seggewiss H, Tavazzi L, Thiene G, Yilmaz A, Charron P, Elliott PM; European Society of Cardiology Working Group on Myocardial and Pericardial Diseases. Current state of knowledge on aetiology, diagnosis, management, and therapy of myocarditis: a position statement of the European Society of Cardiology Working Group on Myocardial and Pericardial Diseases. Eur Heart J. 2013;34:2636-48.
4. Frustaci A, Chimenti C. Immunosuppressive therapy in virus-negative inflammatory cardiomyopathy. Herz. 2012;37:854-8.
5. Karatolios K, Pankuweit S, Kisselbach C, Maisch B. Inflammatory cardiomyopathy. Hellenic J Cardiol. 2006;47:54-65.
6. Pankuweit S, Ruppert V, Eckhardt H, Strache D, Maisch B. Pathophysiology and aetiological diagnosis of inflammatory myocardial diseases with a special focus on parvovirus B19. J Vet Med B Infect Dis Vet Public Health. 2005;52:344-7.
7. Aretz HT, Billingham ME, Edwards WD, Factor SM, Fallon JT, Fenoglio JJ Jr, Olsen EG, Schoen FJ. Myocarditis. A histopathologic definition and classification. Am J Cardiovasc Pathol 1987;1:3–14.
8. Leone O, Veinot JP, Angelini A, Baandrup UT, Basso C, Berry G, Bruneval P, Burke M, Butany J, Calabrese F, d'Amati G, Edwards WD, Fallon JT, Fishbein MC, Gallagher PJ, Halushka MK, McManus B, Pucci A, Rodriguez ER, Saffitz JE, Sheppard MN, Steenbergen C, Stone JR, Tan C, Thiene G, van der Wal AC, Winters GL. 2011 consensus statement on endomyocardial biopsy from the Association for European Cardiovascular Pathology and the Society for Cardiovascular Pathology. Cardiovasc Pathol. 2012;21:245-74.
9. Dennert R, Crijns HJ, Heymans S. Acute viral myocarditis. Eur Heart J. 2008;29:2073-82.
10. Karjalainen J, Heikkila J. Incidence of three presentations of acute myocarditis in young men in military service. A 20-year experience. Eur Heart J 1999;20:1120-5.
11. Schultheiss HP, Kühl U. Overview on chronic viral cardiomyopathy/ chronic myocarditis. Ernst Schering Res Found Workshop. 2006:3-18.
12. Punja M, Mark DG, McCoy JV, Javan R, Pines JM, Brady W. Electrocardiographic manifestations of cardiac infectious-inflammatory disorders. Am J Emerg Med. 2010;28:364-77.
13. Fairweather D, Cooper LT Jr, Blauwet LA. Sex and gender differences in myocarditis and dilated cardiomyopathy. Curr Probl Cardiol. 2013;38:7-46.

14. Schultheiss HP, Kühl U, Cooper LT. The management of myocarditis. Eur Heart J. 2011;32:2616-25.
15. Blauwet LA, Cooper LT. Myocarditis. Prog Cardiovasc Dis 2010;52:274-88.
16. Yilmaz A, Mahrholdt H, Athanasiadis A, Vogelsberg H, Meinhardt G, Voehringer M, Kispert EM, Deluigi C, Baccouche H, Spodarev E, Klingel K, Kandolf R, Sechtem U. Coronary vasospasm as the underlying cause for chest pain in patients with PVB19 myocarditis. Heart. 2008;94:1456-63.
17. Shauer A, Gotsman I, Keren A, Zwas DR, Hellman Y, Durst R, Admon D. Acute viral myocarditis: current concepts in diagnosis and treatment. Isr Med Assoc J. 2013;15:180-5.
18. Deluigi CC, Ong P, Hill S, Wagner A, Kispert E, Klingel K, Kandolf R, Sechtem U, Mahrholdt H. ECG findings in comparison to cardiovascular MR imaging in viral myocarditis. Int J Cardiol. 2013;165:100-6.
19. Magnani JW, Danik HJ, Dec GW Jr, DiSalvo TG. Survival in biopsy-proven myocarditis: a long-term retrospective analysis of the histopathologic, clinical, and hemodynamic predictors. Am Heart J 2006; 151:463-70.
20. James OG, Christensen JD, Wong TZ, Borges-Neto S, Koweek LM. Utility of FDG PET/CT in inflammatory cardiovascular disease. Radiographics. 2011;31:1271-86.
21. Wagner A, Bruder O, Mahrholdt H. Myocarditis: update and critical assessment. Curr Cardiovasc Imaging Rep. 2010;3:57–64.
22. Elamm C, Fairweather D, Cooper LT. Pathogenesis and diagnosis of myocarditis. Heart. 2012;98:835-40.
23. Basso C, Calabrese F, Angelini A, Carturan E, Thiene G. Classification and histological, immunohistochemical, and molecular diagnosis of inflammatory myocardial disease. Heart Fail Rev 2013;18:673-81.
24. Yilmaz A, Klingel K, Kandolf R, Sechtem U. Imaging in inflammatory heart disease: from the past to current clinical practice. Hellenic J Cardiol 2009;50:449-60.
25. Afonso L, Hari P, Pidlaoan V, Kondur A, Jacob S, Khetarpal V. Acute myocarditis: can novel echocardiographic techniques assist with diagnosis? Eur J Echocardiogr 2010;11:E5.
26. Schultz JC, Hilliard AA, Cooper LT Jr, Rihal CS. Diagnosis and treatment of viral myocarditis. Mayo Clin Proc 2009;84:1001-9.
27. Felker GM, Boehmer JP, Hruban RH, Hutchins GM, Kasper EK, Baughman KL, Hare JM. Echocardiographic findings in fulminant and acute myocarditis. J Am Coll Cardiol 2000;36:227-32.
28. Jeserich M, Konstantinides S, Pavlik G, Bode C, Geibel A. Non-invasive imaging in the diagnosis of acute viral myocarditis. Clin Res Cardiol 2009;98:753-63.
29. Urhausen A, Kindermann M, Bohm M, Kindermann W. Images in cardiovascular medicine. Diagnosis of myocarditis by cardiac tissue velocity imaging in an olympic athlete. Circulation 2003;108:e21–2.
30. Skouri HN, Dec GW, Friedrich MG, Cooper LT. Noninvasive imaging in myocarditis. J Am Coll Cardiol 2006;48:2085-93.

31. Smedema JP. Images in cardiovascular medicine: myocardial inflammation in viral peri-myocarditis detected by tissue Doppler echocardiography and magnetic resonance imaging. Cardiovasc J Afr 2007;18:238–240.
32. Di Bella G, Gaeta M, Pingitore A, Oreto G, Zito C, Minutoli F, Anfuso C, Dattilo G, Lamari A, Coglitore S, Carerj S. Myocardial deformation in acute myocarditis with normal left ventricular wall motion--a cardiac magnetic resonance and 2-dimensional strain echocardiographic study. Circ J 2010;74:1205-13.
33. Hsiao JF, Koshino Y, Bonnichsen CR, Yu Y, Miller FA Jr, Pellikka PA, Cooper LT Jr, Villarraga HR. Speckle tracking echocardiography in acute myocarditis. Int J Cardiovasc Imaging 2013;29:275-84.
34. Escher F, Kasner M, Kühl U, Heymer J, Wilkenshoff U, Tschöpe C, Schultheiss HP. New echocardiographic findings correlate with intramyocardial inflammation in endomyocardial biopsies of patients with acute myocarditis and inflammatory cardiomyopathy. Mediators Inflamm. 2013;2013:875420.
35. Kasner M, Sinning D, Escher F, Lassner D, Kühl U, Schultheiss HP, Tschöpe C. The utility of speckle tracking imaging in the diagnostic of acute myocarditis, as proven by endomyocardial biopsy. Int J Cardiol. 2013;168:3023-4.
36. Uppu SC, Shah A, Weigand J, Nielsen JC, Ko HH, Parness IA, Srivastava S. Two-dimensional speckle-tracking derived segmental peak systolic longitudinal strain identifies regional myocardial involvement in patients with myocarditis and normal global left ventricular systolic function. Pediatr. Cardiol 2015;36:950-9.
37. Logstrup BB, Nielsen JM, Kim WY, Poulsen SH. Myocardial oedema in acute myocarditis detected by echocardiographic 2D myocardial deformation analysis. Eur Hear J Cardiovasc Imaging 2016;17:1018-26.
38. Kuhl U, Lauer B, Souvatzoglu M, Vosberg H, Schultheiss HP. Antimyosin scintigraphy and immunohistologic analysis of endomyocardial biopsy in patients with clinically suspected myocarditis-evidence of myocardial cell damage and inflammation in the absence of histologic signs of myocarditis. J Am Coll Cardiol 1998;32:1371–6.
39. Friedrich MG, Sechtem U, Schulz-Menger J, Holmvang G, Alakija P, Cooper LT, White JA, Abdel-Aty H, Gutberlet M, Prasad S, Aletras A, Laissy JP, Paterson I, Filipchuk NG, Kumar A, Pauschinger M, Liu P; International Consensus Group on Cardiovascular Magnetic Resonance in Myocarditis. Cardiovascular magnetic resonance in myocarditis: A JACC White Paper. J Am Coll Cardiol 2009;53:1475-1487.
40. Lurz P, Eitel I Adam J, Steiner J, Grothoff M, Desch S, Fuernau G, de Waha S, Sareban M, Luecke C, Klingel K, Kandolf R, Schuler G, Gutberlet M, Thiele H. Diagnostic performance of CMR imaging compared with EMB in patients with suspected myocarditis. JACC Cardiovasc Imaging 2012;5:513-24.
41. Gutberlet M, Spors B, Thoma T, Bertram H, Denecke T, Felix R, Noutsias M, Schultheiss HP, Kühl U. Suspected chronic myocarditis at cardiac MR: diagnostic accuracy and association with immunohistologically detected inflammation and viral persistence. Radiology 2008;246:401–9.

42. Noutsias M, Pankuweit S, Maisch B. Biomarkers in inflammatory and noninflammatory cardiomyopathy. Herz 2009;34:614-23.
43. Bock CT, Klingel K, Kandolf R. Human parvovirus B19-associated myocarditis. N Engl J Med 2010;362:1248–1249.
44. Yilmaz A, Kindermann I, Kindermann M, Mahfoud F, Ukena C, Athanasiadis A, Hill S, Mahrholdt H, Voehringer M, Schieber M, Klingel K, Kandolf R, Böhm M, Sechtem U. Comparative evaluation of left and right ventricular endomyocardial biopsy: differences in complication rate and diagnostic performance. Circulation. 2010;122:900-9.
45. Escher F, Westermann D, Gaub R, Pronk J, Bock T, Al-Saadi N, Kühl U, Schultheiss HP, Tschöpe C. Development of diastolic heart failure in a 6-year follow-up study in patients after acute myocarditis. Heart 2011;97:709-14.
46. Kühl U, Pauschinger M, Seeberg B, Lassner D, Noutsias M, Poller W, Schultheiss HP. Viral persistence in the myocardium is associated with progressive cardiac dysfunction. Circulation 2005;112:1965-70.
47. Feigenbaum H, Mastouri R, Sawada S. A practical approach to using strain echocardiography to evaluate the left ventricle. Circ J 2012;76:1550-5.
48. Blessberger H, Binder T. Non-invasive imaging: Two dimensional speckle tracking echocardiography: basic principles. Heart 2010; 96:716-22.
49. Mor-Avi V, Lang RM, Badano LP, Belohlavek M, Cardim NM, Derumeaux G, Galderisi M, Marwick T, Nagueh SF, Sengupta PP, Sicari R, Smiseth OA, Smulevitz B, Takeuchi M, Thomas JD, Vannan M, Voigt JU, Zamorano JL. Current and evolving echocardiographic techniques for the quantitative evaluation of cardiac mechanics: ASE/EAE consensus statement on methodology and indications endorsed by the Japanese Society of Echocardiography. Eur J Echocardiogr 2011;12:167-205.
50. Geyer H, Caracciolo G, Abe H, Wilansky S, Carerj S, Gentile F, Nesser HJ, Khandheria B, Narula J, Sengupta PP. Assessment of myocardial mechanics using speckle tracking echocardiography: fundamentals and clinical applications. J Am Soc Echocardiogr 2010;23:351-69.
51. Duan F, Xie M, Wang X, Li Y, He L, Jiang L, Fu Q. Preliminary clinical study of left ventricular myocardial strain in patients with non-ischemic dilated cardiomyopathy by three-dimensional speckle tracking imaging. Cardiovascular Ultrasound 2012;10:8.
52. Ammar KA, Paterick TE, Khandheria BK, Jan MF, Kramer C, Umland MM, Tercius AJ, Baratta L, Tajik AJ. Myocardial mechanics: understanding and applying three-dimensional speckle tracking echocardiography in clinical practice. Echocardiography 2012;29:861-72.
53. Leung DY, Ng AC. Emerging clinical role of strain imaging in echocardiography. Heart Lung Circ. 2010;19:161–74.
54. Saito K, Okura H, Watanabe N, Hayashida A, Obase K, Imai K, Maehama T, Kawamoto T, Neishi Y, Yoshida K. Comprehensive evaluation of left ventricular strain using speckle tracking echocardiography in normal adults: comparison of three-dimensional and two-dimensional approaches. J Am Soc Echocardiogr. 2009;22:1025-30.

55. Zhang X, Wei X, Liang Y, Liu M, Li C, Tang H. Differential changes of left ventricular myocardial deformation in diabetic patients with controlled and uncontrolled blood glucose: a three-dimensional speckle-tracking echocardiography–based study. J Am Soc Echocardiogr. 2013;26:499-506.
56. Urbano-Moral JA, Patel AR, Maron MS, Arias-Godinez JA, Pandian NG. Three-dimensional speckle-tracking echocardiography: methodological aspects and clinical potential. Echocardiography 2012;29:997-1010.
57. Nelson MR, Hurst RT, Raslan SF, Cha S, Wilansky S, Lester SJ. Echocardiographic measures of myocardial deformation by speckle-tracking technologies: the need for standardization? J Am Soc Echocardiogr 2012;25:1189-94.
58. Yingchoncharoen T, Agarwal S, Popovic ZB, Marwick TH. Normal ranges of left ventricular strain: a meta-analysis. J Am Soc Echocardiogr. 2013;26:185-91.
59. Serri K, Reant P, Lafitte M, Berhouet M, Le Bouffos V, Roudaut R, Lafitte S. Global and regional myocardial function quantification by two-dimensional strains: application in hypertrophic cardiomyopathy. J Am Coll Cardiol 2006;47:1175–81.
60. Gayat E, Ahmad H, Weinert L, Lang RM, Mor-Avi V. Reproducibility and inter-vendor variability of left ventricular deformation measurements by three-dimensional speckle-tracking echocardiography. J Am Soc Echocardiogr 2011;24:878-85.
61. Muraru D, Cucchini U, Mihaila S, Miglioranza MH, Aruta P, Cavalli G, Cecchetto A, Padayattil-Jose S, Peluso D, Iliceto S, Badano LP. Left ventricular myocardial strain by three-dimensional speckle-tracking echocardiography in healthy subjects: reference values and analysis of their physiologic and technical determinants. J Am Soc Echocardiogr 2014;27:858-71.
62. Kleijn SA, Aly MF, Terwee CB, van Rossum AC, Kamp O. Three-dimensional speckle tracking echocardiography for automatic assessment of global and regional left ventricular function based on area strain. J Am Soc Echocardiogr 2011;24:314-21.
63. Marwick TH, Leano RL, Brown J, Sun JP, Hoffmann R, Lysyansky P, Becker M, Thomas JD. Myocardial strain measurement with 2-dimensional speckle-tracking echocardiography: definition of normal range. JACC Cardiovasc Imaging 2009;2:80-4.
64. Nishikage T, Nakai H, Mor-Avi V, Lang RM, Salgo IS, Settlemier SH, Husson S, Takeuchi M. Quantitative assessment of left ventricular volume and ejection fraction using two-dimensional speckle tracking echocardiography. Eur J Echocardiogr. 2009;10:82–88.
65. Smedsrud MK, Pettersen E, Gjesdal O, Svennevig JL, Andersen K, Ihlen H, Edvardsen T. Detection of left ventricular dysfunction by global longitudinal systolic strain in patients with chronic aortic regurgitation. J Am Soc Echocardiogr. 2011;24:1253-9.
66. Dandel M., Hetzer R. Echocardiographic strain and strain rate imaging – clinical applications. Int J Cardiol. 2009;132:11–24.
67. Dalen H, Thorstensen A, Aase SA, Ingul CB, Torp H, Vatten LJ, Stoylen A. Segmental and global longitudinal strain and strain rate based on echocardiography of 1266 healthy individuals: the HUNT study in Norway. Eur J Echocardiogr 2010;11:176-83.

68. Kaku K, Takeuchi M, Tsang W, Takigiku K, Yasukochi S, Patel AR, Mor-Avi V, Lang RM, Otsuji Y. Age-related normal range of left ventricular strain and torsion using three-dimensional speckle-tracking echocardiography. J Am Soc Echocardiogr. 2014; 27:55-64.
69. Galderisi M, Esposito R, Schiano-Lomoriello V, Santoro A, Ippolito R, Schiattarella P, Strazzullo P, de Simone H. Correlates of global area strain in native hypertensive patients: a three-dimensional speckle-tracking echocardiography study. Eur Heart J Cardiovasc Imaging 2012;13:730-8.
70. Jasaityte R, Heyde B, Ferferieva V, Amundsen B, Barbosa D, Loeckx D, Kiss G, Orderund F, Claus P, Torp H, D'hooge J. Comparison of a new methodology for the assessment of 3D myocardial strain from volumetric ultrasound with 2D speckle tracking. Int J Cardiovasc Imaging 2012;28:1049-60.
71. Delgado V, Tops LF, van Bommel RJ, van der Kley F, Marsan NA, Klautz RJ, Versteegh MI, Holman ER, Schalij MJ, Bax JJ. Strain analysis in patients with severe aortic stenosis and preserved left ventricular ejection fraction undergoing surgical valve replacement. Eur Heart J 2009;30:3037–47.
72. de Isla LP, de Agustin A, Rodrigo JL, Almeria C, del Carmen Manzano M, Rodriguez E, Garcia A, Macaya C, Zamorano J. Chronic mitral regurgitation: A pilot study to assess preoperative left ventricular contractile function using speckle-tracking echocardiography. J Am Soc Echocardiogr 2009;22:831–38.
73. Okada M, Tanaka H, Matsumoto K, Ryo K, Kawai H, Hirata K. Subclinical myocardial dysfunction in patients with reverse-remodeled dilated cardiomyopathy. J Am Soc Echocardiogr 2012;25:726-32.
74. Heggemann F, Weiss C, Hamm K, Kaden J, Süselbeck T, Papavassiliu T, Borggrefe M, Haghi D. Global and regional myocardial function quantification by two-dimensional strain in Takotsubo cardiomyopathy. Eur J Echocardiogr 2009;10:760–4.
75. Burri MV, Nanda NC, Lloyd SG, Hsiung MC, Dod HS, Beto RJ, Bhardwaj R, Jain A, Jackson J, Agarwal A, Chaurasia P, Prasad AN, Manda J, Pothineni KR. Assessment of systolic and diastolic left ventricular and left atrial function using vector velocity imaging in Takotsubo cardiomyopathy. Echocardiography 2008;25:1138–44.
76. Porciani MC, Cappelli F, Perfetto F, Ciaccheri M, Castelli G, Ricceri I, Chiostri M, Franco B, Padeletti L. Rotational mechanics of the left ventricle in AL amyloidosis. Echocardiography 2010;27:1061–68.
77. Sengupta PP, Krishnamoorthy VK, Abhayaratna WP, Korinek J, Belohlavek M, Sundt TM 3rd, Chandrasekaran K, Mookadam F, Seward JB, Tajik AJ, Khandheria BK. Disparate patterns of left ventricular mechanics differentiate constrictive pericarditis from restrictive cardiomyopathy. JACC Cardiovasc Imaging 2008;1:29–38.
78. Fonseca CG, Dissanayake AM, Doughty RN, Whalley GA, Gamble GD, Cowan BR, Occleshaw CJ, Young AA. Three-dimensional assessment of left ventricular systolic strain in patients with type 2 diabetes mellitus, diastolic dysfunction, and normal ejection fraction. Am J Cardiol 2004; 94:1391-5.

79. Behar V, Adam D, Lysyansky P, Friedman Z. The combined effect of nonlinear filtration and window size on the accuracy of tissue displacement estimation using detected echo signals. Ultrasonics 2004;41:743-53.
80. Belghitia H, Brette S, Lafitte S, Reant P, Picard F, Serri K, Lafitte M, Courregelongue M, Dos Santos P, Douard H, Roudaut R, DeMaria A. Automated function imaging: a new operator-independent strain method for assessing left ventricular function. Arch Cardiovasc Dis 2008;101:163-9.
81. Jasaityte R, Heyde B, D'hooge J. Current state of three-dimensional myocardial strain estimation using echocardiography. J Am Soc Echocardiogr. 2013;26:15-28.
82. Tschöpe C, Bock CT, Kasner M, Noutsias M, Westermann D, Schwimmbeck PL, Pauschinger M, Poller WC, Kühl U, Kandolf R, Schultheiss HP. High prevalence of cardiac parvovirus B19 infection in patients with isolated left ventricular diastolic dysfunction. Circulation 2005; 111:879–86.
83. Aretz HT. Myocarditis: the Dallas criteria. Hum Pathol. 1987;18:619-24.
84. Escher F, Kuhl U, Sabi T, Suckau L, Lassner D, Poller W, Schultheiss HP, Noutsias M. Immunohistological detection of Parvovirus B19 capsid proteins in endomyocardial biopsies from dilated cardiomyopathy patients. Med Sci Monit. 2008;14:CR333-338.
85. Noutsias M, Pauschinger M, Ostermann K, Escher F, Blohm JH, Schultheiss H, Kühl U. Digital image analysis system for quantification of infiltrates and cell adhesion molecules in inflammatory cardiomyopathy. Med Sci Monit. 2002;8:MT59-71.
86. Udink ten Cate FEA, Adelmann RO, Junker P, Hackenbroch M, Sreeram N. Screening children with suspected myocarditis for global and regional myocardial dysfunction using two-dimensional speckle tracking echocardiography: is it of use? Int J Cardiol. 2012;157:278-81.
87. De Cobelli F, Pieroni M, Esposito A, Chimenti C, Belloni E, Mellone R, Canu T, Perseghin G, Gaudio C, Maseri A, Frustaci A, Del Maschio A. Delayed gadolinium-enhanced cardiac magnetic resonance in patients with chronic myocarditis presenting with heart failure or recurrent arrhythmias. J Am Coll Cardiol 2006;47:1649–54.
88. Lynch M, O'Donnell R Weintraub NL, Lopez-Candales A. Assessment of mitral annular velocity vector imaging in acute myocarditis. Echocardiography. 2013;30:E227-30.
89. Kühl U, Pauschinger M, Bock T, Klingel K, Schwimmbeck CP, Seeberg B, Krautwurm L, Poller W, Schultheiss HP, Kandolf R. Parvovirus B19 infection mimicking acute myocardial infarction. Circulation. 2003;108:945–50.
90. Mahrholdt H, Wagner A, Deluigi CC, Kispert E, Hager S, Meinhardt G, Vogelsberg H, Fritz P, Dippon J, Bock CT, Klingel K, Kandolf R, Sechtem U. Presentaton, patterns of myocardial damage, and clinical course of viral myocarditis. Circulation 2006;114:1581-90.
91. Bültmann BD, Klingel K, Sotlar K, Bock CT, Baba HA, Sauter M, Kandolf R. Fatal parvovirus B19-associated myocarditis clinically mimicking ischemic heart disease: an endothelial cell-mediated disease. Hum Pathol. 2003;34:92–5.

92. Lamparter S, Schoppet M, Pankuweit S, Maisch B. Acute parvovirus B19 infection associated with myocarditis in an immunocompetent adult. Hum Pathol. 2003;34:725–8.
93. Escher F, Lassner D, Kühl U, Gross U, Westermann D, Poller W, Skurk C Weitmann K, Hoffmann W, Tschöpe C, Schultheiss HP. Analysis of endomyocardial biopsies in suspected myocarditis- diagnostic value of left versus right ventricular biopsy. Int J Cardiol. 2014;177:76-8.
94. Caforio AL, Calabrese F, Angelini A, Tona F, Vinci A, Bottaro S, Ramondo A, Carturan E, Iliceto S, Thiene G, Daliento L. A prospective study of biopsy-proven myocarditis: prognostic relevance of clinical and aetiopathogenetic features at diagnosis. Eur Heart J 2007;28:1326-33.
95. Bowles NE, Ni J, Kearney DL, Pauschinger M, Schultheiss HP, McCarthy R, Hare J, Bricker JT, Bowles KR, Towbin JA. Detection of viruses in myocardial tissues by polymerase chain reaction. Evidence of adenovirus as a common cause of myocarditis in children and adults. J Am Coll Cardiol 2003;42:466–72.
96. Kühl U, Noutsias N, Seeberg B, Schuktheiss HP. Immunohistological evidence for a chornic intramyocardial inflammatory process in dilated cardiomyopathy. Heart 1996;75:295-300.
97. Kühl U, Noutsias M, Seeberg B, Schannwell M, Welp LB, Schultheiss HP. Chronic inflammation in the myocardium of patients with clinically suspected dilated cardiomyopathy. J Cardiac Failure 1994;1:13-25.
98. Kiihl U, Noutsias M, Schultheiss HP. Immunohistochemistry in dilated cardiomyopathy. Eur Heart J 1995;16 Suppl O:100-6.
99. Prochorec-Sobieszek M, Bilinska ZT, Grzybowski J, Mazurkiewicz L, Skwarek M, Walczak E, Michalak E, Cedro K, Chmielak Z, Debski A, Demkow M, Witkowski A, Wagner T, Ruzyllo W. Assessment of the inflammatory process by endomyocardial biopsy in patients with dilated cardiomyopathy based on pathological and immunohistochemical methods. Kardiol Pol. 2006;64:479-87.
100. Noustias M, Seeberg B, Schultheiss HP, Kiihl U. Expression of cell adhesion molecules in dilated cardiomyopathy: evidence for endothelial activation in inflammation cardiomyopathy. Circulation 1999;99:2124-31.
101. Schaper J, Froede R, Hein S, Buck A, Hashizume H, Speiser B, Friedl A, Bleese N. Impairment of the myocardial ultrastructure and changes of the cytoskeleton in dilated cardiomyopathy. Circulation1991;83:504–14.
102. Di Somma S, Marotta M, Salvatore G, Cudemo G, Cuda G, De Vivo F, Di Benedetto MO, Ciaramella F, Caputo G, de Divitiis O. Changes in myocardial cytoskeletal intermediate filaments and myocyte contractile dysfunction in dilated cardiomyopathy: an in vivo study in humans. Heart 2000;84:659-67.
103. Leitman, M, Bachner-Hinenzon, N, Adam D, Fuchs T, Theodorovich N, Peleg E, Krakover R, Moravsky G, Uriel N, Vered Z. Speckle tracking imaging in acute inflammatory pericardial diseases. Echocardiogr. 2011;28:548-55.

104. Kraigher-Krainer E, Shah AM, Gupta DK, Santos A, Claggett B, Pieske B, Zile MR, Voors AA, Lefkowitz MP, Packer M, McMurray JJ, Solomon SD; PARAMOUNT Investigators. Impaired systolic function by strain imaging in heart failure with preserved ejection fraction. J Am Coll Cardiol. 2014; 63:447-56.
105. Ha SJ, Woo JS, Kwon SH, Oh CH, Kim KS, Bae JH, Kim WS. Acute regional myocarditis with normal ventricular wall motion diagnosed by two-dimensional speckle tracking imaging. Korean J Intern Med. 2013;28:732-5.
106. Yoneyama A, Koyama J, Tomita T, Kumazaki S, Tsutsui H, Watanabe N, Kinoshita O, Ikeda U. Relationship of plasma brain-type natriuretic peptide levels to left ventricular longitudinal function in patients with congestive heart failure assessed by strain Doppler imaging. Int J Cardiol. 2008;130:56-63.
107. Rangel I, Goncalves A, de Sousa C, Almeida PB, Rodrigues J, Macedo F, Silva Cardoso J, Maciel MJ. Global longitudinal strain as a potential prognostic marker in patients with chronic heart failure and systolic dysfunction. Rev Port Caridol. 2014;33:403-9.
108. Obaid FA, Maskon O, Abdolwahid F. Systolic function and intraventricular mechanical dyssynchrony assessed by advanced speckle tracking imaging with N-terminal prohormone of brain natriuretic peptide for outcome prediction in chronic heart failure patients. Sultan Qaboos Univ Med J. 2013;13:551-9.
109. Unger ED, Dubin RF, Deo R, Daruwalla V, Friedman JL, Medina C, Beussink L, Freed BH, Shah SJ. Association of chronic kidney disease with abnormal cardiac mechanics and adverse outcomes in patients with heart failure and preserved ejection fraction. Eur J Heart Fail. 2016; 18:103-12.
110. Edwards NC, Hirth A, Ferro CJ, Townend JN, Steeds RP. Subclinical abnormalities of left ventricular myocardial deformation in early-stage chronic kidney disease: the precursor of uremic cardiomyopathy? J Am Soc Echocardiogr 2008;21:1293–8.
111. Hassanin N, Alkemary A. Early detection of subclinical uremic cardiomyopathy using two-dimensional speckle tracking echocardiography. Echocardiography. 2016;33:527-36.
112. Panoulas VF, Sulemane S, Konstantinou K, Bratsas A, Elliott SJ, Dawson D, Frankel AH, Nihoyannopoulos P. Early detection of subclinical left ventricular dysfunction in patients with chronic kidney disease. Eur Heart J Cardiovasc Imaging. 2015;16:539-48.
113. Kosmala W, Plaksej R, Strotmann JM, Weigel C, Herrmann M, Mende H, Störk S, Angermann CE, Wagner JA, Weidemann F. Progression of left ventricular functional abnormalities in hypertensive patients with heart failure: an ultrasonic two-dimensional speckle tracking study. J AM Soc Echocardiogr. 2008;21:1309-17.
114. Edvardsen T, Helle-Valle T, Smiseth OA. Systolic dysfunction in heart failure with normal ejection fraction: speckle-tracking echocardiography. Prog Cardiovasc Dis 2006;49:207-14.
115. Delgado V, Mollema SA, Ypenburg C, Tops LF, van der Wall EE, Schalij MJ, Bax JJ. Relation between global left ventricular longitudinal strain assessed with novel automated function imaging and biplane left ventricular ejection fraction in patients with coronary artery disease. J Am Soc Echocardiogr. 2008;21:1244-50.

116. Marciniak A, Claus P, Sutherland GR, Marciniak K, Karu T, Baltabaeva A, Merli E, Bijnens B, Jahangiri M. Changes in systolic left ventricular function in isolated mitral regurgitation. A strain rate imaging study. Eur Heart J 2007;28:2627-36.
117. Maffessanti F, Nesser HJ, Weinert L, Steringer-Mascherbauer R, Niel J, Gorissen W, Sugeng L, Lang RM, Mor-Avi V. Quantitative evaluation of regional left ventricular function using three-dimensional speckle tracking echocardiography in patients with and without heart disease. Am J Cardiol 2009;104:1755-62.
118. Pizzino F, Vizzari G, Qamar R, Bomzer C, Carerj S, Zito C, Khandheria BK. Multimodality imaging in cardiooncology. J Oncol. 2015;2015:263950.
119. Vitarelli A, Martino F, Capotosto L, Martino E, Colantoni, Ashurov V, Ricci S, Conde Y, Maramao F, Vitarelli M, De Chiara S, Zanoni C. Early myocardial deformation changes in hypercholesterolemic and obese children and adolescent: a 2D and 3D speckle tracking echocardiography study. Medicine (Baltimore) 2014;93:e71.
120. Ma C, Chen J, Yang J, Tang L, Chen X, Li N, Liu S, Zhang Y. Quantitative assessment of left ventricular function by 3-dimensional speckle-tracking echocardiography in patients with chronic heart failure: a meta-analysis. J Ultrasound Med. 2014;33:287-95.
121. Reant P, Barbot L, Touche C, Dijos M, Arsac F, Pillois X, Landelle R, Roudaut R, Lafitte S. Evaluation of global left ventricular systolic function using three-dimensional echocardiography speckle-tracking strain parameters. J Am Soc Echocardiogr 2012;25:68-79.
122. Trache T, Stöbe S, Tarr A, Pfeiffer D, Hagendorff A. The agreement between 3D, standard 2D and triplane 2D speckle tracking: effects of image quality and 3D volume rate. Echo Res Pract. 2014;1:71-83.
123. Li SN, Wong SJ, Cheung YF. Novel area strain based on three-dimensional wall motion analysis for assessment of global left ventricular performance after repair of tetralogy of Fallot. J Am Soc Echocardiogr 2011;24:819-25.
124. Seo Y, Ishizu T, Atsumi A, Kawamura R, Aonuma K. Three-dimensional speckle tracking echocardiography. Circ J. 2014;78:1290-301.
125. Huttin O, Zhang L, Lamarie J, Mandry D, Juilliere Y, Lemoine S, Micard E, Marie PY, Sadoul N, Girerd N, Selton-Suty C. Global and regional myocardial deformation mechanics of microvascular obstruction in acute myocardial infarction: a three dimensional speckle-tracking imaging study. Int J Cardiovasc Imaging. 2015; 31:1337-46.
126. Nagata Y, Takeuchi M, Wu VC, Izumo M, Suzuki K, Sato K, Seo Y, Akashi YJ, Aonuma K, Otsuji Y. Prognostic value of LV deformation parameters using 2D and 3D speckle-tracking echocardiography in asymptomatic patients with severe aortic stenosis and preserved LV ejection fraction. JACC Cardiovasc Imaging. 2015; 8:235-45.
127. Abate E, Hoogslag GE, Antoni ML, Nucifora G, Delgado V, Holman ER, Schalij MJ, Bax JJ, Marsan NA. Value of three-dimensional speckle-tracking longitudinal strain for predicting improvement of left ventricular function after acute myocardial infarction. Am J Cardiol 2012;110:961–7.

8. Abbreviations

2D- two-dimensional

3D- three-dimensional

AF- atrial fibrillation

AH- arterial hypertension

AMs- adhesion molecules

AoV- aortic valve

AP- angina pectoris

AUC- area under the curve

AV- atrioventricular

BMI- body mass index

CAD- coronary artery disease

CAMs- cell adhesion molecules

CD- cluster of differentiation

CI- confidence interval

CK- creatine kinase

CKD- chronic kidney disease

CM – cardiomyopathy

CMR- cardiac magnetic resonance

CMV- cytomegalovirus

COPD- chronic obstructive pulmonary disease

CRP- C-reactive protein

DCM- dilated cardiomyopathy

df- degrees of freedom

DM- diabetes mellitus

DNA- deoxyribonucleic acid

EBV- Epstein–Barr virus

ECG- electrocardiogram

EF- ejection fraction

EMB- endomyocardial biopsy

EMBs- endomyocardial biopsies

ESC- European Society of Cardiology

GAS- global area strain

GCS- global circumferential strain

GFR- glomerular filtration rate

GLS- global longitudinal strain

GLSR- global longitudinal systolic strain rate

GLASR- global longitudinal late diastolic strain rate

GLESR- global longitudinal early diastolic strain rate

GRS- global radial strain

ge- genome equivalents

HbA1c- glycated hemoglobin

HCM- hypertrophic cardiomyopathy

HF- heart failure

HFpEF- heart failure with preserved ejection fraction

HHV- human herpes virus

HHV6- human herpes virus 6

HIV- Human immunodeficiency virus

HLA- human leukocyte antigens

ICAM-1- intercellular adhesion molecule 1

iCM- inflammatory cardiomyopathy

IVS- interventricular septum

LA- left atrium

LBBB- left bundle branch block

LV- left ventricular

LVEDD- left ventricular end-diastolic dimension

LVEDP- left ventricular end-diastolic pressure

LVEDV- left ventricular end-diastolic volume

LVEF- left ventricular ejection fraction

LVESD- left ventricular end-systolic dimension

LVESV- left ventricular end-systolic volume

LVOT- left ventricular outflow tract velocity

LVOT Vmax- maximal left ventricular outflow tract velocity

LVSF- left ventricular shortening fraction

MRI- magnetic resonance imaging

mRNA- messenger ribonucleic acid

NTproBNP- N-terminal pro B-type natriuretic peptide

NYHA- New York Heart Association

PAP- pulmonary artery pressure

PCR- polymerase chain reaction

PV- pulmonary valve

PVB19- parvovirus B19

PW- posterior wall

RA- right atrium

RBBB- right bundle branch block

RNA- ribonucleic acid

ROC- receiver operating characteristic

RT-PCR- reverse transcription polymerase chain reaction

RV- right ventricular

SD- standard deviation

SR- strain rate

STE- speckle tracking echocardiography

STEMI- ST-elevation myocardial infarction

TAPSE- tricuspid annular plane systolic excursion

TD- tissue Doppler

TDI- tissue Doppler imaging

TSH- thyroid-stimulating hormone

TV- tricuspid valve

VA- late diastolic mitral inflow velocity

VCAM-1- vascular cell adhesion molecule 1

VE- early diastolic mitral inflow velocity

Vmax- maximal velocity

WHO- World Health Organization

WMAs- wall motion abnormalities

9. Eidesstattliche Versicherung

„Ich, Aleksandar Aleksandrov, versichere an Eides statt durch meine eigenhändige Unterschrift, dass ich die vorgelegte Dissertation mit dem Thema: „Myocardial deformation imaging in patients with inflammatory cardiomyopathy“ selbstständig und ohne nicht offengelegte Hilfe Dritter verfasst und keine anderen als die angegebenen Quellen und Hilfsmittel genutzt habe.

Alle Stellen, die wörtlich oder dem Sinne nach auf Publikationen oder Vorträgen anderer Autoren beruhen, sind als solche in korrekter Zitierung (siehe „Uniform Requirements for Manuscripts (URM)“ des ICMJE -*www.**icmje**.org*) kenntlich gemacht. Die Abschnitte zu Methodik (insbesondere praktische Arbeiten, Laborbestimmungen, statistische Aufarbeitung) und Resultaten (insbesondere Abbildungen, Graphiken und Tabellen) entsprechen den URM (s.o) und werden von mir verantwortet.

Meine Anteile an etwaigen Publikationen zu dieser Dissertation entsprechen denen, die in der untenstehenden gemeinsamen Erklärung mit dem/der Betreuer/in, angegeben sind. Sämtliche Publikationen, die aus dieser Dissertation hervorgegangen sind und bei denen ich Autor bin, entsprechen den URM (s.o) und werden von mir verantwortet.

Die Bedeutung dieser eidesstattlichen Versicherung und die strafrechtlichen Folgen einer unwahren eidesstattlichen Versicherung (§156,161 des Strafgesetzbuches) sind mir bekannt und bewusst.“

Datum 30.01.2017 Unterschrift

Anteilserklärung an etwaigen erfolgten Publikationen

Aleksandar Aleksandrov hatte folgenden Anteil an den folgenden Publikationen:

Publikation 1: Carsten Tschöpe, Burkert Pieske, Mario Kasner, Heinz-Peter Schultheiss, Felicitas Escher, Aleksandar Aleksandrov, Nidal Al-Saadi, Markus Makowski, Frank Spillmann, Martin Genger, Uwe Kühl, Michel Noutsias, Daniel Morris. Multimodality Imaging Approach in the Diagnosis of Chronic Myocarditis with Preserved Left Ventricular Ejection Fraction (MCpEF): The Role of 2D Speckle-Tracking Echocardiography. International Journal of Cardiology. 2017 (under review)

Beitrag im Einzelnen (bitte kurz ausführen): 2D speckle tracking echocardiography Messungen gemacht, statistische Datenverarbeitung

Unterschrift, Datum und Stempel des betreuenden Hochschullehrers/der betreuenden Hochschullehrerin

Unterschrift des Doktoranden/der Doktorandin

10. Curriculum vitae

Mein Lebenslauf wird aus datenschutzrechtlichen Gründen in der elektronischen Version meiner Arbeit nicht veröffentlicht.

Mein Lebenslauf wird aus datenschutzrechtlichen Gründen in der elektronischen Version meiner Arbeit nicht veröffentlicht.

Mein Lebenslauf wird aus datenschutzrechtlichen Gründen in der elektronischen Version meiner Arbeit nicht veröffentlicht.

11. List of publications

1. Kasner M, Aleksandrov A, Escher F, Al-Saadi N, Makowski M, Spillmann F, Genger M, Schultheiss HP, Kühl U, Pieske B, Morris DA, Noutsias M, Tschöpe C. Multimodality imaging approach in the diagnosis of chronic myocarditis with preserved left ventricular ejection fraction (MCpEF): The role of 2D speckle-tracking echocardiography. Int J Cardiol. 2017;243:374-8.
2. Atanassova PA, Massaldjieva RI, Dimitrov BD, Aleksandrov AS, Semerdjieva MA, Tsvetkova SB, Chalakova NT, Chompalov KA. Early neurological and cognitive impairments in subclinical cerebrovascular disease. Neurol India. 2016;64(4):646-55.
3. Kasner M, Aleksandrov AS, Westermann D, Lassner D, Gross M, von Haehling S, Anker SD, Schultheiss HP, Tschöpe C. Functional iron deficiency and diastolic function in heart failure with preserved ejection fraction. Int J Cardiol. 2013;168(5):4652-7.
4. Demirevska L, Aleksandrov A, Gotchev D, Nedkova M, Balabanski V. Practical protocol for perioperative management of patients treated with K antagonists. Military Medicine. LXVIII 2016;4:9-13.
5. Demirevska L, Aleksandrov A, Gotchev D, Balabanski V, Nedkova M. Congestive heart failure indused by nonsteroidal anti-inflammatory drugs. Military Medicine. LXVIII 2016;4:42-4.
6. Co-Author of the book “The statins in the cardiovascular continuum”, edited by Prof. Nina Gotcheva and Assoc. Prof. Borislav Georgiev, 2013, Sofia.
7. Co-Author of the book “Pharmacotherapy in the cardiology”, edited by Prof. Mila Vlaskovska and Assoc. Prof. Nina Gotcheva, 2012, Sofia.
8. Co-Author of the book “Sudden cardial death”, edited by Assoc. Prof. Nina Gotcheva and Assoc. Prof. Tosho Balabanski, 2012 Sofia.
9. Daskalov I, Aleksandrov A, Gotchev D. Pulmonary hypertension – contemporary classification and diagnostic algorithm. Medinfo 2011;01:36-40.
10. Ivanov S, Daskalov I, Aleksandrov A, Gotchev D. Miocardites. Medinfo 2010;10:65-6.
11. Demirevska L, Daskalov I, Aleksandrov A, Gotchev D, Ivanov S. Pericarditis. Tuberculous pericarditis. Medinfo 2010;09:59-61.

12. Aleksandrov A, Daskalov I, Ivanov S, Demirevska L, Gotchev D. Treatment of arterial hypertension. Medinfo 2010;01:14-8.
13. Daskalov I, Aleksandrov A, Demirevska L, Ivanov S, Gotchev D. Valsartan following percutaneous coronary interventions. Medinfo 2009;09:48-54.
14. Aleksandrov A, Ivanov S, Daskalov I, Demirevska L, Gotchev D. New trends in the antithrombotic therapy of acute coronary syndrome. Medinfo 2009;01:22-6.
15. Daskalov I, Aleksandrov A, Demirevska L, Ivanov S, Gotchev D. Fondaparinux in the treatment of acute coronary syndrome. Bulgarian Cardiology 2008;4.
16. Demirevska L, Ivanov S, Daskalov I, Aleksandrov A. Amiodarone and thyroid gland dysfunction. Medinfo 2008;09:56-60.
17. Daskalov I, Demirevska L, Aleksandrov A, Ivanov S, Gotchev D. The new European guidelines for the treatment of arterial hypertension. Therapy with angiotensin receptor blockers. Medinfo 2008;09:5-10.
18. Demirevska L, Daskalov I, Aleksandrov A, Ivanov S, Gotchev D. Cardiac sarcoidosis. In Spiro 2008;3:23-5.
19. Atanasova P, Aleksandrov A. Cerebrovascular risk factors in healthy adults without cerebrovascular accidents. Union of Scientist research, Plovdiv, series G: Medicine, Pharmacy and Dentistry. Scientific session Medicine and Dentistry, Plovdiv, June, 2007.
20. Gardjeva PA, Dimitrova SZ, Kostadinov ID, Murdjeva MA, Peychev LP, Lukanov LK, Stanimirova IV, Alexandrov AS. A study of chemical composition and antimicrobial activity of Bulgarian propolis. Folia Med. 2007;49(3-4):63-9.
21. Gardjeva P, Alexandrov A, Dimitrova S, et al. A study on chemical composition and antifungal activity of Bulgarian propolis. Union of Scientist research, Plovdiv, series G: Medicine, Pharmacy and Dentistry. Scientific session Medicine and Dentistry 2006;7:201-5.
22. Moshekov E, Aleksandrov A, Mladenova M, Dimitrova E, Bakardzhiev I, Mateeva M. Colonic atresia. Clinical observation and therapeutic approach in three cases. Praemedicus since 1925 2006;26(1-2):87-9.
23. Atanasova P, Krastev N, Bahchevanov K, Mihaylova A, Paunova H, Aleksandrov A, Kostadinova M, Masaldzhieva P. Minimal hepatic encephalopathy – pathogenic, diagnostic and clinical aspects. Bulgarian Neurology 2006;6(1):12-7.

12. Acknowledgements

I would like cordially to thank the following persons and institutions, without whom this work and my presence in Berlin would have been impossible.

Prof. Dr. med. Carsten Tschöpe
PD Dr. med. Mario Kasner
Prof. Dr. rer. nat. Nonka Mateva
PD Dr. med. Dobromir Gotchev
Mrs Martina Weiland
Dr. Stanislav Ivanov
The colleagues from the Cardiology Department of Charité-CBF
The colleagues from the Cardiology Department at the Military Medical Academy, Sofia, Bulgaria
My wonderful family